Ofioliti, 2011, 36 (1), 1-35

EARLY JURASSIC TO EARLY LATE CRETACEOUS RADIOLARIANS FROM THE SANTA ROSA ACCRETIONARY COMPLEX (NORTHWESTERN COSTA RICA)

Alexandre Nicolas Bandini°,*,✉, Peter Oliver Baumgartner°, Kennet Flores°,, Paulian Dumitrica°**
and **Sarah-Jane Jackett*****

° *Institut de Géologie et de Paléontologie, Université de Lausanne, Switzerland.*
* *School of Earth and Environment, The University of Western Australia, Crawley, Australia.*
** *American Museum of Natural History, New York, USA.*
*** *Integrated Ocean Drilling Program, Texas A&M University, College Station, USA.*
✉ *Corresponding author, email: alexandre.bandini@uwa.edu.au*

Keywords: *Radiolaria, radiolarites, basalts, Mesozoic, Jurassic, Cretaceous, Caribbean Plate, Santa Rosa Accretionary Complex. Santa Elena Peninsula, Costa Rica.*

ABSTRACT

In the circum-Pacific ophiolitic belts, when no other biogenic constituents are found, radiolarians have the potential to provide significant biostratigraphic information. The Santa Rosa Accretionary Complex, which crops out in several half-windows (Carrizal, Sitio Santa Rosa, Bahia Nancite, Playa Naranjo) along the south shores of the Santa Elena Peninsula in northwestern Costa Rica, is one of these little-known ophiolitic mélanges. It contains various oceanic assemblages of alkaline basalt, radiolarite and polymictic breccias. The radiolarian biochronology presented in this work is mainly based by correlation on the biozonations of Carter et al. (2010), Baumgartner et al. (1995b), and O'Dogherty (1994) and indicate an Early Jurassic to early Late Cretaceous (early Pliensbachian to earliest Turonian) age for the sediments associated with oceanic basalts or recovered from blocks in breccias or megabreccias. The 19 illustrated assemblages from the Carrizal tectonic window and Sitio Santa Rosa contain in total 162 species belonging to 65 genera. The nomenclature of tectonic units is the one presented by (Baumgartner and Denyer, 2006). This study brings to light the Early Jurassic age of a succession of radiolarite, which was previously thought to be of Cretaceous age, intruded by alkaline basalts sills (Unit 3). The presence of Early Jurassic large reworked blocks in a polymictic megabreccia, firstly reported by De Wever et al. (1985) is confirmed (Unit 4). Therefore, the alkaline basalt associated with the radiolarites of these two units (and maybe also Units 5 and 8) could be of Jurassic age. In the Carrizal tectonic window, Middle to early Late Jurassic radiolarian chert blocks associated with massive tholeitic basalts and Early Cretaceous brick-red ribbon cherts overlying pillow basalts are interpreted as fragments of a Middle Jurassic oceanic basement accreted to an Early Cretaceous oceanic Plate, in an intra-oceanic subduction context. Whereas, the knobby radiolarites and black shales of Playa Carrizal are indicative of a shallower middle Cretaceous paleoenvironment. Other remnants of this oceanic basin are found in Units 2, 6, and 7, which documented the rapid approach of the depocentre to a subduction trench during the late Early Cretaceous (Albian-Cenomanian), to possibly early Late Cretaceous (Turonian).

INTRODUCTION

The Santa Elena Peninsula, located in northwestern Costa Rica, is 8 to 16 km wide and protrudes about 40 km westwards into the Pacific Ocean (Fig. 1). During the last fifty years, several geological studies have been carried out, showing that much of the peninsula is made up of serpentinized peridotites, cut locally by mafic dykes (Azéma and Turnon, 1980). The large serpentinite unit is thrust on top of a relative autochthonous unit, which crops out along the south coast of the peninsula and is formed by red and brown radiolarian cherts associated with massive and pillow basalts, but also with volcanic sandstones and breccias. Radiolarites are in places cut by sills of potassic alkaline basalts (e.g., Harrison, 1953; Dengo, 1962; Azéma and Turnon, 1980; De Wever et al., 1985; Donnelly, 1994; Meschede and Frisch, 1994).

Initially, the Santa Elena Peninsula rock units were considered as part of a single ophiolitic suite with the volcano-sedimentary sequence being the upper part of this suite locally preserved in grabens and related to the oceanic assemblage that composes the Nicoya Peninsula (Dengo, 1962; Kuijpers, 1980; Schmidt-Effing, 1980). Subsequently Azéma and Turnon (1980) observed an important fault interpreted as a major overthrust separating two composite tectonic units of different origin (Azéma and Tournon, 1980; Tournon, 1984; Bourgois et al., 1984; Baumgartner, 1984; Azéma et al., 1985). According to this hypothesis, the ultramafic peridotites form the allochthonous upper unit, which corresponds to a south-directed nappe emplaced during the Late Cretaceous and called herein the Santa Elena Nappe. The relative autochthonous unit constitutes the underlying tectonic unit, which was correlated with the Nicoya Complex (Bourgois et al., 1984; Baumgartner, 1984; Azéma et al., 1985). Tournon (1980) provided a drawing of the coastal section at Santa Rosa indicating a complex interlayering of sedimentary and igneous lithologies. Astorga (1992) and Tournon (1994), based on the distribution of radiolarian ages by De Wever et al. (1985), interpreted the outcrops of the Santa Rosa area as a single stratigraphic sequence ranging in age form the late Early Jurassic to the Late Cretaceous, set in a simple anticline. However, more recent fieldwork indicates that this relative autochthonous unit is not a continuous sequence, but a stack of tectonic units piled-up in an accretionary complex called the Santa Rosa Accretionary Complex (Baumgartner and Denyer, 2006).

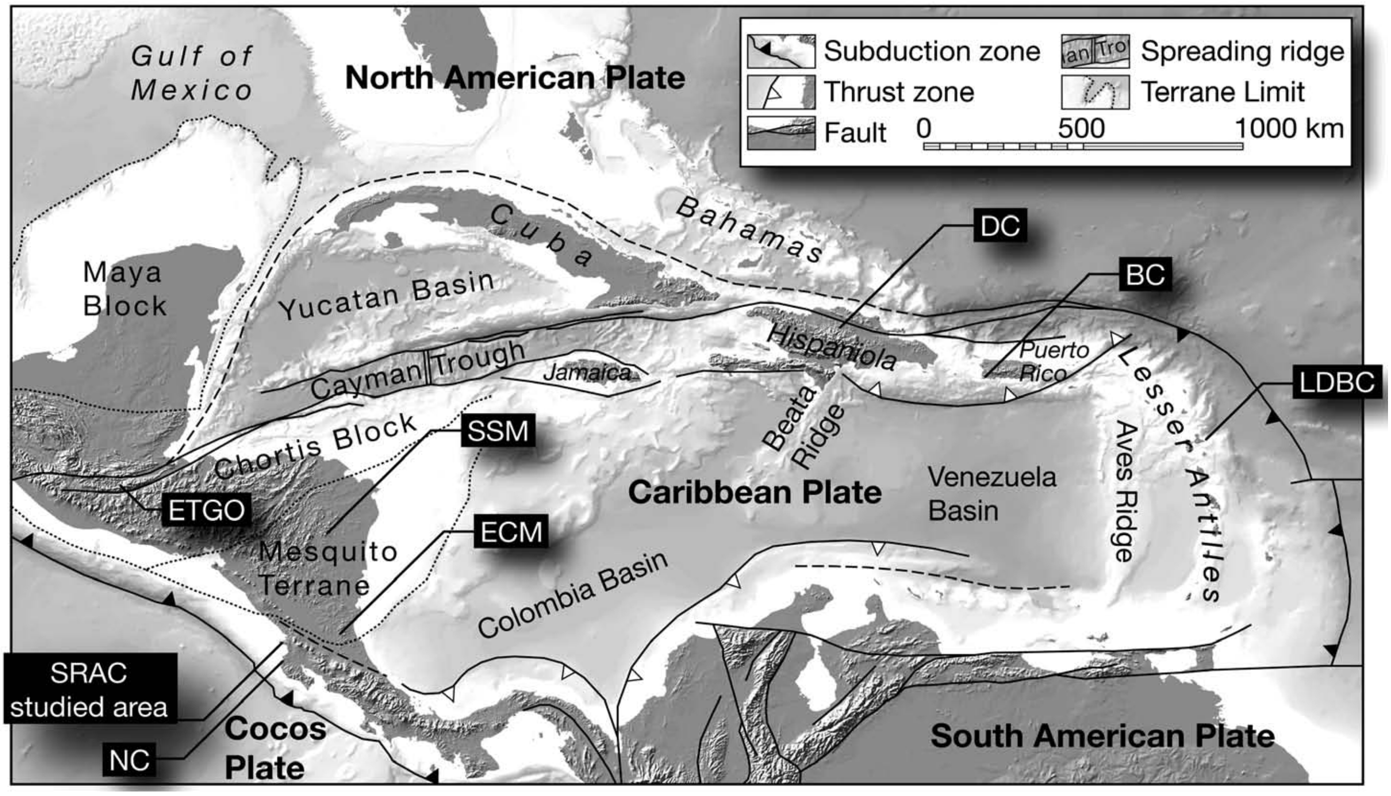

Fig. 1 - Circum-Caribbean region map modified from Mann et al. (1991), Baumgartner et al. (2008), and Pindell and Kennan (2009) with Plate-boundaries and morphology, showing main tectonic features and radiolarite localities discussed in text. From west to east, ETGO: El Tambor Group Ophiolites, SRAC: Santa Rosa Accretionary Complex (studied area), NC: Nicoya Complex, SSM: Siuna Serpentinite Mélange, ECM: El Castillo Mélange, DC: Duarte Complex, BC: Bermeja Complex, and LDBC: La Désirade Basement Complex of Guadeloupe.

This study aims at providing new micropaleontological data and discussing the preliminary radiolarian biochronology published in two previous publications (Schmidt-Effing, 1980; De Wever et al., 1985). Radiolaria are the only fossils that are abundant throughout the accretionary complex and their biochronology is critical to the understanding of the origin of the remnants of oceanic and trench fill units of the Santa Rosa Accretionary Complex and more generally the paleogeography of the trailing edge of the Caribbean Plate.

GEOLOGICAL SETTING

We distinguish from bottom to top three tectonic units in the area of the Santa Elena Peninsula (Fig. 2): 1) the Islas Murciélagos pillow and massive basalts; 2) the relative autochthonous of the Santa Elena Nappe composed of the Santa Rosa Accretionary Complex and the Nancite Complex; 3) the Santa Elena Nappe composed of ultramafics.

The Islas Murciélagos

The Islas Murciélagos pillow and massive basalts show no clear structural relationship with the following two units. Their geochemistry suggests a primitive island arc origin similar to the dolerites of the Santa Elena Nappe. A pillow basalt from Islas Murciélagos yields a $^{40}Ar/^{39}Ar$ date of 109.0±2.0 Ma (Hauff et al., 2000). No fossil-bearing sediments are known from this unit.

The relative autochtonous

The relative autochthonous of the Santa Elena Nappe is composed of the Santa Rosa Accretionary Complex (SRAC) and the Nancite Complex, which comprises layered gabbros, plagiogranites and associated basaltic dykes.

The Santa Rosa Accretionary Complex

Baumgartner and Denyer (2006) named the SRAC after Sitio Santa Rosa, where the most complete sequence is exposed. They describe it as a tectonic pile of sedimentary and volcanic packages. Polarity indicators in all sedimentary packages show younging to the east. Sedimentary environments within individual stratigraphic packages range from oceanic (radiolarites with alkaline basalt sills) to trench fill (arc-derived turbidites and collapse megabreccias). Bedded radiolarites are of middle Cretaceous ages whereas reworked blocks of highly deformed radiolarite in breccias are of Jurassic ages.

The SRAC is exposed in a few isolated outcrops, because the Santa Elena overthrust undulates and is offset by local faults. In many places its intersection with the surface is below the actual sea level. Megabreccias with pluri-decametric blocks, which are contemporaneous of the emplacement of the Santa Elena Nappe, are associated with this roughly horizontal thrust (e.g., outcrops in western Playa Carrizal, Isla Pelada and northern Playa Naranjo, Baumgartner and Denyer, 2006).

Overall, basaltic units dominate the SRAC. From west to east, several tectonic half-windows occur along the southern coast of the peninsula: the Carrizal tectonic window, located west and east of Playa Guarumo and extending through to Playa Carrizal; the Sitio Santa Rosa, where a stack of tectonic units including alkaline pillow basalts, basaltic breccias, red and brown radiolarites, radiolarite-basalt breccias, tuffs and sills of alkaline basalts (Tournon, 1984; 1994; Frisch et al., 1992) crop out. Basalt and radiolarite associated with the SRAC also crop out in the Potrero Grande tectonic window. The easternmost exposures include outcrops at Bahia Nancite, Playa Tule and the cliffs north of Playa Naranjo. The samples described in this study are from outcrops located in the Carrizal tectonic window (area between Playa Guarumo and Playa Carrizal) and Sitio Santa Rosa (between Playa Danta and Punta El Respinge) (see Fig. 2).

The area both west and east of Playa Guarumo is dominated by steeply dipping massive and pillowed basalt flows with rare and thin interpillow sediments that are hydrothermally altered and did not provide radiolarian assemblages. Between Playa Guarumo and Playa Carizal, several hundreds of meters of mostly massive tholeitic basalt organized in flows show some interlayered radiolarite successions. Most of the thinly bedded radiolarites occur as 1-3 m thick and 10-20 m long lenses set in a tectonized basaltic matrix. Also, sill-like basalt lenses occur within the thicker radiolarite sequences and show chilled margins. The first radiolarite occurrence east of Playa Guarumo seems to be floored by red chert interbedded with volcanic breccias and hyaloclastites that would indicate a stratigraphic contact on the Playa Guarumo basalt. Dark grey basalt in pillows, exceptionally vesicular, is rather rare and our geochemical raw data indicate no common origin with the alkaline basalts of Santa Rosa. At Playa Carrizal, a 30 m long and 6 m thick outcrop shows a distinctly wavy bedded radiolarite sequence ("knobby") that contains a black shale interval. One radiolarian assemblage from this area was previously described by De Wever et al. (1985, SE50) and provided a late Aptian-Albian age.

Baumgartner and Denyer (2006) described 8 tectonic units at Sitio Santa Rosa forming the Santa Rosa Accretionary Complex. They observed decimeter to meter wide intensive and roughly shear zones separating each unit from the other, and interpreted these units as being tectonically stacked and constituting part of an accretionary complex.

Unit 1. It is 100 m thick and includes at its base pillow basalts with minor basaltic breccias overlaid by ribbon-bedded radiolarite with soft sediment deformation.

Unit 2. It is a 300 m thick disorganized and poorly stratified polymictic breccias to megabreccias that include radiolaritic blocks of up to 10 m in size. De Wever et al. (1985) reported a radiolarian assemblage (SE 83) in radiolarite microbreccias of early Albian age, with older reworked specimens of Late Jurassic and Early Cretaceous age.

Unit 3. It is a 300 m thick unit dominated by thin-bedded radiolarite with interlayered alkaline basaltic sills with chilled margins, which overlies basaltic breccias and tuffaceous mudstone.

Unit 4. This is a 125 m thick chaotic breccia including among other decametric blocks of folded radiolarite and alkaline basalts. De Wever et al. (1985) dated one of these blocks (SE 85) yielding an Early Jurassic to early Middle Jurassic radiolarian assemblage.

Unit 5. It is a 100 m thick unit entirely composed of massive alkaline basalts.

Unit 6. This unit is 150 m thick and begins with centimeter bedded volcaniclastic turbidites interbedded with brown

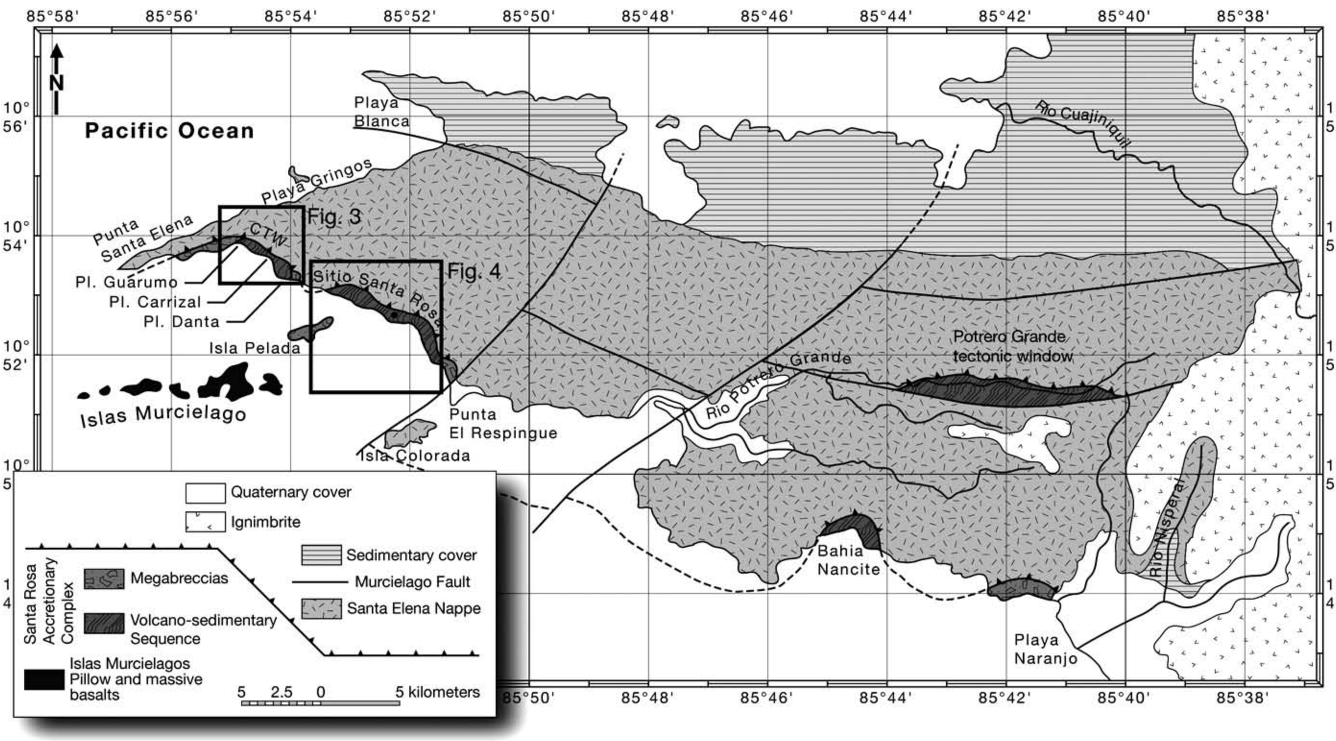

Fig. 2 - Geological map of the Santa Elena Peninsula, modified from Tournon (1994). Rectangles indicate the two sampled areas (see Figs. 3 and 4). CTW: Carrizal tectonic window.

siliceous mudstones and forming an upward coarsening sequence. It ends with metric to decametric strata of debris flows.

Unit 7. It is a 300 m thick unit with a base of radiolarites that grade upsection into grey tuffaceous mudstones and ending with decimetric debris flows truncated at its top by a megabreccia (decametric radiolaritic blocks in a polymictic boulder breccia). A radiolarite microbreccia from this unit yielded a radiolarian assemblage described by De Wever et al. (1985, SE 113). It provided a Barremian-Cenomanian age with several reworked specimens of Late Jurassic and Early Cretaceous age.

Unit 8. It is over 1 km thick and composed of a pile of layered flows of pillowed and massive alkaline basalts.

The Nancite Complex

The Nancite Complex consists of layered gabbros. It has been erroneously included with the Santa Elena Ultramafics by Gazel et al. (2006). According to Arias (2002) and our own field examination in 2007, the Nancite Complex is clearly exposed in a tectonic window beneath the main overthrust of the Santa Elena Nappe. Therefore, geochemical affinities between these two units cannot be regarded as evidence for a common geodynamic origin. Low TiO_2 contents and high LREE depletion suggest a primitive island arc origin for the Nancite Complex (Arias, 2002). Hauff et al. (2000) report a $^{40}Ar/^{39}Ar$ date of 124.0±4.0 Ma from the layered gabbros. Both the Nancite Complex and the Islas Murcielagos basalts have an age range that makes them approximately contemporaneous with the formation of the SRAC, suggesting a genetic relationship between these units. On-going geochemical analyses of arc-derived clasts sampled from SRAC breccias will confirm or invalidate this hypothesis.

The Santa Elena Nappe

The Santa Elena Ultramafics form a regional southwest-vergent overthrust, the Santa Elena Nappe, over the units discussed previously. It consists of depleted (MORB-like) serpentinized mantle peridiotites, with very low TiO_2 and high Ni and Cr contents. Crosscutting doleritic dykes represent a later phase with a geochemistry that suggests a primitive island arc origin (Gazel et al., 2006). Again, these dykes show geochemical similarities (Gazel et al., 2006) with the basaltic dykes cutting through the Nancite Complex located in the relative autochthonous beneath the Santa Elena Nappe, but this does not warrant for a genetic relationship between the two units. Moreover, the Santa Elena Ultramafics and the crosscutting dolerites are, so far, undated. Sr, Nd, and Pb isotopic ratios of the Santa Elena Nappe and the Santa Rosa Accretionary Complex samples do not correspond to the Galapagos Mantle array, and suggest different mantle reservoirs and geochemical characteristics than the CLIP and the Nicoya Complex. Of the above units, only the SRAC contains radiolarian-bearing sedimentary sequences further discussed below.

RADIOLARIAN BIOCHRONOLOGY

The dominant radiolarian-bearing lithologies of the studied samples are ribbon chert and siliceous mudstone. The procedure described by Bandini et al. (2008, p. 8) was used for radiolarian extractions. Apart from radiolarians, no other biogenic constituents were found in the residues. The following samples descriptions are given with coordinates (WGS 84, degrees) and are ordered from west to east, according to the distribution of tectonic units. They include descriptions of the outcrops, faunal content and biochronological ages. The remaining material and SEM stubs are stored in the collection of the Musée de Géologie de Lausanne, Université de Lausanne, Switzerland (MGL no. 97024-97042).

More than 50 samples were collected for radiolarian dating in the Santa Elena Peninsula, of which 19 yielded identifiable radiolarians (Figs. 3 and 4). The supraspecies taxonomy used in this study follows De Wever et al. (2001) and O'Dogherty et al. (2009a; 2009b). The radiolarian biostratigraphy is mainly based on the Early-early Middle Jurassic radiolarian zonation of Carter et al. (2010), the Middle Jurassic-Early Cretaceous zonation of the InterRad Jurassic-Cretaceous Working Group (Baumgartner et al., 1995b) and the middle Cretaceous zonation of O'Dogherty (1994). These zonations have been established using the Unitary Association method (Guex 1991). In total, 162 species, belonging to 65 genera were present in these samples, ranging in age from middle Early Jurassic to early Late Cretaceous (early Pliensbachian to earliest Turonian).

Carrizal tectonic window

This tectonic window comprises at least two separate sequences, each including a different facies of radiolarite: decimeter thick beds of radiolarite (samples CR-SE04, CR-SE05, CR-SE06, CR-SE07, CR-SE09, CR-SE10, and CR-SE11, Fig. 3) associated with tholeitic basalts between Playa Guarumo and Playa Carrizal; and a sequence of knobby radiolarite (samples POCR07-28, POCR07-31, POCR07-35, and POCR07-36, Fig. 3).

CR-SE10 and CR-SE11

Samples CR-SE10 and CR-SE11 (Fig. 5a) were collected in a 10 m sequence of ribbon cherts, which at their base seem to be interbedded with basaltic breccia and hyaloclastites that form the top of a thick sequence of basalt flows cropping out from Playa Guarumo to this locality. The sequence is topped by a sharp contact with the following basalt flow.

CR-SE10 (Table 1 and Plate 3) - In this radiolarian assemblage 3 species included in the zonations of Baumgartner et al. (1995b) and O'Dogherty (1994) were found. *Thanarla pulchra* (Squinabol) and *Acaeniotyle umbilicata* (Rüst) assign this assemblage to the late Berriasian to late Aptian interval.

CR-SE11 (Table 1 and Plate 4) - The species *Hiscocapsa uterculus* (Parona), *Pseudodictyomitra carpatica* gr. (Lozyniak), and *Thanarla brouweri* (Tan) are present in the zonation of O'Dogherty (1994) and indicate a range from UA 1 to 5 (latest Barremian to early Aptian).

CR-SE09

The sample CR-SE09 (Fig. 5b) is from near the base of a 10 to 15 m thick highly deformed radiolarite sequence. Chert ribbons are centimeter thick, mostly dark brown with brick-red (hydrothermally altered) intervals. Radiolarite is in irregular, probably intrusive contact with the surrounding basalt outcrops.

CR-SE09 (Table 2 and Plate 3) - Both species *Svinitzium kamoensis* (Mizutani and Kido) and *Zhamoidellum ventricosum*

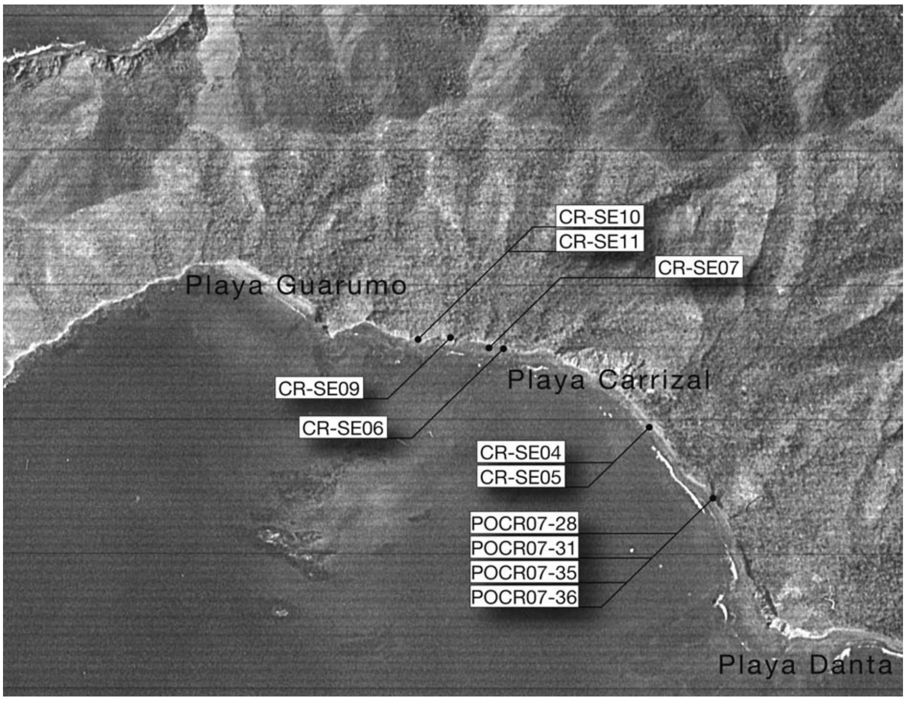

Fig. 3 - Position of the samples from the Carrizal tectonic window (Santa Rosa Accretionary Complex).

Table 1 - List of Early Cretaceous radiolarian species from samples CR-SE10 and CR-SE11 from the Carrizal tectonic window of the Santa Rosa Accretionary Complex with ranges from diagnostic species (see chapter on radiolarian biochronology).

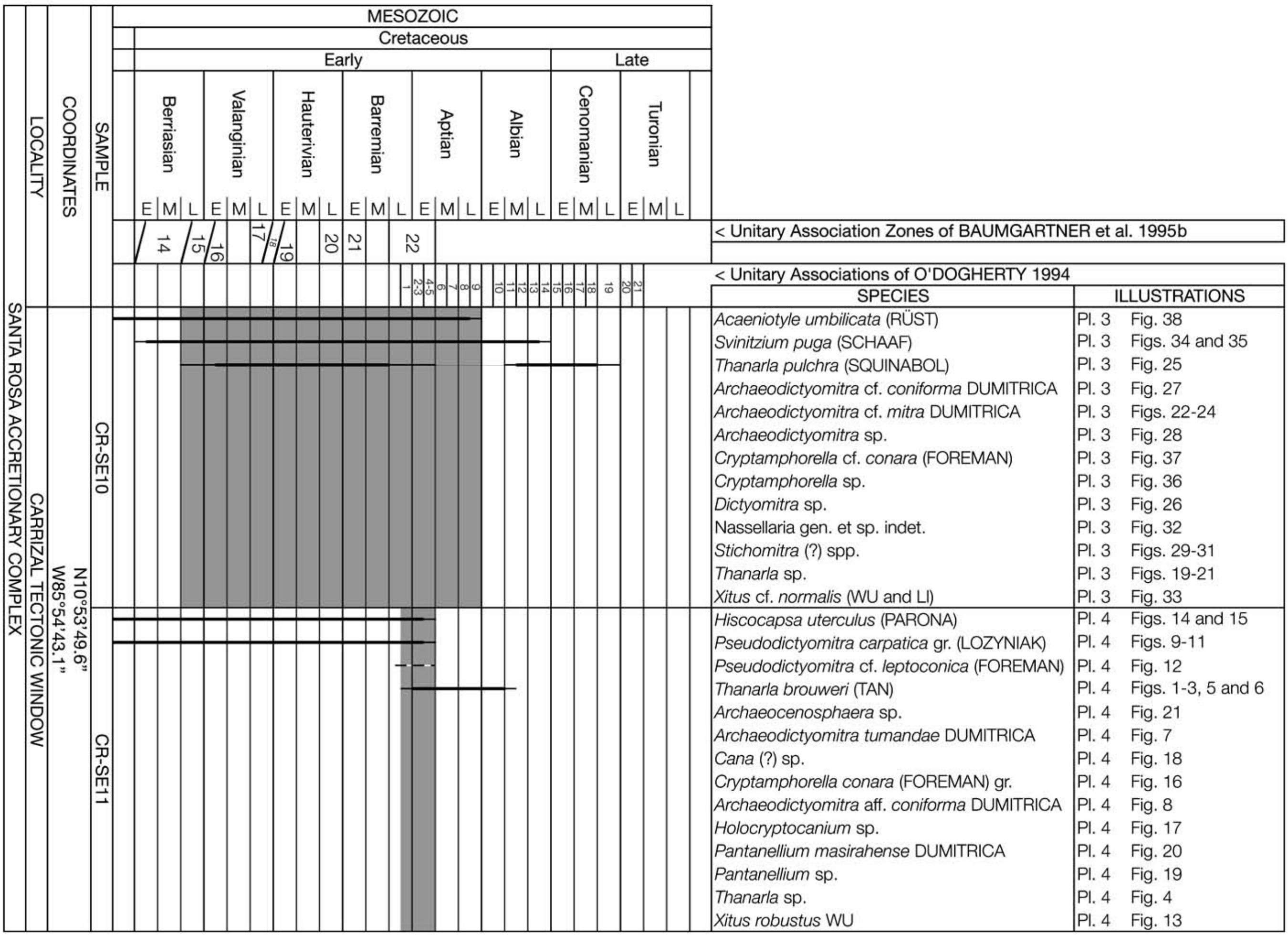

	LOCALITY	COORDINATES	SAMPLE	SPECIES	ILLUSTRATIONS
SANTA ROSA ACCRETIONARY COMPLEX	CARRIZAL TECTONIC WINDOW	N10°53'49.6" W85°54'43.1"	CR-SE10	*Acaeniotyle umbilicata* (RÜST)	Pl. 3 Fig. 38
				Svinitzium puga (SCHAAF)	Pl. 3 Figs. 34 and 35
				Thanarla pulchra (SQUINABOL)	Pl. 3 Fig. 25
				Archaeodictyomitra cf. *coniforma* DUMITRICA	Pl. 3 Fig. 27
				Archaeodictyomitra cf. *mitra* DUMITRICA	Pl. 3 Figs. 22-24
				Archaeodictyomitra sp.	Pl. 3 Fig. 28
				Cryptamphorella cf. *conara* (FOREMAN)	Pl. 3 Fig. 37
				Cryptamphorella sp.	Pl. 3 Fig. 36
				Dictyomitra sp.	Pl. 3 Fig. 26
				Nassellaria gen. et sp. indet.	Pl. 3 Fig. 32
				Stichomitra (?) spp.	Pl. 3 Figs. 29-31
				Thanarla sp.	Pl. 3 Figs. 19-21
				Xitus cf. *normalis* (WU and LI)	Pl. 3 Fig. 33
			CR-SE11	*Hiscocapsa uterculus* (PARONA)	Pl. 4 Figs. 14 and 15
				Pseudodictyomitra carpatica gr. (LOZYNIAK)	Pl. 4 Figs. 9-11
				Pseudodictyomitra cf. *leptoconica* (FOREMAN)	Pl. 4 Fig. 12
				Thanarla brouweri (TAN)	Pl. 4 Figs. 1-3, 5 and 6
				Archaeocenosphaera sp.	Pl. 4 Fig. 21
				Archaeodictyomitra tumandae DUMITRICA	Pl. 4 Fig. 7
				Cana (?) sp.	Pl. 4 Fig. 18
				Cryptamphorella conara (FOREMAN) gr.	Pl. 4 Fig. 16
				Archaeodictyomitra aff. *coniforma* DUMITRICA	Pl. 4 Fig. 8
				Holocryptocanium sp.	Pl. 4 Fig. 17
				Pantanellium masirahense DUMITRICA	Pl. 4 Fig. 20
				Pantanellium sp.	Pl. 4 Fig. 19
				Thanarla sp.	Pl. 4 Fig. 4
				Xitus robustus WU	Pl. 4 Fig. 13

Thin lines are used for first and last appearance intervals. Geographic coordinates are provided (WGS 84, degrees) (see also Figs. 2, 3, and 5a). The numbers correspond to those from Plates 3 and 4.

Table 2 - List of Middle to Late Jurassic radiolarian species from sample CR-SE09 from the Carrizal tectonic window of the Santa Rosa Accretionary Complex with ranges from diagnostic species (see chapter on radiolarian biochronology).

SANTA ROSA ACCRETIONARY COMPLEX	LOCALITY	COORDINATES	SAMPLE	SPECIES	ILLUSTRATIONS
SANTA ROSA ACCRETIONARY COMPLEX	CARRIZAL TECT. W.	N10°53'49.7" W85°54'39.8"	CR-SE09	*Praewilliriedellum convexum* (YAO)	Pl. 3 Figs. 15-18
				Svinitzium kamoensis (MIZUTANI and KIDO)	Pl. 3 Fig. 10
				Zhamoidellum ventricosum DUMITRICA	Pl. 3 Fig. 13
				Zhamoidellum aff. *ovum* DUMITRICA	Pl. 3 Fig. 14
				Archaeodictyomitra aff. *excellens* (TAN)	Pl. 3 Fig. 8
				Hsuum sp.	Pl. 3 Fig. 11
				Nassellaria gen. et sp. indet.	Pl. 3 Fig. 9
				Transhsuum sp.	Pl. 3 Fig. 12

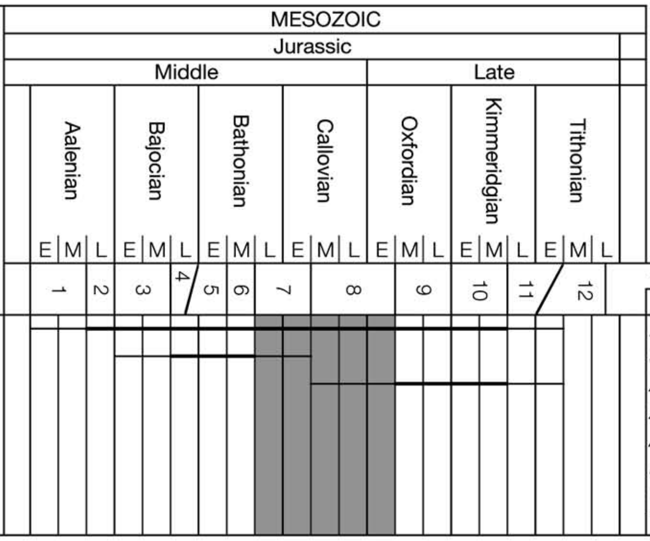

< Unitary Association Zones of BAUMGARTNER et al. 1995b

Thin lines are used for first and last appearance intervals. Geographic coordinates are provided (WGS 84, degrees) (see also Figs. 2, 3 and 5b). The numbers correspond to those from Plate 3.

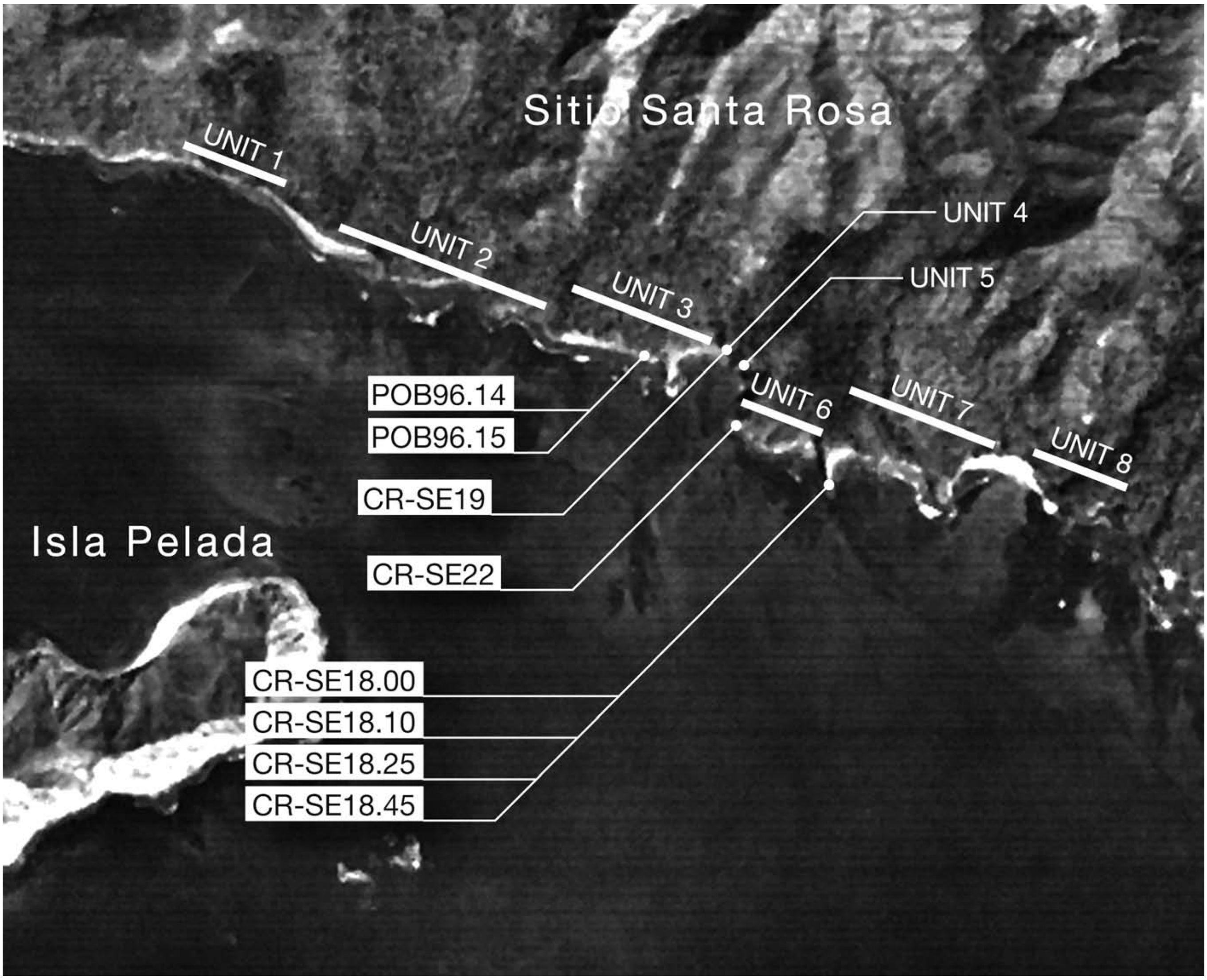

Fig. 4 - Units of the Santa Rosa Accretionary Complex (Baumgartner and Denyer, 2006) and position of the samples from the Sitio Santa Rosa tectonic window.

Fig. 5 - Outcrop photographs of the Santa Rosa Accretionary Complex (northwestern Costa Rica). Carrizal tectonic window: a) Ribbon cherts (late Berriasian to late Aptian interval), which seem to be interbedded with basaltic breccia (CR-SE10 and 11, N10°53'49.6'' W85°54'43.1''); b) Middle-early Late Jurassic (late Bathonian-early Callovian to middle Callovian-early Oxfordian) highly deformed radiolarite beds with centimeter thick ribbons, mostly dark brown with brick-red (hydrothermally altered) intervals (CR-SE09, N10°53'49.7'' W85°54'39.8''); c) Early Valanginian to late Aptian Knobby radiolarite (POCR07-31, 35, and 36, for localisation see Fig. 3); d) Late middle to late Aptian anoxic event (POCR07-28, for localisation see Fig. 3); e) Tight chevron folding at the top of the section of knobby radiolarites (for localisation see Fig. 3); Sitio Santa Rosa: f) Top of Unit 3 of Baumgartner and Denyer (2006), Pliensbachian to early Toarcian parallel-bedded ribbon chert with meter-thick sills (POB 96.14 and 96.15, for localisation see Fig. 4).

Dumitrica are present in the zonation proposed by Baumgartner et al. (1995b). *Svinitzium kamoensis* (Mizutani and Kido) (= *Dictyomitrella* (?) *kamoensis*, in Baumgartner et al., 1985) last appears in UAZ 7 (late Bathonian-early Callovian), and *Zhamoidellum ventricosum* Dumitrica first appears in UAZ 8 (middle Callovian-early Oxfordian). This assemblage could correspond to an interval ranging from UAZ 7 to 8 (late Bathonian-early Callovian to middle Callovian-early Oxfordian).

CR-SE06 and CR-SE07

Samples CR-SE06 and CR-SE07 are from an elongated, 2 m by 20 m size lense of red radiolarite embedded in sheared basalt.

CR-SE06 (Table 3 and Plate 2) - *Xitus spicularius* (Aliev) *sensu* O'Dogherty (1994) and *Svinitzium puga* (Schaaf) are present in the mid-Cretaceous zonation of O'Dogherty (1994) and corresponds to UA 6 to 14 of middle Aptian to late Albian age.

Table 3 - List of Early Cretaceous radiolarian species from samples CR-SE06 and CR-SE07 from the Carrizal tectonic window of the Santa Rosa Accretionary Complex with ranges from the diagnostic species (see chapter on radiolarian biochronology).

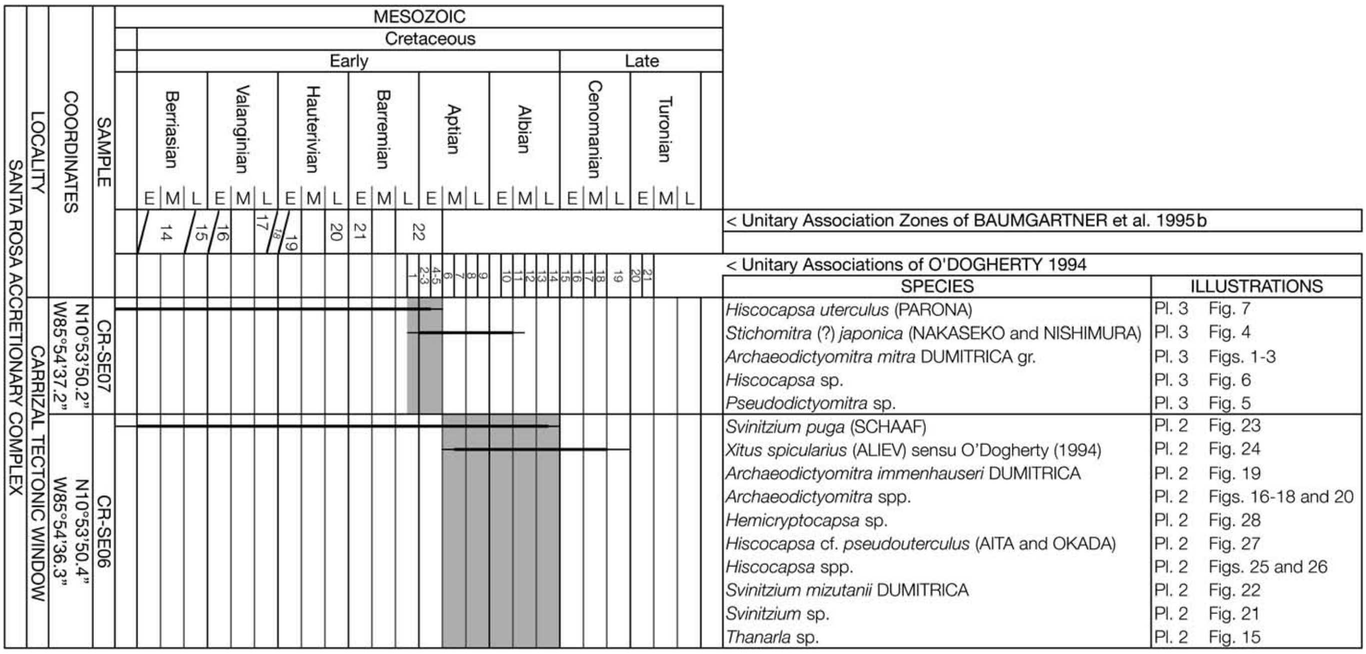

SANTA ROSA ACCRETIONARY COMPLEX	LOCALITY	COORDINATES	SAMPLE	SPECIES	ILLUSTRATIONS
SANTA ROSA ACCRETIONARY COMPLEX	CARRIZAL TECTONIC WINDOW	N10°53'50.2" W85°54'37.2"	CR-SE07	*Hiscocapsa uterculus* (PARONA)	Pl. 3 Fig. 7
				Stichomitra (?) *japonica* (NAKASEKO and NISHIMURA)	Pl. 3 Fig. 4
				Archaeodictyomitra mitra DUMITRICA gr.	Pl. 3 Figs. 1-3
				Hiscocapsa sp.	Pl. 3 Fig. 6
				Pseudodictyomitra sp.	Pl. 3 Fig. 5
		N10°53'50.4" W85°54'36.3"	CR-SE06	*Svinitzium puga* (SCHAAF)	Pl. 2 Fig. 23
				Xitus spicularius (ALIEV) sensu O'Dogherty (1994)	Pl. 2 Fig. 24
				Archaeodictyomitra immenhauseri DUMITRICA	Pl. 2 Fig. 19
				Archaeodictyomitra spp.	Pl. 2 Figs. 16-18 and 20
				Hemicryptocapsa sp.	Pl. 2 Fig. 28
				Hiscocapsa cf. *pseudouterculus* (AITA and OKADA)	Pl. 2 Fig. 27
				Hiscocapsa spp.	Pl. 2 Figs. 25 and 26
				Svinitzium mizutanii DUMITRICA	Pl. 2 Fig. 22
				Svinitzium sp.	Pl. 2 Fig. 21
				Thanarla sp.	Pl. 2 Fig. 15

Thin lines are used for first and last appearance intervals. Geographic coordinates are provided (WGS 84, degrees) (see also Figs. 2 and 3). The numbers correspond to those from Plates 2 and 3.

CR-SE07 (Table 3 and Plate 3) - The species *Hiscocapsa uterculus* (Parona) is present in the zonation of Baumgartner et al. (1995b) and ranges from UAZ 11 to 22 (late Kimmeridgian-early Tithonian to late Barremian-early Aptian). It is also present in the middle Cretaceous zonation proposed by O'Dogherty (1994) where it ranges from UA 1 (latest Barremian) to 5 (late early Aptian). The species *Stichomitra* (?) *japonica* (Nakaseko and Nishimura) is present in the zonation proposed by O'Dogherty (1994) and ranges from UA 1 (latest Barremian) to 11 (middle Albian). The illustrated assemblage could correspond to a latest Barremian-early Aptian interval. However, the first appearance of *Stichomitra* (?) *japonica* (Nakaseko and Nishimura) coincides with the lower limit of the O'Dogherty's zonation and thus, could be a little bit older.

CR-SE04 and CR-SE05

Samples CR-SE04 and CR-SE05 are from the same 2 m by 10 m radiolarite lens cropping out at low tide on the shore immediately below the megabreccia of the Santa Elena thrust and associated with blocks of massive basalt. Middle Jurassic radiolarite clasts (or blocks) seem to be reworked into late Early Cretaceous radiolarite.

CR-SE04 (Table 4 and Plate 1) - According to Baumgartner et al. (1995b), the presence of *Emiluvia nana* Baumgartner and *Tethysetta dhimenaensis* ssp. A *sensu* Baumgartner et al. (1995a) correspond to UAZ 6 to 8 of middle Bathonian-early Oxfordian age.

CR-SE05 (Table 4 and Plate 1 and 2) - According to O'Dogherty (1994), the co-occurence of *Pseudodictyomitra carpatica* gr. (Lozyniak) and *Stichomitra* (?) *communis* Squinabol corresponds to UA 5 of late early Aptian age.

Knobby radiolarite

Samples POCR07-28, POCR07-31, POCR07-35, and POCR07-36 (Fig. 5c-e) are from a 30 m long and 6 m high outcrop of mostly knobby radiolarite. The base of the outcrop above the beach gravel is characterized by 1 m of parallel-bedded cherts of greenish-greyish color, in the center of which a 30 cm thick black shale horizon with a central 10 cm thick black chert layer (POCR07-28, Fig. 5d) is visible. This interval could be related to an anoxic event. Brick red knobby cherts (POCR07- 31, 35 and 36, Fig. 5c) start about 1 m above the green chert. Since the whole outcrop is affected by isoclinal chevron folds (Fig. 5e), neither the polarity nor the stratigraphic sequence of the studied samples is clear.

The age of the radiolarian assemblages of this section coincide approximately with the upper limit of the zonation of Baumgartner et al. (1995b) and the lower limit of the zonation of O'Dogherty (1994) (late Barremian-early Aptian). Therefore we consider herein only the range of species that doesn't have their last appearance in the UAZ 22 of Baumgartner et al. (1995b) or their first appearance in the UA 1 of O'Dogherty (1994).

POCR07-28 (Table 5, Plate 5) - In this assemblage, seven species included in the zonation of O'Dogherty (1994) were found. The co-occurrence of *Hiscocapsa grutterinki* (Tan) and *Becus horridus* (Squinabol) assigns the assemblage to UA 7-9. The corresponding time interval ranges from late middle to late Aptian.

POCR07-31 (Table 5, Plate 6) - According to O'Dogherty (1994), the presence of *Archaeodictyomitra lacrimula* (Foreman) and *Stichomitra* (?) *communis* Squinabol corresponds to UA 5-6 of late early to early middle Aptian age.

POCR07-35 (Table 5, Plate 6) - The species *Pseudodictyomitra lanceloti* Schaaf assigns the lower limit of this assemblage to the UAZ 20 of Baumgartner et al. (1995b). The species *Thanarla pacifica* Nakaseko and Nishimura assigns the upper limit of this assemblage to the UA 6 of

Table 4 - List of Middle Jurassic to Early Cretaceous radiolarian species from samples CR-SE04 and CR-SE05 from the Carrizal tectonic window of the Santa Rosa Accretionary Complex with ranges from diagnostic species (see chapter on radiolarian biochronology).

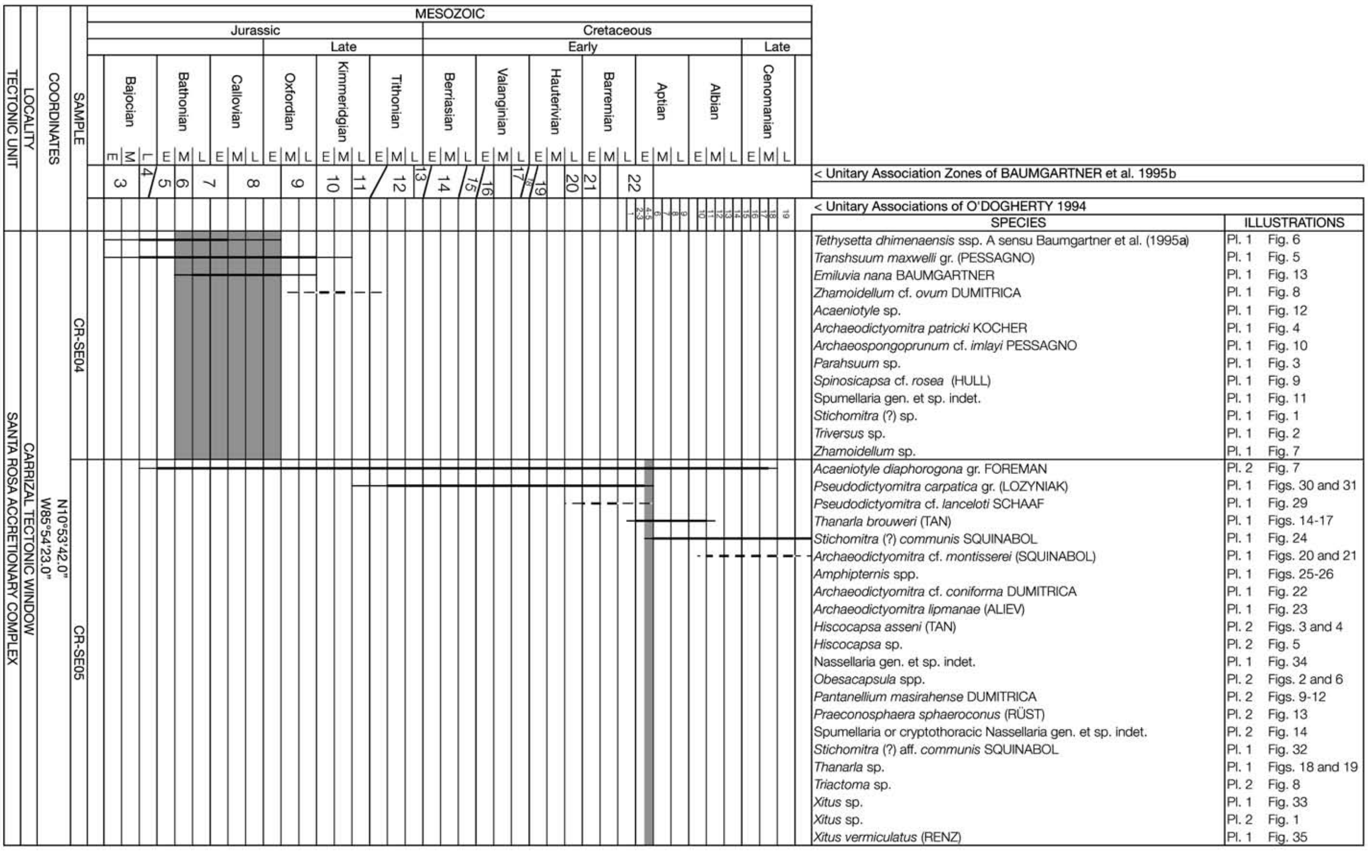

TECTONIC UNIT	LOCALITY	COORDINATES	SAMPLE	SPECIES	ILLUSTRATIONS
SANTA ROSA ACCRETIONARY COMPLEX	CARRIZAL TECTONIC WINDOW	N10°53'42.0" W85°54'23.0"	CR-SE04	*Tethysetta dhimenaensis* ssp. A sensu Baumgartner et al. (1995a)	Pl. 1 Fig. 6
				Transhsuum maxwelli gr. (PESSAGNO)	Pl. 1 Fig. 5
				Emiluvia nana BAUMGARTNER	Pl. 1 Fig. 13
				Zhamoidellum cf. *ovum* DUMITRICA	Pl. 1 Fig. 8
				Acaeniotyle sp.	Pl. 1 Fig. 12
				Archaeodictyomitra patricki KOCHER	Pl. 1 Fig. 4
				Archaeospongoprunum cf. *imlayi* PESSAGNO	Pl. 1 Fig. 10
				Parahsuum sp.	Pl. 1 Fig. 3
				Spinosicapsa cf. *rosea* (HULL)	Pl. 1 Fig. 9
				Spumellaria gen. et sp. indet.	Pl. 1 Fig. 11
				Stichomitra (?) sp.	Pl. 1 Fig. 1
				Triversus sp.	Pl. 1 Fig. 2
				Zhamoidellum sp.	Pl. 1 Fig. 7
			CR-SE05	*Acaeniotyle diaphorogona* gr. FOREMAN	Pl. 2 Fig. 7
				Pseudodictyomitra carpatica gr. (LOZYNIAK)	Pl. 1 Figs. 30 and 31
				Pseudodictyomitra cf. *lanceloti* SCHAAF	Pl. 1 Fig. 29
				Thanarla brouweri (TAN)	Pl. 1 Figs. 14-17
				Stichomitra (?) *communis* SQUINABOL	Pl. 1 Fig. 24
				Archaeodictyomitra cf. *montisserei* (SQUINABOL)	Pl. 1 Figs. 20 and 21
				Amphipternis spp.	Pl. 1 Figs. 25-26
				Archaeodictyomitra cf. *coniforma* DUMITRICA	Pl. 1 Fig. 22
				Archaeodictyomitra lipmanae (ALIEV)	Pl. 1 Fig. 23
				Hiscocapsa asseni (TAN)	Pl. 2 Figs. 3 and 4
				Hiscocapsa sp.	Pl. 2 Fig. 5
				Nassellaria gen. et sp. indet.	Pl. 1 Fig. 34
				Obesacapsula spp.	Pl. 2 Figs. 2 and 6
				Pantanellium masirahense DUMITRICA	Pl. 2 Figs. 9-12
				Praeconosphaera sphaeroconus (RÜST)	Pl. 2 Fig. 13
				Spumellaria or cryptothoracic Nassellaria gen. et sp. indet.	Pl. 2 Fig. 14
				Stichomitra (?) aff. *communis* SQUINABOL	Pl. 1 Fig. 32
				Thanarla sp.	Pl. 1 Figs. 18 and 19
				Triactoma sp.	Pl. 2 Fig. 8
				Xitus sp.	Pl. 1 Fig. 33
				Xitus sp.	Pl. 2 Fig. 1
				Xitus vermiculatus (RENZ)	Pl. 1 Fig. 35

Thin lines are used for first and last appearance intervals and dashed lines for ranges of uncertain determination species ("cf."). Geographic coordinates are provided (WGS 84, degrees) (see also Figs. 2 and 3). The numbers correspond to those from Plates 1 and 2.

O'Dogherty (1994). The corresponding time interval ranges from late Hauterivian to early middle Aptian.

POCR07-36 (Table 5, Plate 7) - The presences of *Hiscocapsa uterculus* (Parona), *Pseudodictyomitra carpatica* gr. (Lozyniak), and *Crucella bossoensis* Jud assign this assemblage to the UAZ 16 of Baumgartner et al. (1995b) to UAZ 5 of O'Dogherty (1994) of early Valanginian to early Aptian age.

Sitio Santa Rosa Tectonic window

This tectonic window comprises 8 units described by Baumgartner and Denyer (2006, see Geological Setting, Figs. 4 and 5).

Unit 3 (POB96.14 and POB96.15)

Samples POB96.14 and POB96.15 (Fig. 5f) were collected near the top of Unit 3 (Baumgartner and Denyer, 2006), in a thinly parallel-bedded ribbon chert between two meter-thick alkaline sills. Geopetal infills in radiolarians show that the stratigraphic top of the vertically dipping section is constantly to the east. This can be confirmed by the ages found in the two studied samples separated by 5.5 m, which come from the topmost 20 m of a radiolarite section that was more than 100 m thick even before the intrusion of the sills. The base of this sedimentary sequence could be considerably older than the late Early Jurassic ages determined at its top.

POB96.14 (Table 6 and Plate 8) - In this assemblage, seven species included in the zonation of Carter et al. (2010) assign the assemblage to the UA 5 to 21, Pliensbachian in age.

POB96.15 (Table 6 and Plate 9) - In this assemblage, six species are included in the zonation of Carter et al. (2010). *Eucyrtidiellum disparile* gr. Nagai and Mizutani and *Katroma bicornus* De Wever assign the assemblage to the UA 24 to 26, of early Toarcian age.

Unit 4 (CR-SE19)

Sample CR-SE 19 (Fig. 6a) was collected in Unit 4 caracterized by chaotic mélange of radiolarite and alkaline basalt blocks set in a polymictic green breccia including arc-derived basalts. The studied sample is from the same block as the Early Jurassic sample SE85 of De Wever et al. (1985).

CR-SE19 (Table 7 and Plate 10) - In this assemblage, four species included in the zonation of Carter et al. (2010) were found. *Cyclastrum asuncionense* Whalen and Carter and *Paleosaturnalis tetraradiatus* (Kozur and Mostler) assign the assemblage to the UA 2 to 4, early-middle Pliensbachian in age.

Unit 6 (CR-SE22)

The sample CR-SE22 comes from the base of the trench fill Unit 6.

Table 5 - List of Middle Jurassic to Late Cretaceous radiolarian species from samples POCR07-28, 31, 35, and 36 from the Carrizal tectonic window (see also Figs. 2, 3, and 5c-e) of the Santa Rosa Accretionary Complex with ranges from diagnostic species (see chapter on radiolarian biochronology).

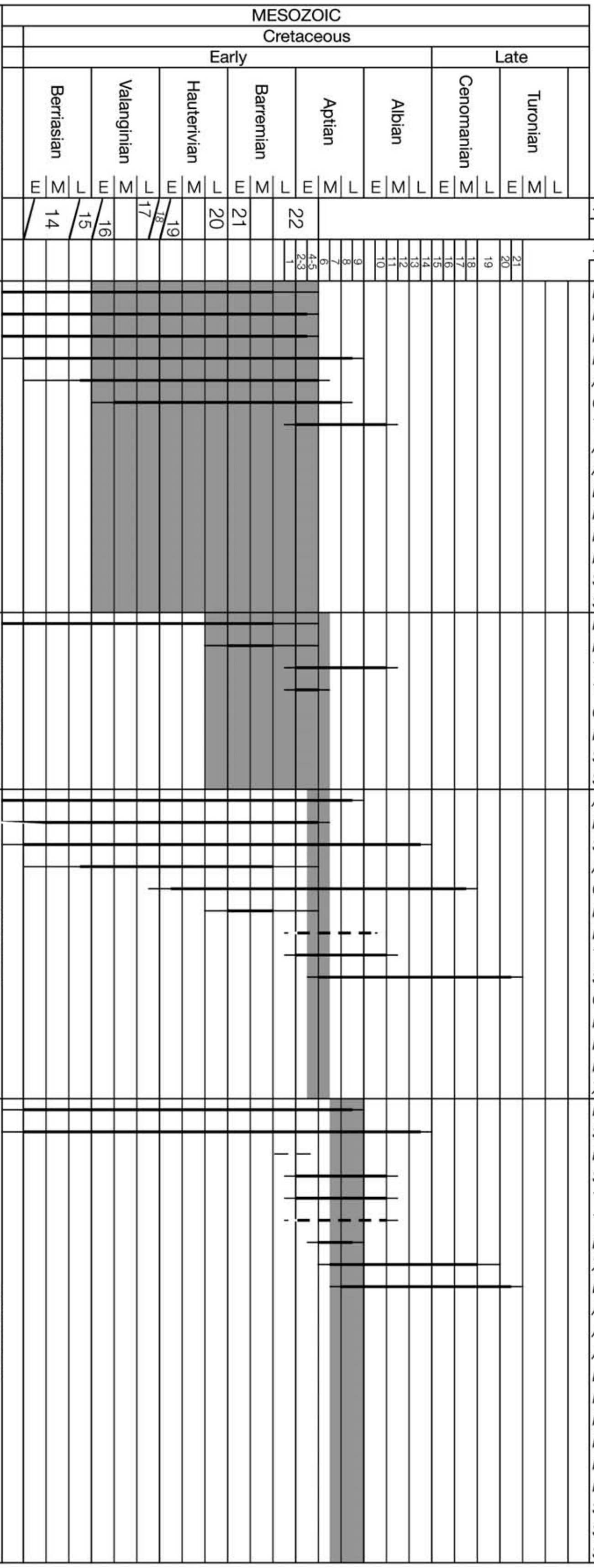

< Unitary Association Zones of BAUMGARTNER et al. 1995b

< Unitary Associations of O'DOGHERTY 1994

LOCALITY	SAMPLE	SPECIES	ILLUSTRATIONS
SANTA ROSA ACCRETIONARY COMPLEX CARRIZAL TECTONIC WINDOW (KNOBBY RADIOLARITE)	POCR07-36	*Pantanellium squinaboli* (TAN)	Pl. 7 Figs. 14-16
		Hiscocapsa uterculus (PARONA)	Pl. 7 Fig. 8
		Pseudodictyomitra carpatica gr. (LOZYNIAK)	Pl. 7 Fig. 6
		Hiscocapsa grutterinki (TAN)	Pl. 7 Fig. 9
		Archaeodictyomitra lacrimula (FOREMAN)	Pl. 7 Fig. 3
		Crucella bossoensis JUD	Pl. 7 Fig. 18
		Thanarla brouweri (TAN)	Pl. 7 Figs. 1 and 2
		Alievium regulare (WU and LI)	Pl. 7 Figs. 10-12
		Archaeospongoprunum sp.	Pl. 7 Fig. 20
		Dicroa sp.	Pl. 7 Fig. 13
		Pantanellium masirahense DUMITRICA	Pl. 7 Fig. 17
		Praeconosphaera sphaeroconus (RÜST)	Pl. 7 Fig. 19
		Pseudodictyomitra sp.	Pl. 7 Fig. 5
		Spinosicapsa (?) sp.	Pl. 7 Fig. 7
		Stichomitra (?) sp.	Pl. 7 Fig. 4
	POCR07-35	*Pantanellium squinaboli* (TAN)	Pl. 6 Fig. 24
		Pseudodictyomitra lanceloti SCHAAF	Pl. 6 Fig. 20
		Thanarla brouweri (TAN)	Pl. 6 Fig. 17
		Thanarla pacifica NAKASEKO and NISHIMURA	Pl. 6 Fig. 18
		Cryptamphorella conara (FOREMAN) gr.	Pl. 6 Fig. 23
		Pseudodictyomitra aff. *carpatica* gr. (LOZYNIAK)	Pl. 6 Fig. 19
		Spinosicapsa sp.	Pl. 6 Fig. 22
		Spinosicapsa typica (RÜST)	Pl. 6 Fig. 21
	POCR07-31	*Acaeniotyle umbilicata* (RÜST)	Pl. 6 Fig. 11
		Pantanellium squinaboli (TAN)	Pl. 6 Fig. 12
		Svinitzium puga (SCHAAF)	Pl. 6 Fig. 7
		Archaeodictyomitra lacrimula (FOREMAN)	Pl. 6 Fig. 9
		Godia coronata (TUMANDA)	Pl. 6 Fig. 16
		Pseudodictyomitra lanceloti SCHAAF	Pl. 6 Fig. 6
		Hiscocapsa cf. *asseni* (TAN)	Pl. 6 Fig. 8
		Thanarla brouweri (TAN)	Pl. 6 Figs. 1 and 2
		Stichomitra (?) *communis* SQUINABOL	Pl. 6 Figs. 3 and 4
		Crucella sp.	Pl. 6 Fig. 14
		Pantanellium sp.	Pl. 6 Fig. 13
		Praeconosphaera sphaeroconus (RÜST)	Pl. 6 Fig. 15
		Pseudodictyomitra cf. *nodocostata* DUMITRICA	Pl. 6 Fig. 5
		Xitus sp.	Pl. 6 Fig. 10
	POCR07-28	*Hiscocapsa grutterinki* (TAN)	Pl. 5 Fig. 21
		Svinitzium puga (SCHAAF)	Pl. 5 Fig. 9
		Pseudodictyomitra cf. *leptoconica* (FOREMAN)	Pl. 5 Figs. 8 and 10
		Stichomitra (?) *japonica* (NAKASEKO and NISHIMURA)	Pl. 5 Fig. 13
		Thanarla brouweri (TAN)	Pl. 5 Figs. 2 and 4
		Thanarla cf. *brouweri* (TAN)	Pl. 5 Fig. 3
		Pseudodictyomitra lodogaensis PESSAGNO	Pl. 5 Fig. 11
		Xitus spicularius (ALIEV) sensu O'Dogherty (1994)	Pl. 5 Figs. 16-18
		Becus horridus (SQUINABOL)	Pl. 5 Fig. 23
		Archaeodictyomitra leptocostata (WU and LI)	Pl. 5 Fig. 7
		Archaeodictyomitra mitra DUMITRICA	Pl. 5 Fig. 5
		Archaeodictyomitra sp.	Pl. 5 Fig. 1
		Dictyomitra sp.	Pl. 5 Fig. 6
		Holocryptocanium sp.	Pl. 5 Fig. 22
		Pantanellium cf. *masirahense* DUMITRICA	Pl. 5 Figs. 24-26
		Praeconocaryomma sp.	Pl. 5 Fig. 27
		Praeconosphaera sp.	Pl. 5 Figs. 28 and 29
		Praexitus cf. *verrucosus* DUMITRICA	Pl. 5 Fig. 19
		Stichomitra (?) cf. *stocki* (CAMPBELL and CLARK)	Pl. 5 Fig. 14
		Stichomitra (?) spp.	Pl. 5 Figs. 12 and 15
		Svinitzium aff. *mizutani* DUMITRICA	Pl. 5 Fig. 20

Thin lines are used for first and last appearance intervals and dashed lines for ranges of uncertain determination species ("cf."). The numbers correspond to those from Plates 5, 6, and 7.

Table 6 - List of Early Jurassic radiolarian species from samples POB96.14 and .15 from the Sitio Santa Rosa tectonic window (see also Figs. 2, 4, and 5f) of the Santa Rosa Accretionary Complex with ranges from diagnostic species (see chapter on radiolarian biochronology).

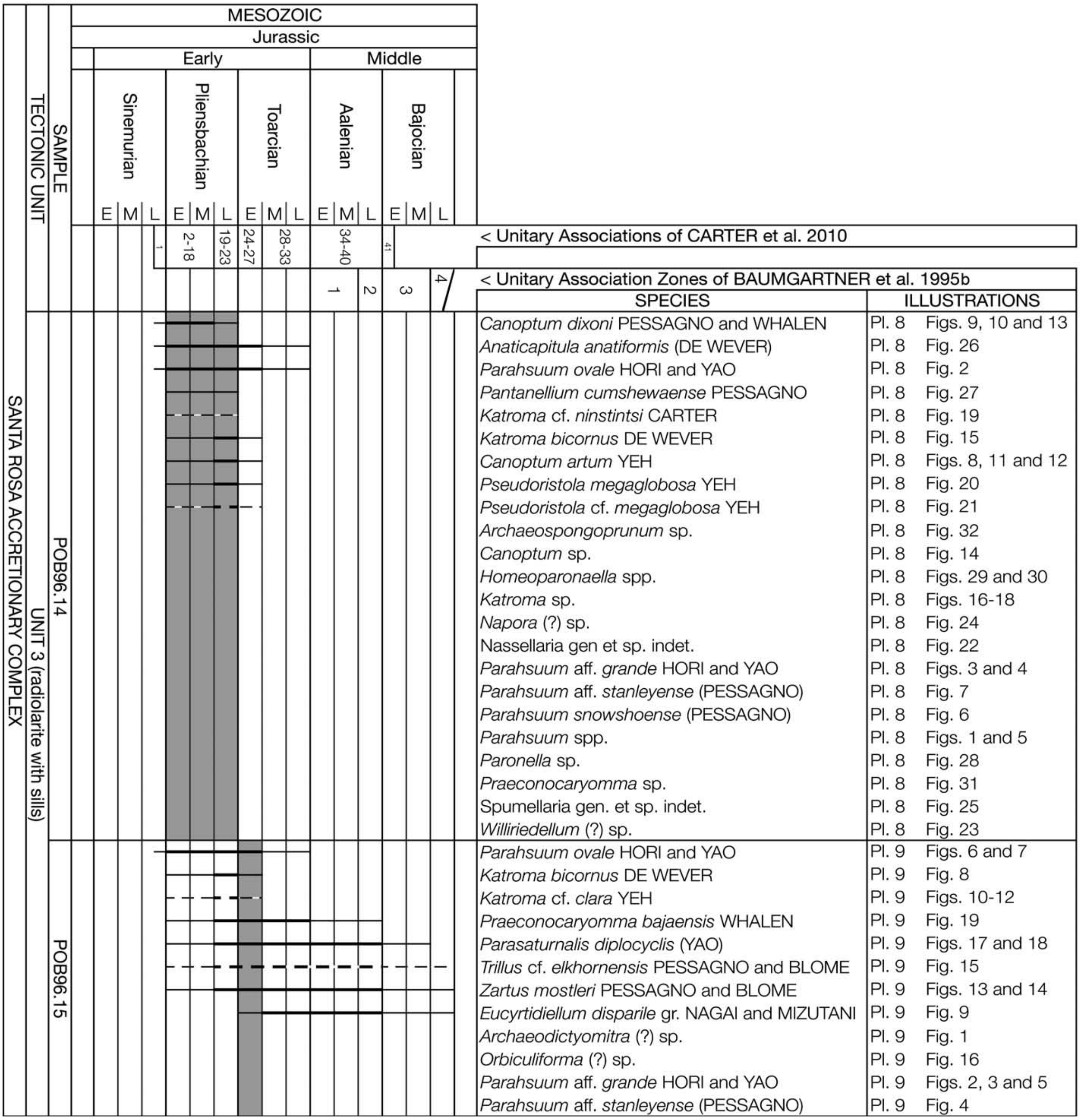

SPECIES	ILLUSTRATIONS
Canoptum dixoni PESSAGNO and WHALEN	Pl. 8 Figs. 9, 10 and 13
Anaticapitula anatiformis (DE WEVER)	Pl. 8 Fig. 26
Parahsuum ovale HORI and YAO	Pl. 8 Fig. 2
Pantanellium cumshewaense PESSAGNO	Pl. 8 Fig. 27
Katroma cf. *ninstintsi* CARTER	Pl. 8 Fig. 19
Katroma bicornus DE WEVER	Pl. 8 Fig. 15
Canoptum artum YEH	Pl. 8 Figs. 8, 11 and 12
Pseudoristola megaglobosa YEH	Pl. 8 Fig. 20
Pseudoristola cf. *megaglobosa* YEH	Pl. 8 Fig. 21
Archaeospongoprunum sp.	Pl. 8 Fig. 32
Canoptum sp.	Pl. 8 Fig. 14
Homeoparonaella spp.	Pl. 8 Figs. 29 and 30
Katroma sp.	Pl. 8 Figs. 16-18
Napora (?) sp.	Pl. 8 Fig. 24
Nassellaria gen et sp. indet.	Pl. 8 Fig. 22
Parahsuum aff. *grande* HORI and YAO	Pl. 8 Figs. 3 and 4
Parahsuum aff. *stanleyense* (PESSAGNO)	Pl. 8 Fig. 7
Parahsuum snowshoense (PESSAGNO)	Pl. 8 Fig. 6
Parahsuum spp.	Pl. 8 Figs. 1 and 5
Paronella sp.	Pl. 8 Fig. 28
Praeconocaryomma sp.	Pl. 8 Fig. 31
Spumellaria gen. et sp. indet.	Pl. 8 Fig. 25
Williriedellum (?) sp.	Pl. 8 Fig. 23
Parahsuum ovale HORI and YAO	Pl. 9 Figs. 6 and 7
Katroma bicornus DE WEVER	Pl. 9 Fig. 8
Katroma cf. *clara* YEH	Pl. 9 Figs. 10-12
Praeconocaryomma bajaensis WHALEN	Pl. 9 Fig. 19
Parasaturnalis diplocyclis (YAO)	Pl. 9 Figs. 17 and 18
Trillus cf. *elkhornensis* PESSAGNO and BLOME	Pl. 9 Fig. 15
Zartus mostleri PESSAGNO and BLOME	Pl. 9 Figs. 13 and 14
Eucyrtidiellum disparile gr. NAGAI and MIZUTANI	Pl. 9 Fig. 9
Archaeodictyomitra (?) sp.	Pl. 9 Fig. 1
Orbiculiforma (?) sp.	Pl. 9 Fig. 16
Parahsuum aff. *grande* HORI and YAO	Pl. 9 Figs. 2, 3 and 5
Parahsuum aff. *stanleyense* (PESSAGNO)	Pl. 9 Fig. 4

Thin lines are used for first and last appearance intervals and dashed lines for ranges of uncertain determination species ("cf."). The numbers correspond to those from Plates 8 and 9.

CR-SE22 (Table 8 and Plate 11) - The presence of *Stichomitra* (?) *tosaensis* (Nakaseko and Nishimura), *Archaeodictyomitra montisserei* (Squinabol), *Rhopalosyringium mosquense* (Smirnova and Aliev), *Pseudodictyomitra pseudomacrocephala* (Squinabol), and *Archaeodictyomitra undata* (Squinabol) are present in the zonation of O'Dogherty (1994) and assign this assemblage to the UA 10 to 21 interval of late early Albian to late early Turonian age.

Unit 7 (CR-SE18.00, CR-SE18.10, CR-SE18.25, and CR-SE18.45)

Unit 7 of Baumgartner and Denyer (2006) is an intact stratigraphic sequence that documents the drift of the sedimentation site from a pelagic open ocean paleoenvironment into the trench (Fig. 6b - f). The lowermost (western) 40 m of the vertically dipping section are made of red ribbon radiolarites (Fig. 6b) that grade upsection into less and less bedded

Fig. 6 - Outcrop photographs of the Santa Rosa Accretionary Complex (northwestern Costa Rica). Sitio Santa Rosa: a) Unit 4 of Baumgartner and Denyer (2006), early-middle Pliensbachian thin bedded and deformed cherts block in a chaotic mélange of radiolarite and alkaline basalt blocks set in a polymictic green breccia including arc-derived basalts (CR-SE19, N10°52'53.4'' W85°52'39.3''); Unit 7 (see also Fig. 7): b) Late early to early middle Albian radiolarites at Punta Roja (samples CR-SE18.00, 18.10, 18.25, and 18.45, N10°52'42.2'' W85°52'29.1''); c) Overlying the radiolarites the first dm-thick sandy to muddy turbidites beds interbedded with siliceous mudstone; d) Sandy turbidites; e) Metric pebble to cobble beds interpreted as debris flows; f) Megabreccia containing blocks of up to 10-20 m size of radiolarites set in a matrix of green radiolarite-basalt breccia.

brown siliceous mudstones. At 45 m above the base, the first dm-thick sandy to muddy turbidites are interbedded with the siliceous mudstone (Fig. 6c) that gradually change color to greenish gray due to the increase of volcanic (arc-derived?) mud. Sandy turbidites (Fig. 6d) grade upsection to metric pebble to cobble beds interpreted as debris flows (Fig. 6e). At about 125 m above the base, an erosional unconformity separates the stratified section from a megabreccia that contains blocks of up to 10-20 m size of radiolarites set in a matrix of green radiolarite-basalt breccia (Fig. 6f). The studied samples are from the first 34 m of pelagic to hemipelagic section that includes the first turbidites.

CR-SE18.00 (base of the section, Table 9 and Plate 12) - The occurrence of *Crolanium spineum* (Pessagno), also present in the zonation of O'Dogherty (1994), indicates a late early Albian to early Cenomanian (UA 10 to 15) age without

Table 7 - List of Early Jurassic radiolarian species from sample CR-SE19 from the Sitio Santa Rosa tectonic window (see also Figs. 2, 4, and 6a) of the Santa Rosa Accretionary Complex with ranges from diagnostic species (see chapter on radiolarian biochronology).

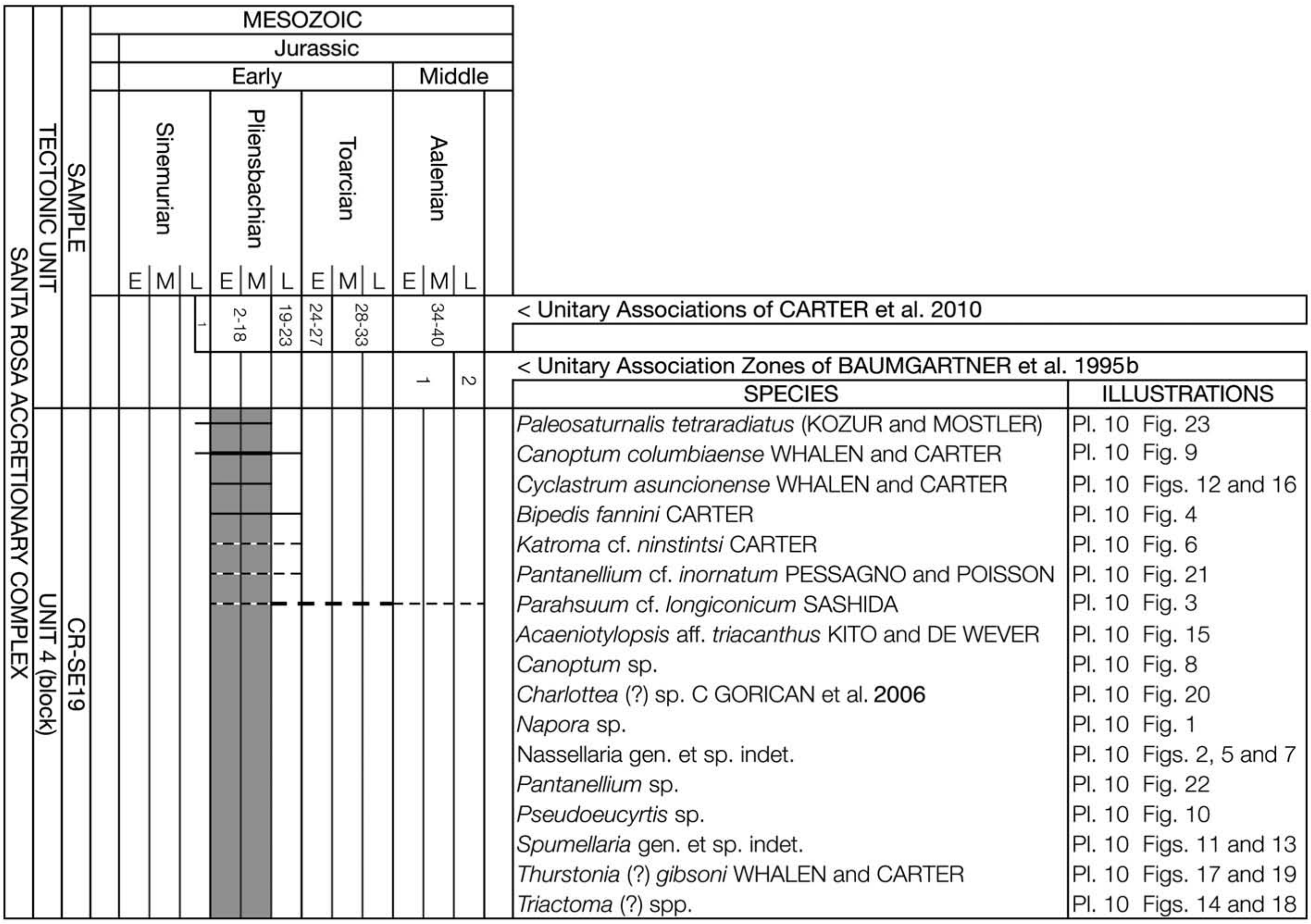

SPECIES	ILLUSTRATIONS
Paleosaturnalis tetraradiatus (KOZUR and MOSTLER)	Pl. 10 Fig. 23
Canoptum columbiaense WHALEN and CARTER	Pl. 10 Fig. 9
Cyclastrum asuncionense WHALEN and CARTER	Pl. 10 Figs. 12 and 16
Bipedis fannini CARTER	Pl. 10 Fig. 4
Katroma cf. *ninstintsi* CARTER	Pl. 10 Fig. 6
Pantanellium cf. *inornatum* PESSAGNO and POISSON	Pl. 10 Fig. 21
Parahsuum cf. *longiconicum* SASHIDA	Pl. 10 Fig. 3
Acaeniotylopsis aff. *triacanthus* KITO and DE WEVER	Pl. 10 Fig. 15
Canoptum sp.	Pl. 10 Fig. 8
Charlottea (?) sp. C GORICAN et al. **2006**	Pl. 10 Fig. 20
Napora sp.	Pl. 10 Fig. 1
Nassellaria gen. et sp. indet.	Pl. 10 Figs. 2, 5 and 7
Pantanellium sp.	Pl. 10 Fig. 22
Pseudoeucyrtis sp.	Pl. 10 Fig. 10
Spumellaria gen. et sp. indet.	Pl. 10 Figs. 11 and 13
Thurstonia (?) *gibsoni* WHALEN and CARTER	Pl. 10 Figs. 17 and 19
Triactoma (?) spp.	Pl. 10 Figs. 14 and 18

Thin lines are used for first and last appearance intervals and dashed lines for ranges of uncertain determination species ("cf."). The numbers correspond to those from Plate 10.

further precision. However, it seems to be restricted to the late early to early middle Albian interval by stratigraphic superposition with sample CR-SE18.45 (see below).

CR-SE18.10 (10 m above base, Table 9 and Plate 12) - The species *Pseudodictyomitra pentacolaensis* Pessagno and *Pseudodictyomitra pseudomacrocephala* (Squinabol) are present in the middle Cretaceous zonation proposed by O'Dogherty (1994) and are correlative of UA 10 (late early Albian) to 19 (late Cenomanian). However, this interval seems to be restricted to the late early to early middle Albian by stratigraphic superposition with sample CR-SE18.45 (see below).

CR-SE18.25 (25 m above base, Table 9 and Plate 12) - The co-occurrence of *Xitus spicularius* (Aliev) *sensu* O'Dogherty (1994) and *Pseudodictyomitra pseudomacrocephala* (Squinabol), also present in the zonation of O'Dogherty (1994), indicates a late early Albian to late Cenomanian (UA 10 to 19) age without further precision. However, the age of this sample seems to be restricted to the late early to early middle Albian interval by stratigraphic superposition with sample CR-SE18.45 (see below).

CR-SE18.45 (45 m above base, Table 9 and Plate 13) - In this assemblage, three species are included in the zonation of O'Dogherty (1994). *Thanarla brouweri* (Tan) and *Pseudodictyomitra paronai* (Aliev) assign the assemblage to the late early Albian to early middle Albian age (UA 10 to 11).

DISCUSSION OF RESULTS

Carrizal tectonic window

Radiolarite associated with tholeitic basalts

Two different age groups could be determined from radiolarites located between Playa Guarumo and Playa Carrizal (Table 10):

1. Middle to early Late Jurassic ages (middle Bathonian to middle Callovian-early Oxfordian) were found in meter to decameter-sited blocks that are in tectonic and/or intrusive contact with massive, tholeitic basalts.

2. Early Cretaceous ages (total possible range is late Berriasian-earliest Valanginian to late Albian, but more probably Barremian-Albian) were recovered from radiolarite sequences that seem to be, at least in some places, in sedimentary contact with underlying flows.

In contrast with the Santa Rosa units, no detrital sediments were found in the Carrizal tectonic window. We interpret this

Table 8 - List of Early to Late Cretaceous radiolarian species from sample CR-SE22 from the Sitio Santa Rosa tectonic window of the Santa Rosa Accretionary Complex with ranges from diagnostic species (see chapter on radiolarian biochronology).

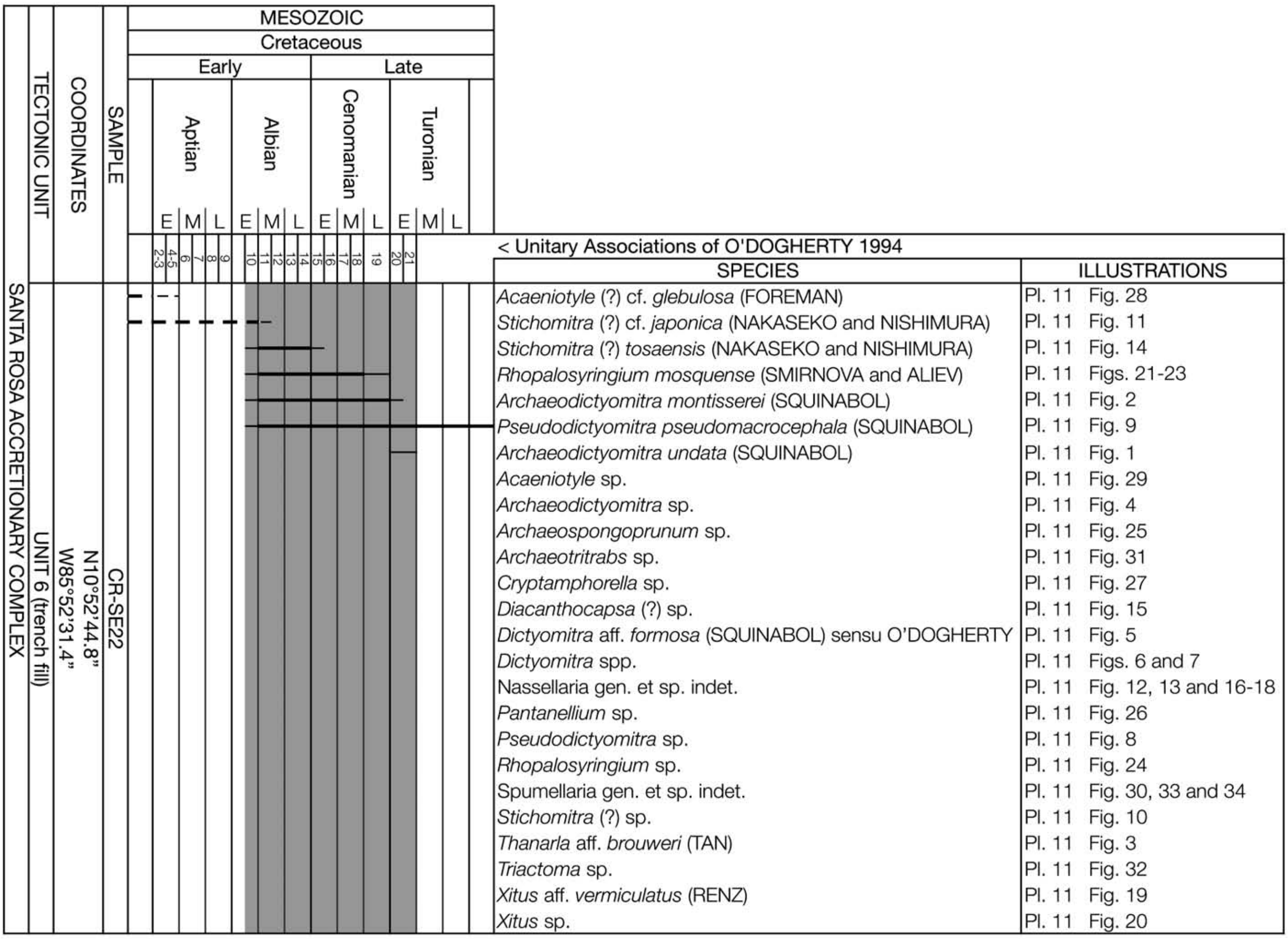

TECTONIC UNIT	COORDINATES	SAMPLE	SPECIES	ILLUSTRATIONS
SANTA ROSA ACCRETIONARY COMPLEX UNIT 6 (trench fill)	N10°52'44.8" W85°52'31.4"	CR-SE22	*Acaeniotyle* (?) cf. *glebulosa* (FOREMAN)	Pl. 11 Fig. 28
			Stichomitra (?) cf. *japonica* (NAKASEKO and NISHIMURA)	Pl. 11 Fig. 11
			Stichomitra (?) *tosaensis* (NAKASEKO and NISHIMURA)	Pl. 11 Fig. 14
			Rhopalosyringium mosquense (SMIRNOVA and ALIEV)	Pl. 11 Figs. 21-23
			Archaeodictyomitra montisserei (SQUINABOL)	Pl. 11 Fig. 2
			Pseudodictyomitra pseudomacrocephala (SQUINABOL)	Pl. 11 Fig. 9
			Archaeodictyomitra undata (SQUINABOL)	Pl. 11 Fig. 1
			Acaeniotyle sp.	Pl. 11 Fig. 29
			Archaeodictyomitra sp.	Pl. 11 Fig. 4
			Archaeospongoprunum sp.	Pl. 11 Fig. 25
			Archaeotritrabs sp.	Pl. 11 Fig. 31
			Cryptamphorella sp.	Pl. 11 Fig. 27
			Diacanthocapsa (?) sp.	Pl. 11 Fig. 15
			Dictyomitra aff. *formosa* (SQUINABOL) sensu O'DOGHERTY	Pl. 11 Fig. 5
			Dictyomitra spp.	Pl. 11 Figs. 6 and 7
			Nassellaria gen. et sp. indet.	Pl. 11 Fig. 12, 13 and 16-18
			Pantanellium sp.	Pl. 11 Fig. 26
			Pseudodictyomitra sp.	Pl. 11 Fig. 8
			Rhopalosyringium sp.	Pl. 11 Fig. 24
			Spumellaria gen. et sp. indet.	Pl. 11 Fig. 30, 33 and 34
			Stichomitra (?) sp.	Pl. 11 Fig. 10
			Thanarla aff. *brouweri* (TAN)	Pl. 11 Fig. 3
			Triactoma sp.	Pl. 11 Fig. 32
			Xitus aff. *vermiculatus* (RENZ)	Pl. 11 Fig. 19
			Xitus sp.	Pl. 11 Fig. 20

Geographic coordinates are provided (WGS 84, degrees) (see also Figs. 2 and 4). Thin lines are used for first and last appearance intervals and dashed lines for ranges of uncertain determination species ("cf."). The numbers correspond to those from Plate 11.

assemblage as a tectonized remnant of an Early Cretaceous ocean floor on which Jurassic radiolarites were present or became gravitationally emplaced onto as blocks.

Knobby radiolarites

At Playa Carrizal, we confirm preliminary radiolarian data from De Wever et al. (1985). Our radiolarian ages may range form early Valanginian to latest Aptian in age for the section of knobby radiolarites studied at this locality (Table 10). A black shale horizon is clearly dated as middle Aptian by a radiolarian assemblage from a black chert interbedded with siliceous black shale. We recovered a big chunk of lignite from one of the black shales that is under study. The apparent down-section younging may be an indication for an inverted polarity of the block, or the result of duplications in the section due to tight chevron folding that affected the whole block.

The radiolarite facies of this outcrop is distinct from all other localities as it presents thicker planar-bedded green cherts around the black shale interval and distinctly wavy-bedded brick red radiolarites in the remainder of the outcrop. Apart from the black shale and thick shaly partings between chert beds, no detrital material has been detected. The knobby bedding has been well described from Mediterranean sections (e.g., Winterer and Bosellini, 1981). The knobby bedding is generally interpreted as the result of diagenetic dissolution and compaction of a calcareous sequence originally containing porcellanite nodules and layers (e.g., Bosellini and Winterer, 1975). This chert facies has never been found in other oceanic units of Northern Costa Rica nor the Mesquito Composite Terrane (Baumgartner et al., 2008). This facies, together with the wood-bearing black shale would argue for a shallower, and/or near-continent or island environment for this sequence. Sheared, very altered basalts are found in the adjacent outcrops around this block, but no stratigraphic relationship can be established. All these outcrops are immediately beneath the tectonic thrust contact with the overlying megabreccia and the serpentinite of the Santa Elena Nappe.

Sitio Santa Rosa tectonic window

Unit 3

The Unit 3 of Baumgartner and Denyer (2006) is an exclusively oceanic unit made of very evenly bedded centimetric ribbon radiolarite that was intruded by many metric to plurimetric alkaline sills that followed bedding planes (Fig. 7). Baumgartner and Denyer considered this unit to be

Table 9 - List of Early to Late Cretaceous radiolarian species from sample CR-SE18.00, 18.10, 18.25, and 18.45 from the Sitio Santa Rosa tectonic window of the Santa Rosa Accretionary Complex with ranges from diagnostic species (see chapter on radiolarian biochronology).

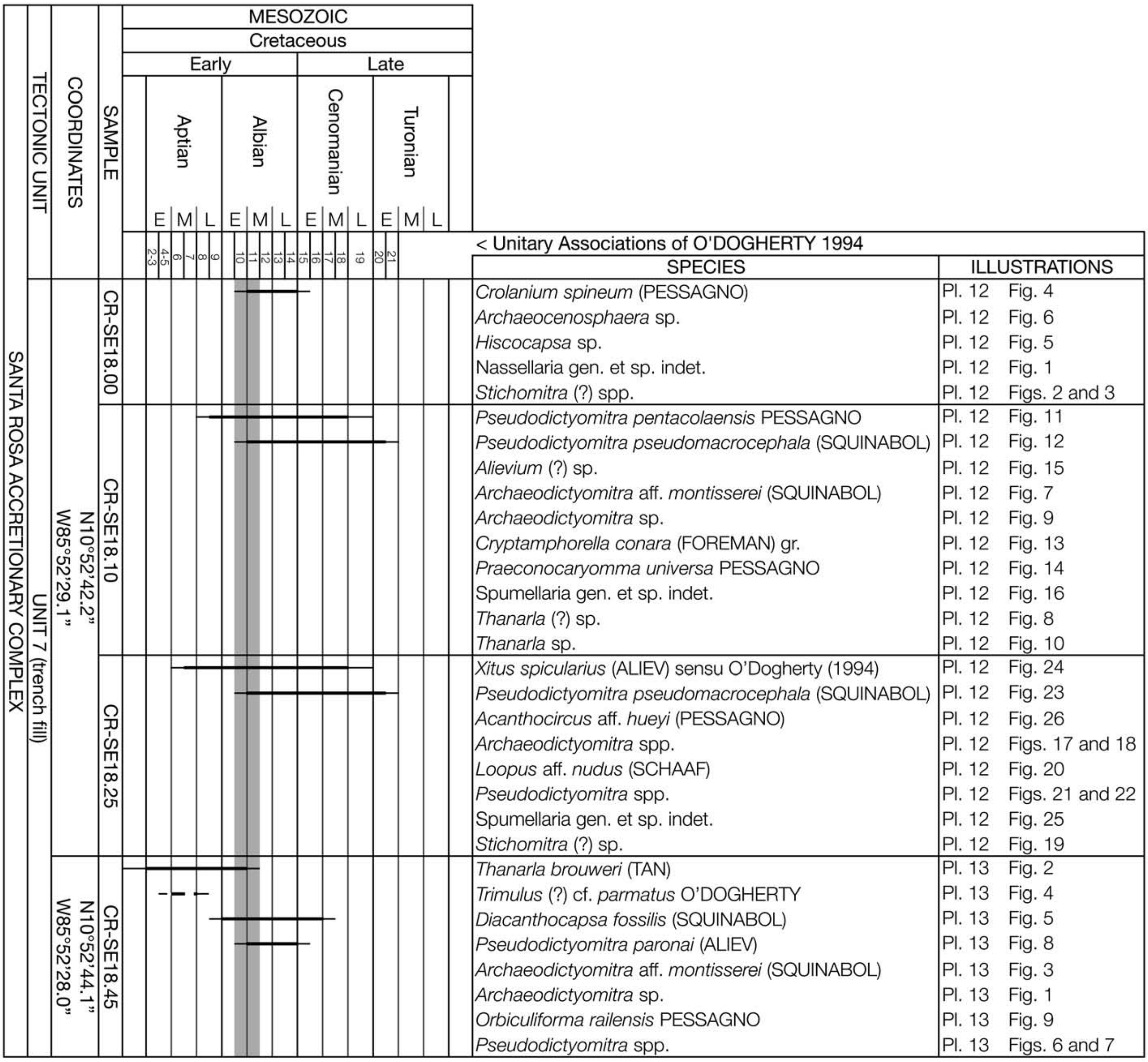

TECTONIC UNIT	COORDINATES	SAMPLE	SPECIES	ILLUSTRATIONS
SANTA ROSA ACCRETIONARY COMPLEX UNIT 7 (trench fill)	N10°52'42.2" W85°52'29.1"	CR-SE18.00	*Crolanium spineum* (PESSAGNO)	Pl. 12 Fig. 4
			Archaeocenosphaera sp.	Pl. 12 Fig. 6
			Hiscocapsa sp.	Pl. 12 Fig. 5
			Nassellaria gen. et sp. indet.	Pl. 12 Fig. 1
			Stichomitra (?) spp.	Pl. 12 Figs. 2 and 3
		CR-SE18.10	*Pseudodictyomitra pentacolaensis* PESSAGNO	Pl. 12 Fig. 11
			Pseudodictyomitra pseudomacrocephala (SQUINABOL)	Pl. 12 Fig. 12
			Alievium (?) sp.	Pl. 12 Fig. 15
			Archaeodictyomitra aff. *montisserei* (SQUINABOL)	Pl. 12 Fig. 7
			Archaeodictyomitra sp.	Pl. 12 Fig. 9
			Cryptamphorella conara (FOREMAN) gr.	Pl. 12 Fig. 13
			Praeconocaryomma universa PESSAGNO	Pl. 12 Fig. 14
			Spumellaria gen. et sp. indet.	Pl. 12 Fig. 16
			Thanarla (?) sp.	Pl. 12 Fig. 8
			Thanarla sp.	Pl. 12 Fig. 10
		CR-SE18.25	*Xitus spicularius* (ALIEV) sensu O'Dogherty (1994)	Pl. 12 Fig. 24
			Pseudodictyomitra pseudomacrocephala (SQUINABOL)	Pl. 12 Fig. 23
			Acanthocircus aff. *hueyi* (PESSAGNO)	Pl. 12 Fig. 26
			Archaeodictyomitra spp.	Pl. 12 Figs. 17 and 18
			Loopus aff. *nudus* (SCHAAF)	Pl. 12 Fig. 20
			Pseudodictyomitra spp.	Pl. 12 Figs. 21 and 22
			Spumellaria gen. et sp. indet.	Pl. 12 Fig. 25
			Stichomitra (?) sp.	Pl. 12 Fig. 19
	N10°52'44.1" W85°52'28.0"	CR-SE18.45	*Thanarla brouweri* (TAN)	Pl. 13 Fig. 2
			Trimulus (?) cf. *parmatus* O'DOGHERTY	Pl. 13 Fig. 4
			Diacanthocapsa fossilis (SQUINABOL)	Pl. 13 Fig. 5
			Pseudodictyomitra paronai (ALIEV)	Pl. 13 Fig. 8
			Archaeodictyomitra aff. *montisserei* (SQUINABOL)	Pl. 13 Fig. 3
			Archaeodictyomitra sp.	Pl. 13 Fig. 1
			Orbiculiforma railensis PESSAGNO	Pl. 13 Fig. 9
			Pseudodictyomitra spp.	Pl. 13 Figs. 6 and 7

Geographic coordinates are provided (WGS 84, degrees) (see also Figs. 2, 4, 6b). Thin lines are used for first and last appearance intervals and dashed lines for ranges of uncertain determination species ("cf."). The numbers correspond to those from Plates 12 and 13.

of Cretaceous age but so far it is undated. The age of both studied radiolarian assemblages are clearly of Early Jurassic age (Pliensbachian and early Toarcian, Table 10). It means that this whole unit must be compared to the other locality yielding Early Jurassic radiolarians in Unit 4 (see below). Unit 3 and the late Early Jurassic block in Unit 4 must represent remnants of an older oceanic setting than the one hosting the Cretaceous radiolarite sequences.

Unit 4

The studied reworked radiolarite block yielded an Early Jurassic radiolarian assemblage (early-middle Pliensbachian, Table 10), confirming the Early-early Middle Jurassic (Pliensbachian-Aalenian, Fig. 7) age of De Wever (1985, emended by Baumgartner and Denyer 2006). It is set in a mélange that includes decametric blocks of alkaline basalts as well as green conglomerates containing alkaline basalts and a possibly arc-derived matrix. The sequence comprising Units 3 (oceanic), 4 (mélange) and 5 (alkaline basalt) represents a tectonic stack containing the same alkaline basalts and their erosion products that may represent a much older episode than the rest of the SRAC. While the oceanic radiolarites hosting the sills are late Early Jurassic in age, the sills are so far undated (Ar/Ar dating of amphiboles is underway). The breccia of Unit 4 has not been dated, but it is obviously younger than the age of the reworked blocks (Fig. 7).

Table 10 - Synthesis of biochronologic ages from the Santa Rosa Accretionary Complex.

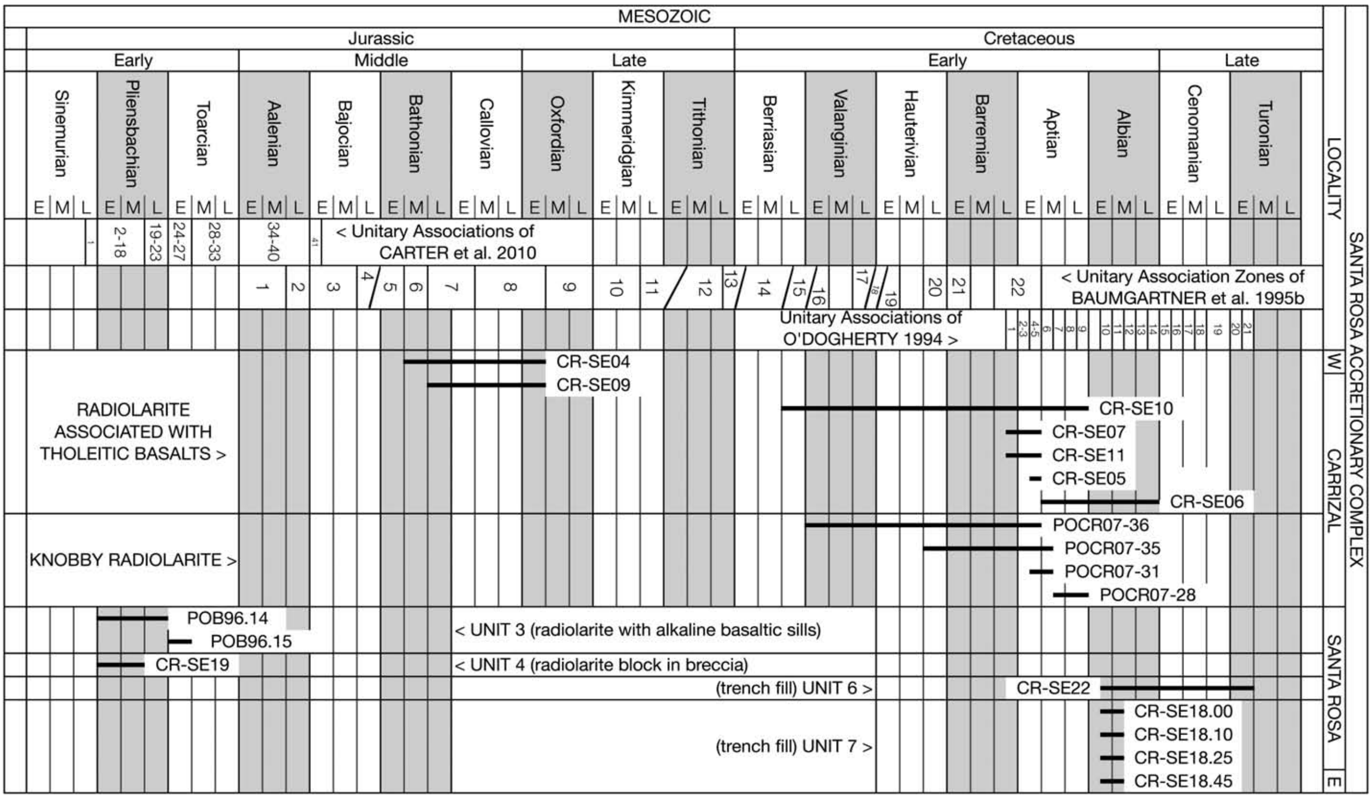

Unit 6

The studied sample is from the base of the Unit 6 where red to brown siliceous mudstones are grading into coarse turbidites and debris flows containing angular basalt-radiolarite breccias (Fig. 7). The late Early-early Late Cretaceous (late early Albian to earliest Turonian, Table 10) radiolarian assemblage dates the onset of proximal sedimentation. This section is interpreted as a rapid approach of the depocentre to the trench area (Baumgartner and Denyer, 2006). Our sample age would correspond to the beginning of this descent in the trench.

Unit 7

The first 45 m of section that yielded radiolarians are in pelagic to hemipelagic facies, with the first turbidites above the topmost sample (Fig. 7). The ages (late early Albian to early middle Albian, Table 10) of the section from the base of Unit 7 date the onset of distal detrital sedimentation and are consistent with the age established in Unit 6 (see above). From the top of Unit 7, De Wever et al. (1985) obtained an Early-early Late Cretaceous radiolarian assemblage (Barremian-Cenomanian) with Late Jurassic reworked specimens (Fig. 7).

CONCLUSION

The new radiolarian ages (Table 10) described in this study confirm the general structure of the SRAC. However, the late Early Jurassic minimum age of the over 100 m thick radiolarite sequence of Unit 3, previously thought to be of Cretaceous age, sheds new light on the history of the accreted material. Although the alkaline sills that intruded the Early Jurassic radiolarites are still undated, they could well be of Jurassic age and by analogy, most of the geochemically similar alkaline basalts (most likely OIB) of the SRAC (Units 3, 4, 5, and possibly 8) could therefore be of Jurassic age. Two alternate hypotheses may account for the presence of important volumes of Jurassic (?) oceanic island basalt that originally formed on an Early Jurassic oceanic floor:

1. In accordance with Baumgartner et al. (2008), this material became accreted to the western American margin and became part of the Mesquito Composite Terrane (possibly during the latest Jurassic-Early Cretaceous times). During the middle Cretaceous accretion of the SRAC, this material became tectonically eroded from the upper Plate and incorporated into the Santa Rosa accretionary prism.
2. The Early Jurassic radiolarites, associated alkaline sills and basalts formed part of the Jurassic crust of an oceanic basin, of which some remnants (Units 3, 4, 5, and possibly 8) were accreted to the Early Cretaceous crust of a younger oceanic basin in an intra-oceanic subduction context. During the late Early-early Late Cretaceous fragments of this Early Cretaceous oceanic crust and the Jurassic remnants were accreted together to the western American margin forming the SRAC.

The important volumes of tholeitic basalt present in the Carrizal tectonic window are tentatively dated by overlying radiolarites as Early Cretaceous (Valanginian to Albian), and correspond to the lowest (westernmost) tectonic units of the SRAC. We interpret these outcrops as remnants of a Cretaceous oceanic floor on which Middle to Late Jurassic radiolarite material was present as blocks or clasts. A variety of paleotectonic settings are conceivable from this evidences such as an Early Cretaceous back-arc opening outboard of a Jurassic intra-oceanic subduction. The knobby radiolarites and black shales of Playa Carrizal are indicative of a shallower, perhaps oceanic island, middle Cretaceous paleoenvironment.

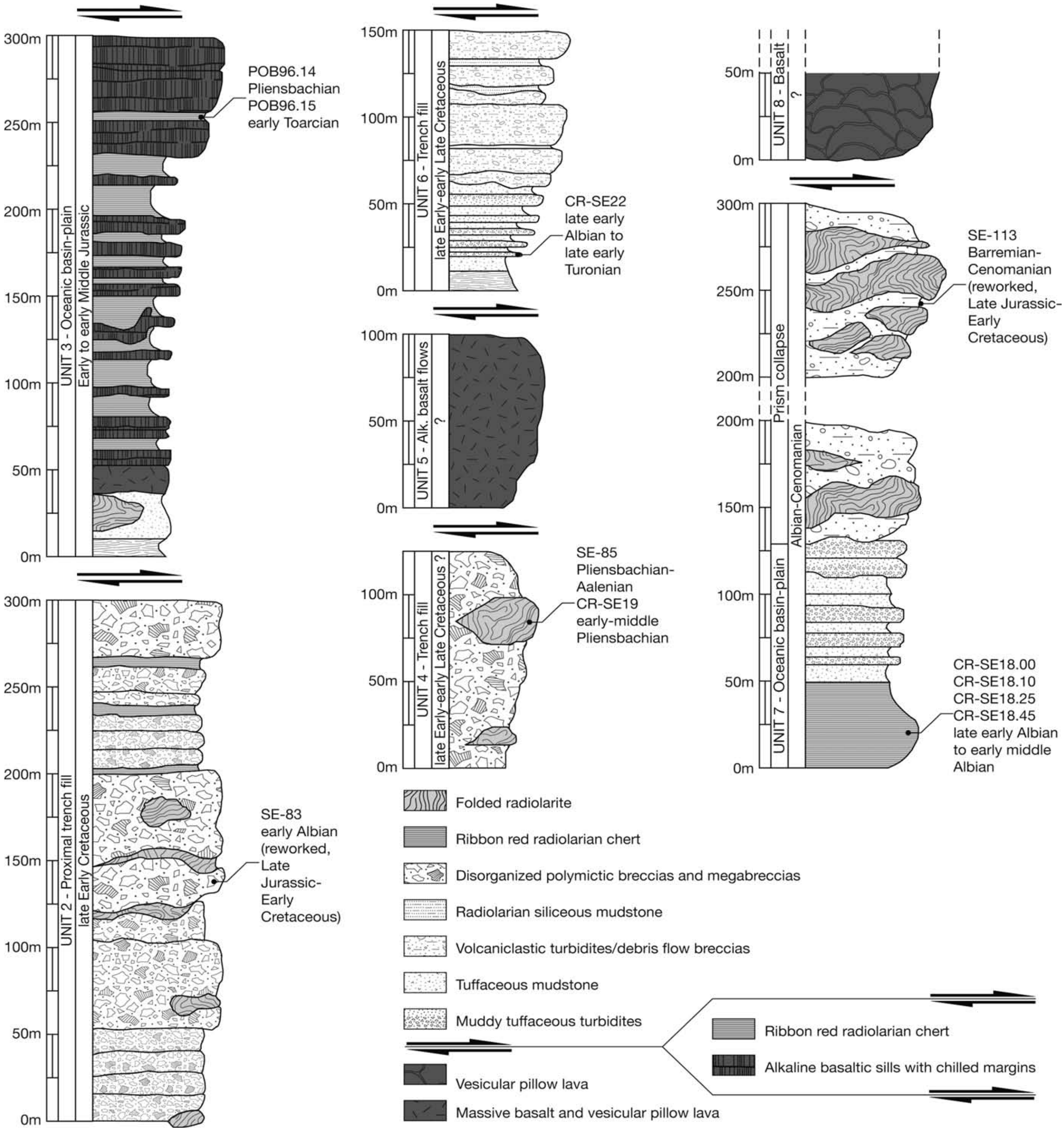

Fig. 7 - Stratigraphic columns and paleoenvironment interpretation of Units of Baumgartner and Denyer (2006) with age and position of samples. SE83, SE85, and SE113 are from De Wever et al. (1985).

The intact stratigraphic sequences (Units 2, 6, and 7) document the approach of a Cretaceous seafloor from a pelagic paleoenvironment into a proximal trench position during Albian-Cenomanian, possibly Turonian times.

ACKNOWLEDGMENTS

The authors are grateful to Spela Gorican, Paleontoloski Institut Ivana Rakova (Ljubljana, Slovenia), and Luis O'Dogherty, Universidad de Cádiz (Spain) for their invaluable comments. A cordial thanks for their very useful commentaries to Marco Chiari, Istituto di Geoscienze e Georisorse (Florence, Italy), and Fabrice Cordey, Université Lyon 1 (France), who have kindly accepted to review this study. We also express our gratitude to Marc-Olivier Diserens, Pascal Tschudin, and Pierre Vonlanthen, Université de Lausanne (Switzerland), for their assistance during the SEM and laboratory work. This work has been supported by the Swiss National Foundation (grant no. 200020-116667), the Société Académique Vaudoise (Bourse Félix Bonjour) and by the Société Paléontologique Suisse.

REFERENCES

Arias M., 2002. Petrografía y geoquímica de las rocas del Complejo Ígneo Estratificado de Bahía Nancite y su relación con los filones basálticos, península de Santa Elena, Costa Rica. Licenc. Thesis, Univ. Costa Rica, 94 pp.

Astorga A., 1992. Descubrimiento de corteza oceánica mesozoica en el norte de Costa Rica y el sur de Nicaragua. Rev. Geol. Am. Central, 14: 109-112.

Azéma J., Bourgois J., Tournon J., Baumgartner P.O. and Desmet A., 1985. L'orogène pré-Sénonien supérieur de la marge pacifique du Costa Rica (Amérique Centrale). Bull. Soc. Géol. France, 1 (2): 173-179.

Azéma J. and Tournon J., 1980. La péninsule de Santa Elena, Costa Rica: un massif ultrabasique charrié en marge pacifique de l'Amérique Centrale, Costa Rica. C. R. Acad. Sci. Paris, 290: 9-12.

Bandini A.N., Flores K., Baumgartner P.O., Jackett S.-J. and Denyer P., 2008. Late Cretaceous and Paleogene Radiolaria from the Nicoya Peninsula, Costa Rica: a tectonostratigraphic application. Stratigraphy, 5 (1): 3-21.

Baumgartner P.O., 1984. El complejo ofiolítico de Nicoya (Costa Rica): Modelos estructurales analizados en función de las edades de los Radiolarios (Calloviense a Santoniense). In: P. Sprechmann (Ed.), Manual de geología de Costa Rica. San José Costa Rica, Ed, Univ. Costa Rica, p. 115-123.

Baumgartner P.O., O'Dogherty L., Gorican S., Dumitrica-Jud R., Dumitrica P., Pillevuit A., Urquhart E., Matsuoka A., Danelian T., Bartolini A.C., Carter E.S., De Wever P., Kito N., Marcucci M. and Steiger T., 1995a. Radiolarian catalogue and systematics of Middle Jurassic to Early Cretaceous Tethyan genera and species. In: P.O. Baumgartner, L. O'Dogherty, S. Gorican, E. Urquhart, A. Pillevuit and P. De Wever (Eds.), Middle Jurassic to Lower Cretaceous Radiolaria of Tethys: Occurrences, systematics, biochronology. Mém. Géol., Lausanne, 23: 37-685.

Baumgartner P.O., Bartolini A., Carter E.S., Conti M., Cortese G., Danelian T., De Wever P., Dumitrica P., Dumitrica-Jud R., Gorican S., Guex J., Hull D.M., Kito N., Marcucci M., Matsuoka A., Murchey B., O'Dogherty L., Savary J., Vishnevskaya V., Widz D. and Yao A., 1995b. Middle Jurassic to Early Cretaceous radiolarian biochronology of Tethys based on Unitary Associations. In: P.O. Baumgartner, L. O'Dogherty, S. Gorican, E. Urquhart, A. Pillevuit and P. De Wever (Eds.), Middle Jurassic to Lower Cretaceous Radiolaria of Tethys: Occurrences, systematics, biochronology. Mém. Géol., Lausanne, 23: 1013-1048.

Baumgartner P.O. and Denyer P., 2006. Evidence for middle Cretaceous accretion at Santa Elena Peninsula (Santa Rosa Accretionary Complex), Costa Rica. Geol. Acta, 4 (1-2): 179-191.

Baumgartner P.O., Flores K., Bandini A.N., Girault F. and Cruz D., 2008. Upper Triassic to Cretaceous radiolaria from Nicaragua and northen Costa Rica - the Mesquito Composite Oceanic Terrane. Ofioliti, 33 (1): 1-19.

Bosellini A. and Winterer E.L., 1975. Pelagic limestone and radiolarite of the Tethyan Mesozoic: a genetic model. Geology, 3: 279-282.

Bourgois J., Azéma J., Baumgartner P.O., Tournon J., Desmet A. and Aubouin J., 1984. The geologic history of the Caribbean-Cocos Plate boundary with special reference to the Nicoya Ophiolite Complex (Costa Rica) and Deep Sea Drilling Project results (legs 67 and 84 off Guatemala): a synthesis. Tectonophysics, 108: 1-32.

Carter E.S., Gorican S., Guex J., O'Dogherty L., De Wever P., Dumitrica P., Hori R.S., Matsuoka A. and Whalen P. 2010. Global radiolarian zonation for the Pliensbachian, Toarcian and Aalenian. Palaeo. Palaeo. Palaeo., 297: 401-419.

De Wever P., Azema J., Tournon J. and Desmet A., 1985. Découverte de materiel oceanique du Lias-Dogger inferieur dans la péninsule de Santa Elena (Costa Rica, Amérique Centrale). C. R. Acad. Sci. Paris, 300: 759-764.

De Wever P., Dumitrica P., Caulet J.-P., Nigrini C. and Caridroit M., 2001. Radiolarians in the sedimentary record. Gordon and Breach Sci. Publ., Amsterdam, 533 pp.

Dengo G., 1962. Estudio Geológico de la Región de Guanacaste, Costa Rica. Inst. Geogr. Nacion., San José, Costa Rica. 112 pp.

Donnelly T.H., 1994. The Caribbean Cretaceous basalt association: a vast igneous province that includes the Nicoya Complex of Costa Rica. Profil, 7: 17-45.

Frisch W., Meschede M. and Sick M., 1992. Origin of the Central America ophiolites: evidence from paleomagnetic results. Geol. Soc. Am. Bull., 104: 1301-1314.

Gazel E., Denyer P. and Baumgartner P.O., 2006. Magmatic and geotectonic significance of Santa Elena Peninsula, Costa Rica. Geol., Acta 4 (1/2): 193-202.

Guex J., 1991. Biochronological correlations. Springer Verlag, Berlin.

Gorican S., Carter E.S., Dumitrica P.,Whalen P.A., Hori R.S., DeWever P., O'Dogherty L., Matsuoka A. and Guex J., 2006. Catalogue and systematics of Pliensbachian. Toarcian and Aalenian radiolarian genera and species. Založba ZRC/ZRC Publishing, ZRC SAZU, Ljubljana.

Harrison J.V., 1953. The geology of the Santa Elena peninsula in Costa Rica, Central America. 7th Pacific Congr., New Zealand, Proceed., 2: 102-104.

Hauff F., Hoernle K. and van den Bogaard P., 2000. Age and geochemistry of basaltic complexes in western Costa Rica: Contributions to the geotectonic evolution of Central America. Geochem., Geophys., Geosyst., 1(5), doi 10.1029/1999GC000020.

Kuijpers E.P., 1980. The geologic history of the Nicoya Ophiolite Complex, Costa Rica and its geotectonic significance. Tectonophysics, 68: 233-255.

Mann P., Schubert C. and Burke K., 1991. Review of Caribbean neotectonics. In: G. Dengo and J.E. Case (Eds.), The Caribbean region. Geol. Soc. Am. The geology of North America, H: 307-338.

Meschede M. and FrischW., 1994. Geochemical characteristics of basaltic rocks from the Central American ophiolites. Profil, 7: 71-85.

O'Dogherty L., 1994. Biochronology and paleontology of Mid-Cretaceous Radiolarians from Northern Apennines (Italy) and Betic Cordillera (Spain). Mém. Géol., Lausanne, 21: I-XV, 1-415.

O'Dogherty L., Carter E.S., Dumitrica P., Gorican S., De Wever P., Hungerbuehler A., Bandini A.N. and Takemura A., 2009a. Catalogue of Mesozoic radiolarian genera. Part 1: Triassic. Geodiversitas, 31 (2): 213-270.

O'Dogherty L., Carter E.S., Dumitrica P., Gorican S., De Wever P., Bandini A.N., Baumgartner P.O. and Matsuoka A., 2009b. Catalogue of Mesozoic radiolarian genera. Part 2: Jurassic-Cretaceous. Geodiversitas, 31 (2): 271-356.

Pindell J.L. and Kennan L. 2009. Tectonic evolution of the Gulf of Mexico, Caribbean and northern South America in the mantle reference frame: an update. In: K.H. James, M.A. Lorente and J.L. Pindell (Eds.), The origin and evolution of the Caribbean Plate. Geol. Soc. London Spec. Publ., 328: 1-55.

Schmidt-Effing R., 1980. Radiolarien der Mittel-Kreide aus dem Santa Elena-Massiv von Costa Rica. N. Jahrb. Geol. Paläont. Abhandl., 160: 241-257.

Tournon J., 1984. Magmatismes du Mésozoïque à l'actuel en Amerique Centrale: l'exemple du Costa Rica, des ophiolites aux andésites. Doct. thesis, Univ. Pierre and Marie Curie, Paris, 335 pp.

Tournon J., 1994. The Santa Elena Peninsula: an ophiolitic nappe and a sedimentary volcanic relative autochthonous. Profil, 7: 87-96.

Winterer E.L. and Bosellini A., 1981. Subsidence and sedimentation on Jurassic passive continental margin, Southern Alps, Italy. AAPG Bull., 65: 394-421.

APPENDIX

A. SPECIES LIST BY LOCALITIES

A.1. Carrizal tectonic window

A.1.1. CR-SE10 and CR-SE11

CR-SE10 (N10°53'49.6'' W85°54'43.1'', Table 1 and Plate 3) - This sample yielded a radiolarian association comprising *Acaeniotyle umbilicata* (Rüst), *Archaeodictyomitra* cf. *mitra* Dumitrica, *Archaeodictyomitra* sp., *Cryptamphorella* cf. *conara* (Foreman), *Cryptamphorella* sp., *Archaeodictyomitra* cf. *coniforma* Dumitrica, *Dictyomitra* sp., Nassellaria gen. et sp. indet., *Stichomitra* (?) sp., *Svinitzium puga* (Schaaf), *Thanarla pulchra* (Squinabol), *Thanarla* sp., *Xitus* cf. *normalis* (Wu and Li).

CR-SE11 (N10°53'49.6'' W85°54'43.1'', Table 1 and Plate 4) - This sample yielded a radiolarian association comprising *Archaeocenosphaera* sp., *Archaeodictyomitra tumandae* Dumitrica, *Cana* (?) sp., *Cryptamphorella conara* (Foreman) gr., *Archaeodictyomitra* aff. *coniforma* Dumitrica, *Hiscocapsa uterculus* (Parona), *Holocryptocanium* sp., *Pantanellium masirahense* Dumitrica, *Pantanellium* sp., *Pseudodictyomitra carpatica* gr. (Lozyniak), *Pseudodictyomitra* cf. *leptoconica* (Foreman), *Thanarla brouweri* (Tan), *Thanarla* sp., *Xitus robustus* Wu.

A.1.2. CR-SE09

CR-SE09 (N10°53'49.7'' W85°54'39.8'', Table 2 and Plate 3) - This sample includes the following radiolarian association: *Archaeodictyomitra* aff. *excellens* (Tan), *Hsuum* sp., Nassellaria gen. et sp. indet., *Praewilliriedellum convexum* (Yao), *Svinitzium kamoensis* (Mizutani and Kido), *Transhsuum* sp., *Zhamoidellum* aff. *ovum* Dumitrica, *Zhamoidellum ventricosum* Dumitrica.

A.1.3. CR-SE06 and CR-SE07

CR-SE06 (N10°53'50.4'' W85°54'36.3'', Table 3 and Plate 2) - This sample yielded a radiolarian association comprising *Archaeodictyomitra immenhauseri* Dumitrica, *Archaeodictyomitra* spp., *Hemicryptocapsa* sp., *Hiscocapsa* cf. *pseudouterculus* (Aita and Okada), *Hiscocapsa* spp., *Svinitzium mizutanii* Dumitrica, *Svinitzium puga* (Schaaf), *Svinitzium* sp., *Thanarla* sp., *Xitus spicularius* (Aliev) *sensu* O'Dogherty (1994).

CR-SE07 (N10°53'50.2'' W85°54'37.2'', Table 3 and Plate 3) - This sample yielded a radiolarian association comprising *Archaeodictyomitra mitra* Dumitrica gr., *Hiscocapsa* sp., *Hiscocapsa uterculus* (Parona), *Pseudodictyomitra* sp., *Stichomitra* (?) *japonica* (Nakaseko and Nishimura).

A.1.4. CR-SE04 and CR-SE05

CR-SE04 (N10°53'42.0'' W85°54'23.0'', Table 4 and Plate 1) - This sample yielded a radiolarian association comprising *Acaeniotyle* sp., *Archaeodictyomitra patricki* Kocher, *Archaeospongoprunum* cf. *imlayi* Pessagno, *Emiluvia nana* Baumgartner, *Parahsuum* sp., *Spinosicapsa* cf. *rosea* (Hull), *Tethysetta dhimenaensis* ssp. A *sensu* Baumgartner et al. (1995a), Spumellaria gen. et sp. indet., *Stichomitra* (?) sp., *Transhsuum maxwelli* gr. (Pessagno), *Triversus* sp., *Zhamoidellum* cf. *ovum* Dumitrica, *Zhamoidellum* sp..

CR-SE05 (N10°53'42.0'' W85°54'23.0'', Table 4 and Plates 1 and 2) - This sample includes the following radiolarian association: *Acaeniotyle diaphorogona* gr. Foreman, *Amphipternis* spp., *Archaeodictyomitra* cf. *montisserei* (Squinabol), *Archaeodictyomitra lipmanae* (Aliev), *Archaeodictyomitra* cf. *coniforma* Dumitrica, *Hiscocapsa asseni* (Tan), *Obesacapsula* sp., *Hiscocapsa* sp., *Obesacapsula* sp., Nassellaria gen. et sp. indet., *Pantanellium masirahense* Dumitrica, *Praeconosphaera sphaeroconus* (Rüst), *Pseudodictyomitra carpatica* gr. (Lozyniak), *Pseudodictyomitra* cf. *lanceloti* Schaaf, Spumellaria or cryptothoracic Nassellaria gen. et sp. indet., *Stichomitra* (?) aff. *communis* Squinabol, *Stichomitra* (?) *communis* Squinabol, *Thanarla brouweri* (Tan), *Thanarla* sp., *Triactoma* sp., *Xitus* sp., *Xitus vermiculatus* (Renz).

A.1.5. Knobby radiolarite (POCR07-28, POCR07-31, POCR07-35, and POCR07-36)

POCR07-28 (Table 5, Plate 5) - 5cm bed of black chert collected between two layers of siliceous black shales. This radiolarian assemblage contains the following species and morphotypes: *Archaeodictyomitra leptocostata* (Wu and Li), *Archaeodictyomitra mitra* Dumitrica, *Archaeodictyomitra* sp., *Becus horridus* (Squinabol), *Dictyomitra* sp., *Hiscocapsa grutterinki* (Tan), *Holocryptocanium* sp., *Pantanellium* cf. *masirahense* Dumitrica, *Praeconocaryomma* sp., *Praeconosphaera* sp., *Praexitus* cf. *verrucosus* Dumitrica, *Pseudodictyomitra* cf. *leptoconica* (Foreman), *Pseudodictyomitra lodogaensis* Pessagno, *Stichomitra* (?) cf. *stocki* (Campbell and Clark), *Stichomitra* (?) *japonica* (Nakaseko and Nishimura), *Stichomitra* (?) sp., *Svinitzium* aff. *mizutanii* Dumitrica, *Svinitzium puga* (Schaaf), *Thanarla brouweri* (Tan), *Thanarla* cf. *brouweri* (Tan), *Xitus spicularius* (Aliev) *sensu* O'Dogherty (1994).

POCR07-31 (Table 5, Plate 6) - This sample yielded an assemblage comprising *Acaeniotyle umbilicata* (Rüst), *Archaeodictyomitra lacrimula* (Foreman), *Crucella* sp., *Godia coronata* (Tumanda), *Hiscocapsa* cf. *asseni* (Tan), *Pantanellium* sp., *Pantanellium squinaboli* (Tan), *Praeconosphaera sphaeroconus* (Rüst), *Pseudodictyomitra* cf. *nodocostata* Dumitrica, *Pseudodictyomitra lanceloti* Schaaf, *Stichomitra* (?) *communis* Squinabol, *Svinitzium puga* (Schaaf), *Thanarla brouweri* (Tan), *Xitus* sp.

POCR07-35 (Table 5, Plate 6) - The following radiolarian assemblage have been extracted from this sample: *Cryptamphorella conara* (Foreman) gr., *Pantanellium squinaboli* (Tan), *Spinosicapsa* sp., *Spinosicapsa typica* (Rüst), *Pseudodictyomitra* aff. *carpatica* gr. (Lozyniak), *Pseudodictyomitra lanceloti* Schaaf, *Thanarla brouweri* (Tan), *Thanarla pacifica* Nakaseko and Nishimura.

POCR07-36 (Table 5, Plate 7) - This sample yielded a radiolarian association including *Alievium regulare* (Wu and Li), *Archaeodictyomitra lacrimula* (Foreman), *Archaeospongoprunum* sp., *Crucella bossoensis* Jud, *Dicroa* sp., *Hiscocapsa grutterinki* (Tan), *Hiscocapsa uterculus* (Parona), *Pantanellium masirahense* Dumitrica, *Pantanellium squinaboli* (Tan), *Spinosicapsa* (?) sp., *Praeconosphaera sphaeroconus* (Rüst), *Pseudodictyomitra carpatica* gr. (Lozyniak), *Pseudodictyomitra* sp., *Stichomitra* (?) sp., *Thanarla brouweri* (Tan).

A.2. Sitio Santa Rosa Tectonic window

A.2.1. Unit 3 (POB96.14 and POB96.15)

POB96.14 (Table 6 and Plate 8) - This sample yielded a radiolarian association comprising *Anaticapitula anatiformis* (De Wever), *Archaeospongoprunum* sp., *Canoptum artum* Yeh, *Canoptum dixoni* Pessagno and Whalen, *Canoptum* sp., Spumellaria gen. et sp. indet., *Homeoparonaella* sp., *Homeoparonaella* sp., *Katroma bicornus* De Wever, *Katroma* cf. *ninstintsi* Carter, *Katroma* sp., *Napora* (?) sp., Nassellaria gen et sp. indet., *Pantanellium cumshewaense* Pessagno, *Parahsuum* aff. *grande* Hori and Yao, *Parahsuum* aff. *stanleyense* (Pessagno), *Parahsuum ovale* Hori and Yao, *Parahsuum snowshoense* (Pessagno), *Parahsuum* sp., *Paronella* sp., *Praeconocaryomma* sp., *Pseudoristola* cf. *megaglobosa* Yeh, *Pseudoristola megaglobosa* Yeh, *Williriedellum* (?) sp.

POB96.15 (Table 6 and Plate 9) - This sample includes the following radiolarian association: *Archaeodictyomitra* (?) sp., *Orbiculiforma* (?) sp., *Eucyrtidiellum disparile* gr. Nagai and Mizutani, *Katroma bicornus* De Wever, *Katroma* cf. *clara* Yeh, *Parahsuum* aff. *stanleyense* (Pessagno), *Parahsuum* aff. *grande* Hori and Yao, *Parahsuum ovale* Hori and Yao, *Parasaturnalis diplocyclis* (Yao), *Praeconocaryomma bajaensis* Whalen, *Trillus* cf. *elkhornensis* Pessagno and Blome, *Zartus mostleri* Pessagno and Blome.

A.2.2. Unit 4 (CR-SE19)

CR-SE19 (N10°52'53.4'' W85°52'39.3'', Table 7 and Plate 10) - This sample yielded a radiolarian association including *Acaeniotylopsis* aff. *triacanthus* Kito and De Wever, *Bipedis fannini* Carter, *Canoptum columbiaense* Whalen and Carter, *Canoptum* sp., *Charlottea* (?) sp. C Gorican et al. (2006), *Cyclastrum asuncionense* Whalen and Carter, *Katroma* cf. *ninstintsi* Carter, *Napora* sp., Nassellaria gen. et sp. indet., *Pantanellium* cf. *inornatum* Pessagno and Poisson, *Pantanellium* sp., *Parahsuum* cf. *longiconicum* Sashida, *Paleosaturnalis tetraradiatus* (Kozur and Mostler), *Pseudoeucyrtis* sp., Spumellaria gen. et sp. indet., *Thurstonia* (?) *gibsoni* Whalen and Carter, *Triactoma* (?) sp., *Triactoma* (?) sp.

A.2.3. Unit 6 (CR-SE22)

CR-SE22 (N10°52'44.8'' W85°52'31.4'', Table 8 and Plate 11) - This sample includes the following radiolarian association: *Acaeniotyle* (?) cf. *glebulosa* (Foreman), *Dictyomitra* aff. *formosa* (Squinabol) *sensu* O'Dogherty (1994), *Archaeodictyomitra montisserei* (Squinabol), *Archaeodictyomitra* sp., *Archaeodictyomitra undata* (Squinabol), *Archaeospongoprunum* sp., *Archaeotritrabs* sp., *Diacanthocapsa* (?) sp., *Dictyomitra* spp., Nassellaria gen. et sp. indet., *Pantanellium* sp., *Cryptamhorella* sp., *Pseudodictyomitra pseudomacrocephala* (Squinabol), *Pseudodictyomitra* sp., *Rhopalosyringium mosquense* (Smirnova and Aliev), *Rhopalosyringium* sp., *Acaeniotyle* sp., Spumellaria gen. et sp. indet., *Stichomitra* (?) cf. *japonica* (Nakaseko and Nishimura), *Stichomitra* (?) sp., *Stichomitra* (?) *tosaensis* (Nakaseko and Nishimura), *Thanarla* aff. *brouweri* (Tan), *Triactoma* sp., *Xitus* aff. *vermiculatus* (Renz), *Xitus* sp.

A.2.4. Unit 7 (CR-SE18.00, CR-SE18.10, CR-SE18.25, and CR-SE18.45)

CR-SE18.00 (base of the section, N10°52'42.2'' W85°52'29.1'', Table 9 and Plate 12) - This sample yielded a radiolarian association including *Archaeocenosphaera* sp., *Crolanium spineum* (Pessagno), *Hiscocapsa* sp., Nassellaria gen. et sp. indet., *Stichomitra* (?) spp..

CR-SE18.10 (10m above base, N10°52'42.2'' W85°52'29.1'', Table 9 and Plate 12) - This sample includes the following radiolarian association: *Alievium* (?) sp., *Archaeodictyomitra* aff. *montisserei* (Squinabol), *Archaeodictyomitra* sp., *Cryptamphorella conara* (Foreman) gr., *Praeconocaryomma universa* Pessagno, *Pseudodictyomitra pentacolaensis* Pessagno, *Pseudodictyomitra pseudomacrocephala* (Squinabol), Spumellaria gen. et sp. indet., *Thanarla* (?) sp., *Thanarla* sp.

CR-SE18.25 (25 m above base, N10°52'42.2'' W85°52'29.1'', Table 9 and Plate 12) - This sample yielded a radiolarian association including *Acanthocircus* aff. *hueyi* (Pessagno), *Archaeodictyomitra* spp., *Loopus* aff. *nudus* (Schaaf), *Pseudodictyomitra pseudomacrocephala* (Squinabol), *Pseudodictyomitra* sp., *Pseudodictyomitra* sp., Spumellaria gen. et sp. indet., *Stichomitra* (?) sp., *Xitus spicularius* (Aliev) *sensu* O'Dogherty (1994).

CR-SE18.45 (45 m above base, N10°52'44.1'' W85°52'28.0'', Table 9 and Plate 13) - This sample yielded a radiolarian association comprising *Archaeodictyomitra* aff. *montisserei* (Squinabol), *Archaeodictyomitra* sp., *Diacanthocapsa fossilis* (Squinabol), *Orbiculiforma railensis* Pessagno, *Pseudodictyomitra paronai* (Aliev), *Pseudodictyomitra* sp., *Pseudodictyomitra* sp., *Thanarla brouweri* (Tan), *Trimulus* (?) cf. *parmatus* O'Dogherty.

B. SPECIES LIST

Acaeniotyle (?) *glebulosa* (Foreman): CR-SE22 (Plate 11, Fig. 28); *Acaeniotyle diaphorogona* gr. Foreman: CR-SE05 (Plate 2, Fig. 7); *Acaeniotyle* spp.: CR-SE04 (Plate 1, Fig. 12), CR-SE22 (Plate 11, Fig. 29); *Acaeniotyle umbilicata* (Rüst): CR-SE10 (Plate 3, Fig. 38), POCR07-31 (Plate 6, Fig. 11); *Acaeniotylopsis* aff. *triacanthus* Kito and De Wever: CR-SE19 (Plate 10, Fig. 15); *Acanthocircus* aff. *hueyi* (Pessagno): CR-SE18.25 (Plate 12, Fig. 26); *Alievium* (?) sp.: CR-SE18.10 (Plate 12, Fig. 15); *Alievium regulare* (Wu and Li): POCR07-36 (Plate 7, Figs. 10-12); *Amphipternis* spp.: CR-SE05 (Plate 1, Figs. 25-28); *Anaticapitula anatiformis* (De Wever): POB96.14 (Plate 8, Fig. 26); *Archaeocenosphaera* spp.: CR-SE18.00 (Plate 12, Fig. 6), CR-SE11 (Plate 4, Fig. 21); *Archaeodictyomitra* (?) sp.: POB96.15 (Plate 9, Fig. 1); *Archaeodictyomitra* aff. *coniforma* Dumitrica: CR-SE11 (Plate 4, Fig. 8); *Archaeodictyomitra* aff. *excellens* (Tan): CR-SE09 (Plate 3, Fig. 8); *Archaeodictyomitra* aff. *montisserei* (Squinabol): CR-SE18.10 (Plate 12, Fig. 7), CR-SE18.45 (Plate 13, Fig. 3); *Archaeodictyomitra* cf. *coniforma* Dumitrica: CR-SE05 (Plate 1, Fig. 22), CR-SE10 (Plate 3, Fig. 27); *Archaeodictyomitra* cf. *mitra* Dumitrica: CR-SE10 (Plate 3, Figs. 22-24); *Archaeodictyomitra* cf. *montisserei* (Squinabol): CR-SE05 (Plate 1, Figs. 20 and 21); *Archaeodictyomitra immenhauseri* Dumitrica: CR-SE06 (Plate 2, Fig. 19); *Archaeodictyomitra lacrimula* (Foreman): POCR07-31 (Plate 6, Fig. 9), POCR07-36 (Plate 7, Fig. 3); *Archaeodictyomitra leptocostata* (Wu and Li): POCR07-28 (Plate 5, Fig. 7); *Archaeodictyomitra lipmanae* (Aliev): CR-SE05 (Plate 1, Fig. 23); *Archaeodictyomitra mitra* Dumitrica gr.: CR-SE07 (Plate 3, Figs. 1-3), POCR07-28 (Plate 5, Fig. 5); *Archaeodictyomitra montisserei* (Squinabol): CR-SE22 (Plate 11, Fig. 2); *Archaeodictyomitra patricki* Kocher: CR-SE04 (Plate 1, Fig. 4); *Archaeodictyomitra* spp.: CR-SE06 (Plate 2, Figs. 16-18, and 20), CR-SE10 (Plate 3, Fig. 28), CR-SE18.10 (Plate 12, Fig. 9), CR-SE18.45 (Plate 13, Fig. 1), CR-SE22 (Plate 11, Fig. 4), POCR07-28 (Plate 5, Fig. 1), CR-SE18.25 (Plate 12, Figs. 17 and 18); *Archaeodictyomitra tumandae* Dumitrica: CR-SE11 (Plate 4, Fig. 7); *Archaeodictyomitra undata* (Squinabol): CR-SE22 (Plate 11, Fig. 1); *Archaeospongoprunum* cf. *imlayi* Pessagno: CR-SE04 (Plate 1, Fig. 10); *Archaeospongoprunum* spp.: CR-SE22 (Plate 11, Fig. 25), POB96.14 (Plate 8, Fig. 32), POCR07-36

(Plate 7, Fig. 20); *Archaeotritrabs* sp.: CR-SE22 (Plate 11, Fig. 31); *Becus horridus* (Squinabol): POCR07-28 (Plate 5, Fig. 23); *Bipedis fannini* Carter: CR-SE19 (Plate 10, Fig. 4); *Cana* (?) sp.: CR-SE11 (Plate 4, Fig. 18); *Canoptum artum* Yeh: POB96.14 (Plate 8, Figs. 8, 11 and 12); *Canoptum columbiaense* Whalen and Carter: CR-SE19 (Plate 10, Fig. 9); *Canoptum dixoni* Pessagno and Whalen: POB96.14 (Plate 8, Figs. 9, 10 and 13); *Canoptum* spp.: CR-SE19 (Plate 10, Fig. 8), POB96.14 (Plate 8, Fig. 14); *Charlottea* (?) sp. C Gorican et al. (2006): CR-SE19 (Plate 10, Fig. 20); *Crolanium spineum* (Pessagno): CR-SE18.00 (Plate 12, Fig. 4); *Crucella bossoensis* Jud: POCR07-36 (Plate 7, Fig. 18); *Crucella* sp.: POCR07-31 (Plate 6, Fig. 14); *Cryptamhorella* sp.: CR-SE22 (Plate 11, Fig. 27); *Cryptamphorella* cf. *conara* (Foreman): CR-SE10 (Plate 3, Fig. 37); *Cryptamphorella conara* (Foreman) gr.: CR-SE11 (Plate 4, Fig. 16), CR-SE18.10 (Plate 12, Fig. 13), POCR07-35 (Plate 6, Fig. 23); *Cryptamphorella* sp.: CR-SE10 (Plate 3, Fig. 36); *Cyclastrum* cf. *asuncionense* Whalen and Carter: CR-SE19 (Plate 10, Figs. 12 and 16); *Diacanthocapsa* (?) sp.: CR-SE22 (Plate 11, Fig. 15); *Diacanthocapsa* cf. *fossilis* (Squinabol): CR-SE18.45 (Plate 13, Fig. 5); *Dicroa* sp.: POCR07-36 (Plate 7, Fig. 13); *Dictyomitra* aff. *formosa* (Squinabol) *sensu* O'Dogherty (1994): CR-SE22 (Plate 11, Fig. 5); *Dictyomitra* spp.: CR-SE10 (Plate 3, Fig. 26), CR-SE22 (Plate 11, Figs. 6 and 7), POCR07-28 (Plate 5, Fig. 6); *Emiluvia nana* Baumgartner: CR-SE04 (Plate 1, Fig. 13); *Eucyrtidiellum disparile* gr. Nagai and Mizutani: POB96.15 (Plate 9, Fig. 9); *Godia coronata* (Tumanda): POCR07-31 (Plate 6, Fig. 16); *Hemicryptocapsa* sp.: CR-SE06 (Plate 2, Fig. 28); *Hiscocapsa asseni* (Tan): CR-SE05 (Plate 2, Figs. 3 and 4); *Hiscocapsa* cf. *asseni* (Tan): POCR07-31 (Plate 6, Fig. 8); *Hiscocapsa* cf. *pseudouterculus* (Aita and Okada): CR-SE06 (Plate 2, Fig. 27); *Hiscocapsa grutterinki* (Tan): POCR07-28 (Plate 5, Fig. 21), POCR07-36 (Plate 7, Fig. 9); *Hiscocapsa* spp.: CR-SE05 (Plate 2, Fig. 5), CR-SE06 (Plate 2, Figs. 25 and 26), CR-SE07 (Plate 3, Fig. 6), CR-SE18.00 (Plate 12, Fig. 5); *Hiscocapsa uterculus* (Parona): CR-SE07 (Plate 3, Fig. 7), CR-SE11 (Plate 4, Figs. 14 and 15), POCR07-36 (Plate 7, Fig. 8); *Holocryptocanium* spp.: CR-SE11 (Plate 4, Fig. 17), POCR07-28 (Plate 5, Fig. 22); *Homeoparonaella* spp.: POB96.14 (Plate 8, Figs. 29 and 30); *Hsuum* sp.: CR-SE09 (Plate 3, Fig. 11); *Katroma bicornus* De Wever: POB96.14 (Plate 8, Fig. 15), POB96.15 (Plate 9, Fig. 8); *Katroma* cf. *clara* Yeh: POB96.15 (Plate 9, Figs. 10-12); *Katroma* cf. *ninstintsi* Carter: CR-SE19 (Plate 10, Fig. 6), POB96.14 (Plate 8, Fig. 19); *Katroma* sp.: POB96.14 (Plate 8, Figs. 16-18); *Loopus* aff. *nudus* (Schaaf): CR-SE18.25 (Plate 12, Fig. 20); *Napora* (?) sp.: POB96.14 (Plate 8, Fig. 24); *Napora* sp.: CR-SE19 (Plate 10, Fig. 1); Nassellaria gen et sp. indet.: CR-SE05 (Plate 1, Fig. 34), CR-SE09 (Plate 3, Fig. 9), CR-SE10 (Plate 3, Fig. 32), CR-SE18.00 (Plate 12, Fig. 1), CR-SE19 (Plate 10, Figs. 2, 5, and 7), CR-SE22 (Plate 11, Figs. 12, 13, and 16-18), POB96.14 (Plate 8, Fig. 22); *Obesacapsula* spp.: CR-SE05 (Plate 2, Figs. 2 and 6); *Orbiculiforma* (?) sp.: POB96.15 (Plate 9, Fig. 16); *Orbiculiforma railensis* Pessagno: CR-SE18.45 (Plate 13, Fig. 9); *Paleosaturnalis tetraradiatus* (Kozur and Mostler): CR-SE19 (Plate 10, Fig. 23); *Pantanellium* cf. *inornatum* Pessagno and Poisson: CR-SE19 (Plate 10, Fig. 21); *Pantanellium* cf. *masirahense* Dumitrica: POCR07-28 (Plate 5, Figs. 24-26); *Pantanellium cumshewaense* Pessagno: POB96.14 (Plate 8, Fig. 27); *Pantanellium masirahense* Dumitrica: CR-SE05 (Plate 2, Figs. 9-12), CR-SE11 (Plate 4, Fig. 20), POCR07-36 (Plate 7, Fig. 17), *Pantanellium* spp.: CR-SE11 (Plate 4, Fig. 19), CR-SE19 (Plate 10, Fig. 22), CR-SE22 (Plate 11, Fig. 26), POCR07-31 (Plate 6, Fig. 13); *Pantanellium squinaboli* (Tan): POCR07-31 (Plate 6, Fig. 12), POCR07-35 (Plate 6, Fig. 24), POCR07-36 (Plate 7, Figs. 14-16); *Parahsuum* aff. *grande* Hori and Yao: POB96.14 (Plate 8, Figs. 3 and 4), POB96.15 (Plate 9, Figs. 2, 3 and 5); *Parahsuum* aff. *stanleyense* (Pessagno): POB96.14 (Plate 8, Fig. 7), POB96.15 (Plate 9, Fig. 4); *Parahsuum* cf. *longiconicum* Sashida: CR-SE19 (Plate 10, Fig. 3); *Parahsuum ovale* Hori and Yao: POB96.14 (Plate 8, Fig. 2), POB96.15 (Plate 9, Figs. 6 and 7); *Parahsuum snowshoense* (Pessagno): POB96.14 (Plate 8, Fig. 6); *Parahsuum* spp.: CR-SE04 (Plate 1, Fig. 3), POB96.14 (Plate 8, Figs. 1 and 5); *Parasaturnalis diplocyclis* (Yao): POB96.15 (Plate 9, Figs. 17 and 18); *Paronella* sp.: POB96.14 (Plate 8, Fig. 28); *Praeconocaryomma bajaensis* Whalen: POB96.15 (Plate 9, Fig. 19); *Praeconocaryomma* sp.: POB96.14 (Plate 8, Fig. 31), POCR07-28 (Plate 5, Fig. 27); *Praeconocaryomma universa* Pessagno: CR-SE18.10 (Plate 12, Fig. 14); *Praeconosphaera* sp.: POCR07-28 (Plate 5, Figs. 28 and 29); *Praeconosphaera sphaeroconus* (Rüst): CR-SE05 (Plate 2, Fig. 13), POCR07-31 (Plate 6, Fig. 15), POCR07-36 (Plate 7, Fig. 19); *Praewilliriedellum convexum* (Yao): CR-SE09 (Plate 3, Figs. 15-18); *Praexitus* cf. *verrucosus* Dumitrica: POCR07-28 (Plate 5, Fig. 19); *Pseudodictyomitra* aff. *carpatica* gr. (Lozyniak): POCR07-35 (Plate 6, Fig. 19); *Pseudodictyomitra carpatica* gr. (Lozyniak): CR-SE05 (Plate 1, Figs. 30 and 31), CR-SE11 (Plate 4, Figs. 9-11), POCR07-36 (Plate 7, Fig. 6); *Pseudodictyomitra* cf. *lanceloti* Schaaf: CR-SE05 (Plate 1, Fig. 29); *Pseudodictyomitra* cf. *leptoconica* (Foreman): CR-SE11 (Plate 4, Fig. 12), POCR07-28 (Plate 5, Figs. 8 and 10); *Pseudodictyomitra* cf. *nodocostata* Dumitrica: POCR07-31 (Plate 6, Fig. 5); *Pseudodictyomitra lanceloti* Schaaf: POCR07-31 (Plate 6, Fig. 6), POCR07-35 (Plate 6, Fig. 20); *Pseudodictyomitra lodogaensis* Pessagno: POCR07-28 (Plate 5, Fig. 11); *Pseudodictyomitra paronai* (Aliev): CR-SE18.45 (Plate 13, Fig. 8); *Pseudodictyomitra pentacolaensis* Pessagno: CR-SE18.10 (Plate 12, Fig. 11); *Pseudodictyomitra pseudomacrocephala* (Squinabol): CR-SE18.10 (Plate 12, Fig. 12), CR-SE18.25 (Plate 12, Fig. 23), CR-SE22 (Plate 11, Fig. 9); *Pseudodictyomitra* spp.: CR-SE07 (Plate 3, Fig. 5), CR-SE18.25 (Plate 12, Figs. 21 and 22), CR-SE18.45 (Plate 13, Figs. 6 and 7), CR-SE22 (Plate 11, Fig. 8), POCR07-36 (Plate 7, Fig. 5); *Pseudoeucyrtis* sp.: CR-SE19 (Plate 10, Fig. 10); *Pseudoristola* cf. *megaglobosa* Yeh: POB96.14 (Plate 8, Fig. 21); *Pseudoristola megaglobosa* Yeh: POB96.14 (Plate 8, Fig. 20); *Rhopalosyringium mosquense* (Smirnova and Aliev): CR-SE22 (Plate 11, Figs. 21-23); *Rhopalosyringium* sp.: CR-SE22 (Plate 11, Fig. 24); *Spinosicapsa* (?) sp.: POCR07-36 (Plate 7, Fig. 7); *Spinosicapsa* cf. *rosea* (Hull): CR-SE04 (Plate 1, Fig. 9); *Spinosicapsa* sp.: POCR07-35 (Plate 6, Fig. 22); *Spinosicapsa typica* (Rüst): POCR07-35 (Plate 6, Fig. 21); Spumellaria gen. et sp. indet.: CR-SE04 (Plate 1, Fig. 11), CR-SE19 (Plate 10, Figs. 11 and 13), CR-SE18.10 (Plate 12, Fig. 16), CR-SE18.25 (Plate 12, Fig. 25), CR-SE22 (Plate 11, Fig. 30, 33, and 34), POB96.14 (Plate 8, Fig. 25); Spumellaria or cryptothoracic Nassellaria gen. et sp. indet.: CR-SE05 (Plate 2, Fig. 14); *Stichomitra* (?) aff. *communis* Squinabol: CR-SE05 (Plate 1, Fig. 32); *Stichomitra* (?) cf. *japonica* (Nakaseko and Nishimura): CR-SE22 (Plate 11, Fig. 11); *Stichomitra* (?) cf. *stocki* (Campbell and Clark): POCR07-28 (Plate 5, Fig. 14); *Stichomitra* (?) *communis* Squinabol:

CR-SE05 (Plate 1, Fig. 24), POCR07-31 (Plate 6, Figs. 3 and 4); *Stichomitra* (?) *japonica* (Nakaseko and Nishimura): CR-SE07 (Plate 3, Fig. 4), POCR07-28 (Plate 5, Fig. 13); *Stichomitra* (?) spp.: CR-SE04 (Plate 1, Fig. 1), CR-SE10 (Plate 3, Figs. 29, 30, and 31), CR-SE18.00 (Plate 12, Figs. 2 and 3), CR-SE18.25 (Plate 12, Fig. 19), CR-SE22 (Plate 11, Fig. 10), POCR07-28 (Plate 5, Figs. 12 and 15), POCR07-36 (Plate 7, Fig. 4); *Stichomitra* (?) *tosaensis* (Nakaseko and Nishimura): CR-SE22 (Plate 11, Fig. 14); *Svinitzium* aff. *mizutanii* Dumitrica: POCR07-28 (Plate 5, Fig. 20); *Svinitzium kamoensis* (Mizutani and Kido): CR-SE09 (Plate 3, Fig. 10); *Svinitzium mizutanii* Dumitrica: CR-SE06 (Plate 2, Fig. 22); *Svinitzium puga* (Schaaf): CR-SE06 (Plate 2, Fig. 23), CR-SE10 (Plate 3, Figs. 34 and 35), POCR07-28 (Plate 5, Fig. 9), POCR07-31 (Plate 6, Fig. 7); *Svinitzium* sp.: CR-SE06 (Plate 2, Fig. 21); *Tethysetta dhimenaensis* ssp. A *sensu* Baumgartner et al. (1995a): CR-SE04 (Plate 1, Fig. 6); *Thanarla* (?) sp.: CR-SE18.10 (Plate 12, Fig. 8); *Thanarla* aff. *brouweri* (Tan): CR-SE22 (Plate 11, Fig. 3); *Thanarla brouweri* (Tan): CR-SE05 (Plate 1, Figs. 14-17), CR-SE11 (Plate 4, Figs. 1-3, 5 and 6), CR-SE18.45 (Plate 13, Fig. 2), POCR07-28 (Plate 5, Figs. 2 and 4), POCR07-31 (Plate 6, Figs. 1 and 2), POCR07-35 (Plate 6, Fig. 17), POCR07-36 (Plate 7, Figs. 1 and 2); *Thanarla* cf. *brouweri* (Tan): POCR07-28 (Plate 5, Fig. 3); *Thanarla pacifica* Nakaseko and Nishimura: POCR07-35 (Plate 6, Fig. 18); *Thanarla pulchra* (Squinabol): CR-SE10 (Plate 3, Fig. 25); *Thanarla* spp.: CR-SE05 (Plate 1, Figs. 18 and 19), CR-SE06 (Plate 2, Fig. 15), CR-SE10 (Plate 3, Figs. 19-21), CR-SE11 (Plate 4, Fig. 4), CR-SE18.10 (Plate 12, Fig. 10); *Thurstonia* (?) *gibsoni* Whalen and Carter: CR-SE19 (Plate 10, Figs. 17 and 19); *Transhsuum maxwelli* gr. (Pessagno): CR-SE04 (Plate 1, Fig. 5); *Transhsuum* sp.: CR-SE09 (Plate 3, Fig. 12); *Triactoma* (?) spp.: CR-SE19 (Plate 10, Figs. 14 and 18); *Triactoma* sp.: CR-SE05 (Plate 2, Fig. 8), CR-SE22 (Plate 11, Fig. 32); *Trillus* cf. *elkhornensis* Pessagno and Blome: POB96.15 (Plate 9, Fig. 15); *Trimulus* (?) cf. *parmatus* O'Dogherty: CR-SE18.45 (Plate 13, Fig. 4); *Triversus* sp.: CR-SE04 (Plate 1, Fig. 2); *Williriedellum* (?) sp.: POB96.14 (Plate 8, Fig. 23); *Xitus* aff. *vermiculatus* (Renz): CR-SE22 (Plate 11, Fig. 19); *Xitus* cf. *normalis* (Wu and Li): CR-SE10 (Plate 3, Fig. 33); *Xitus robustus* Wu: CR-SE11 (Plate 4, Fig. 13); *Xitus spicularius* (Aliev) *sensu* O'Dogherty (1994): CR-SE06 (Plate 2, Fig. 24), CR-SE18.25 (Plate 12, Fig. 24), POCR07-28 (Plate 5, Figs. 16-18); *Xitus* spp.: CR-SE05 (Plate 1, Fig. 33, Plate 2, Fig. 1), CR-SE22 (Plate 11, Fig. 20), POCR07-31 (Plate 6, Fig. 10); *Xitus vermiculatus* (Renz): CR-SE05 (Plate 1, Fig. 35); *Zartus mostleri* Pessagno and Blome: POB96.15 (Plate 9, Figs. 13 and 14); *Zhamoidellum* aff. *ovum* Dumitrica: CR-SE09 (Plate 3, Fig. 14); *Zhamoidellum* cf. *ovum* Dumitrica: CR-SE04 (Plate 1, Fig. 8); *Zhamoidellum* sp.: CR-SE04 (Plate 1, Fig. 7); *Zhamoidellum ventricosum* Dumitrica: CR-SE09 (Plate 3, Fig. 13).

Received, February 1, 2011
Accepted, June 6, 2011

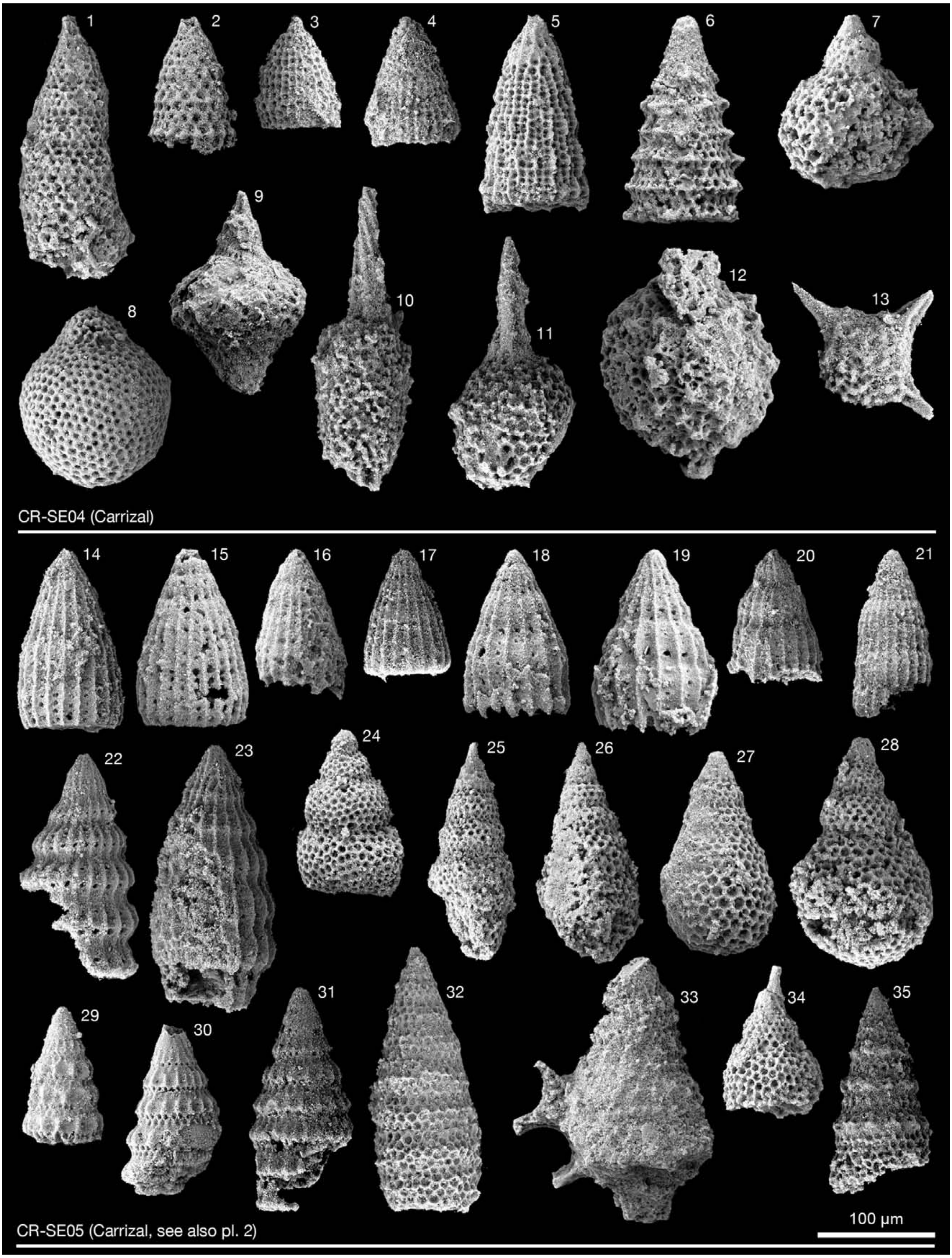

Plate 1 - Scanning Electron Microscope pictures of radiolarians from the Carrizal tectonic window of the Santa Rosa Accretionary Complex, Santa Elena Peninsula, northwestern Costa Rica. Sample CR-SE04 (middle Bathonian-early Oxfordian): 1- *Stichomitra* (?) sp.; 2- *Triversus* sp.; 3- *Parahsuum* sp.; 4- *Archaeodictyomitra patricki* Kocher; 5- *Transhsuum maxwelli* gr. (Pessagno); 6- *Tethysetta dhimenaensis* ssp. A *sensu* Baumgartner et al. (1995a); 7- *Zhamoidellum* sp.; 8- *Zhamoidellum* cf. *ovum* Dumitrica; 9- *Spinosicapsa* cf. *rosea* (Hull); 10- *Archaeospongoprunum* cf. *imlayi* Pessagno; 11- Spumellaria gen. et sp. indet.; 12- *Acaeniotyle* sp.; 13- *Emiluvia nana* Baumgartner. Sample CR-SE05 (late early Aptian, see also Plate 2): 14-17- *Thanarla brouweri* (Tan); 18 and 19- *Thanarla* sp.; 20 and 21- *Archaeodictyomitra* cf. *montisserei* (Squinabol); 22- *Archaeodictyomitra* cf. *coniforma* Dumitrica; 23- *Archaeodictyomitra lipmanae* (Aliev); 24- *Stichomitra* (?) *communis* Squinabol; 25-28- *Amphipternis* spp.; 29- *Pseudodictyomitra* cf. *lanceloti* Schaaf; 30 and 31- *Pseudodictyomitra carpatica* gr. (Lozyniak); 32- *Stichomitra* (?) aff. *communis* Squinabol; 33- *Xitus* sp.; 34- Nassellaria gen. et sp. indet.; 35- *Xitus vermiculatus* (Renz).

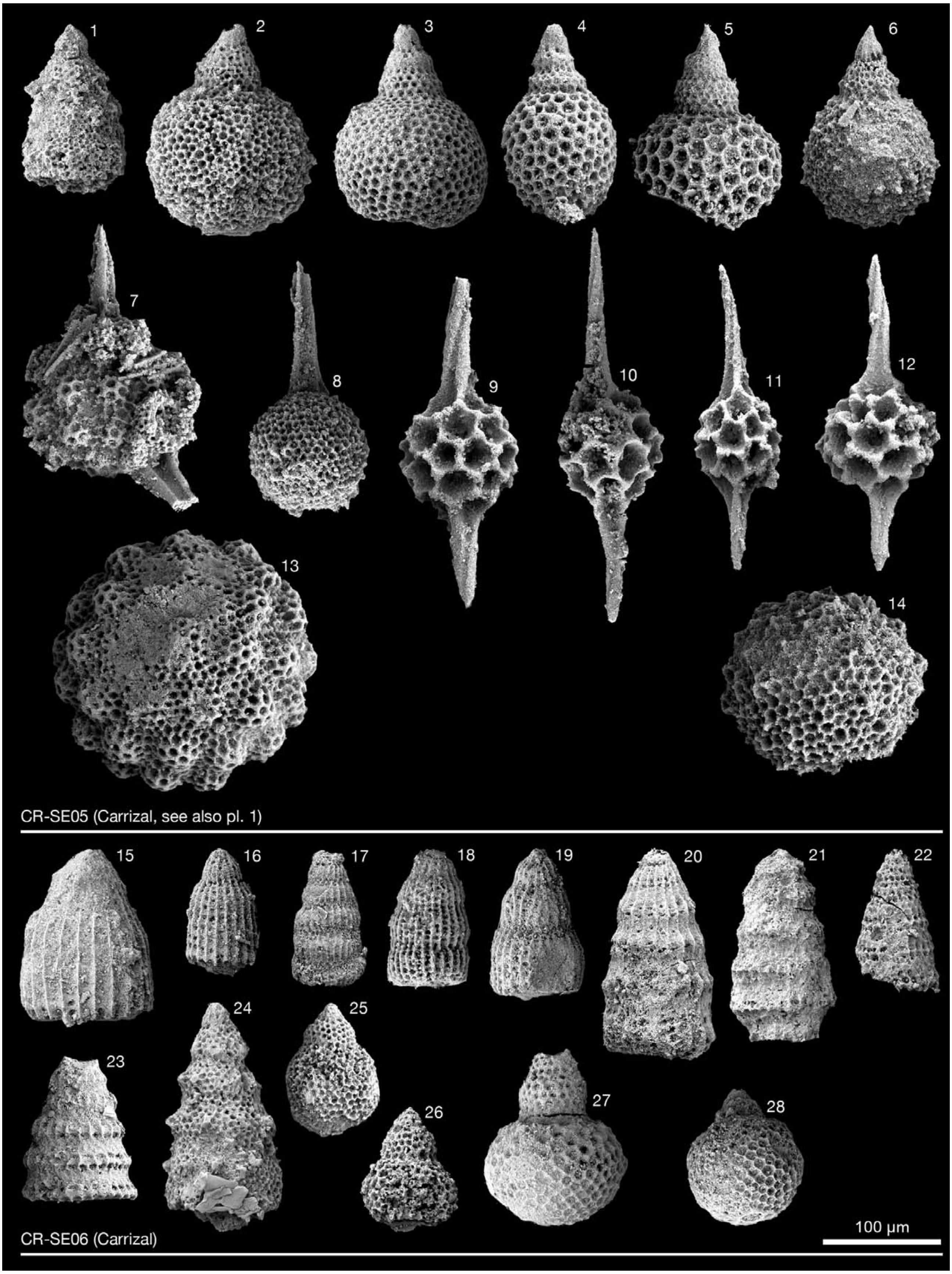

Plate 2 - Scanning Electron Microscope pictures of radiolarians from the Carrizal tectonic window of the Santa Rosa Accretionary Complex, Santa Elena Peninsula, northwestern Costa Rica. Sample CR-SE05 (late early Aptian, see also Plate 1): 1- *Xitus* sp.; 2 and 6- *Obesacapsula* spp.; 3 and 4- *Hiscocapsa asseni* (Tan); 5- *Hiscocapsa* sp.; 7- *Acaeniotyle diaphorogona* gr. Foreman; 8- *Triactoma* sp.; 9-12- *Pantanellium masirahense* Dumitrica; 13- *Praeconosphaera sphaeroconus* (Rüst); 14- Spumellaria or cryptothoracic Nassellaria gen. et sp. indet. Sample CR-SE06 (middle Aptian-late Albian): 15- *Thanarla* sp.; 16-18, and 20- *Archaeodictyomitra* spp.; 19- *Archaeodictyomitra immenhauseri* Dumitrica; 21- *Svinitzium* sp.; 22- *Svinitzium mizutanii* Dumitrica; 23- *Svinitzium puga* (Schaaf); 24- *Xitus spicularius* (Aliev) *sensu* O'Dogherty (1994); 25 and 26- *Hiscocapsa* spp.; 27- *Hiscocapsa* cf. *pseudouterculus* (Aita and Okada); 28- *Hemicryptocapsa* sp.

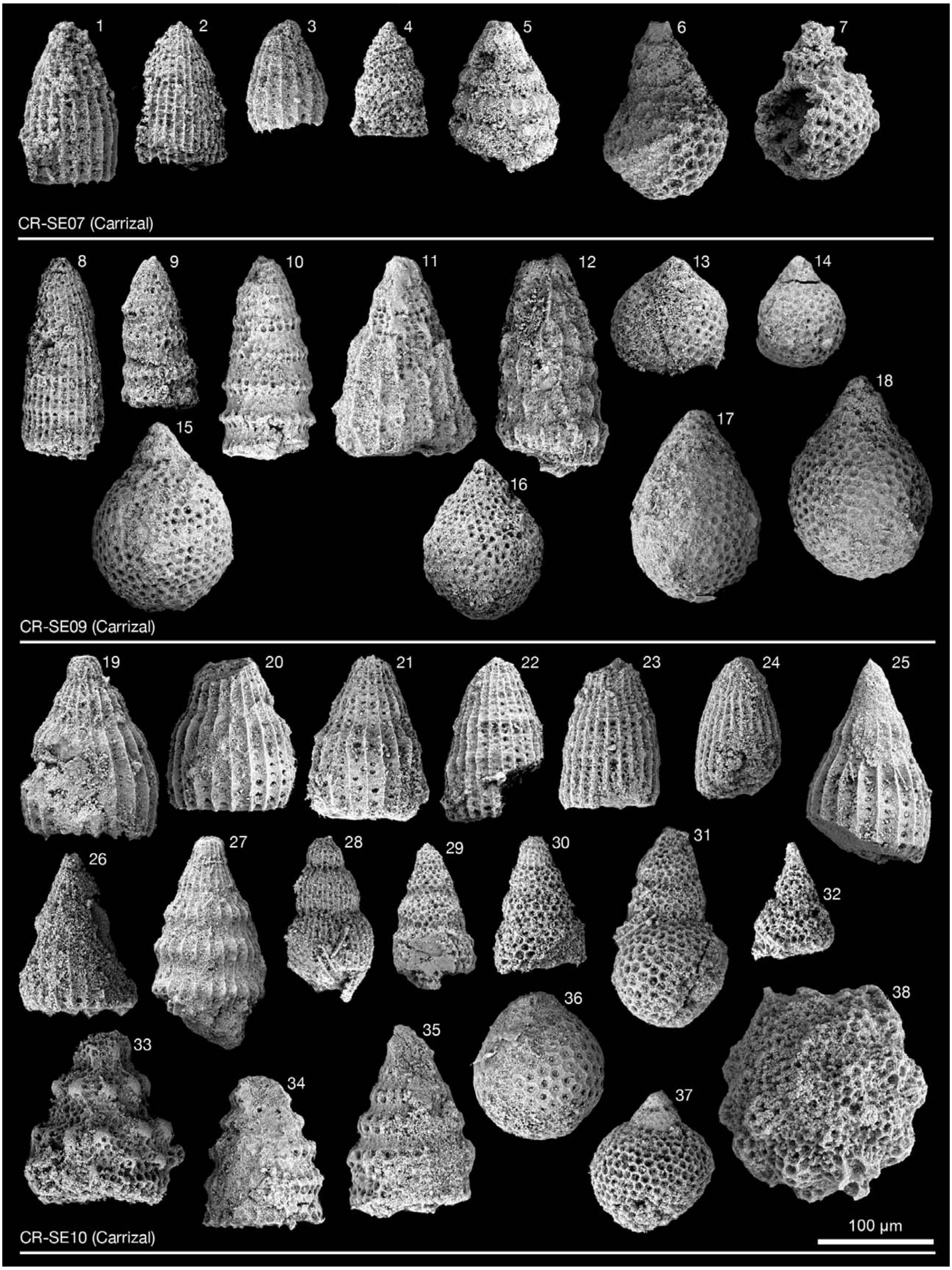

Plate 3 - Scanning Electron Microscope pictures of radiolarians from the Carrizal tectonic window of the Santa Rosa Accretionary Complex, Santa Elena Peninsula, northwestern Costa Rica. Sample CR-SE07 (latest Barremian-early Aptian): 1-3- *Archaeodictyomitra mitra* Dumitrica gr.; 4- *Stichomitra* (?) *japonica* (Nakaseko and Nishimura); 5- *Pseudodictyomitra* sp.; 6- *Hiscocapsa* sp.; 7- *Hiscocapsa uterculus* (Parona). Sample CR-SE09 (late Bathonian-early Oxfordian): 8- *Archaeodictyomitra* aff. *excellens* (Tan); 9- Nassellaria gen. et sp. indet.; 10.- *Svinitzium kamoensis* (Mizutani and Kido); 11- *Hsuum* sp.; 12- *Transhsuum* sp.; 13- *Zhamoidellum ventricosum* Dumitrica; 14- *Zhamoidellum* aff. *ovum* Dumitrica; 15-18- *Praewilliriedellum convexum* (Yao). Sample CR-SE10 (late Berriasian-late Aptian): 19-21- *Thanarla* sp.; 22-24- *Archaeodictyomitra* cf. *mitra* Dumitrica; 25- *Thanarla pulchra* (Squinabol); 26- *Dictyomitra* sp.; 27- *Archaeodictyomitra* cf. *coniforma* Dumitrica; 28- *Archaeodictyomitra* sp.; 29-31- *Stichomitra* (?) spp.; 32- Nassellaria gen. et sp. indet.; 33- *Xitus* cf. *normalis* (Wu and Li); 34 and 35- *Svinitzium puga* (Schaaf); 36- *Cryptamphorella* sp.; 37- *Cryptamphorella* cf. *conara* (Foreman); 38- *Acaeniotyle umbilicata* (Rüst).

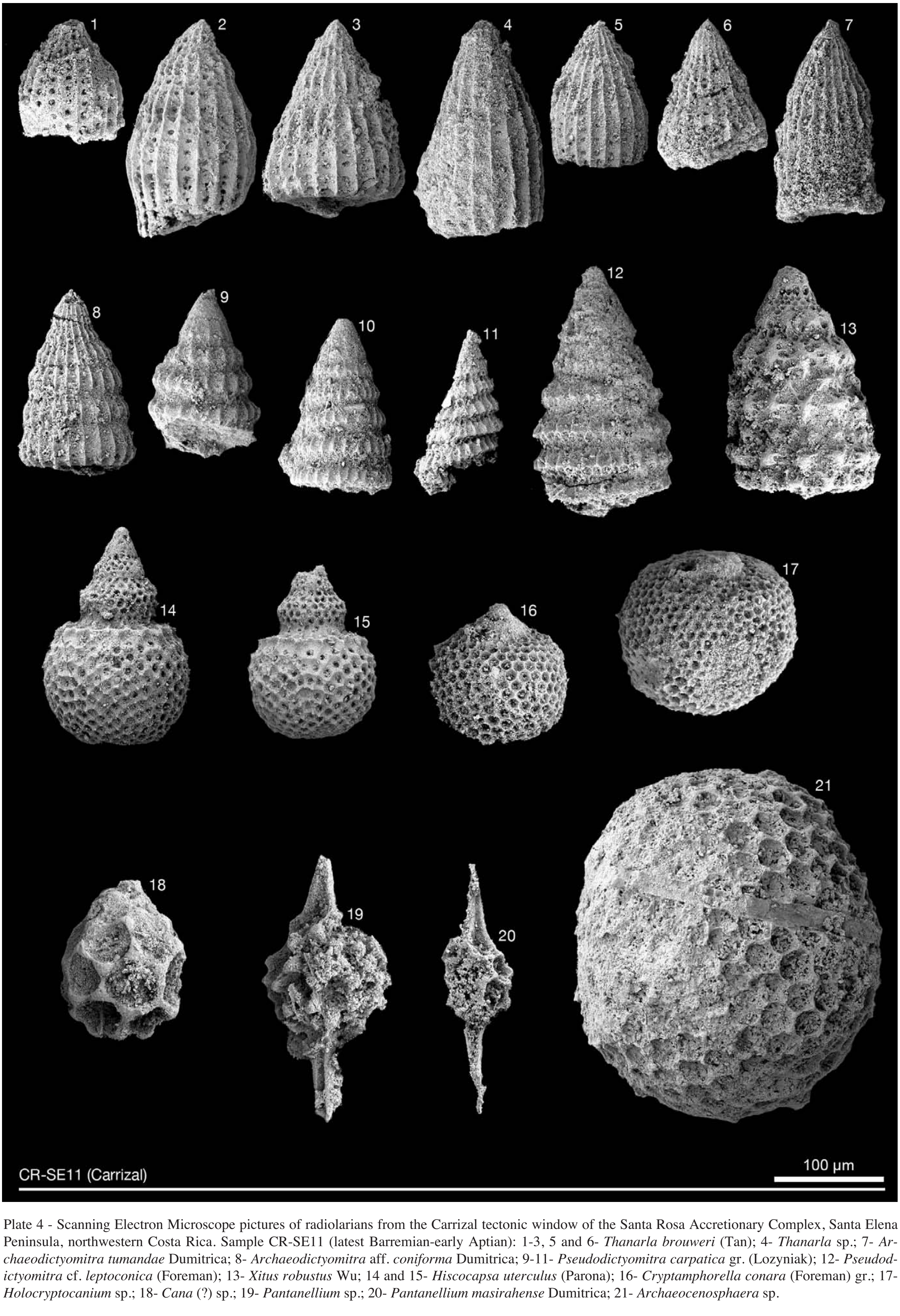

Plate 4 - Scanning Electron Microscope pictures of radiolarians from the Carrizal tectonic window of the Santa Rosa Accretionary Complex, Santa Elena Peninsula, northwestern Costa Rica. Sample CR-SE11 (latest Barremian-early Aptian): 1-3, 5 and 6- *Thanarla brouweri* (Tan); 4- *Thanarla* sp.; 7- *Archaeodictyomitra tumandae* Dumitrica; 8- *Archaeodictyomitra* aff. *coniforma* Dumitrica; 9-11- *Pseudodictyomitra carpatica* gr. (Lozyniak); 12- *Pseudodictyomitra* cf. *leptoconica* (Foreman); 13- *Xitus robustus* Wu; 14 and 15- *Hiscocapsa uterculus* (Parona); 16- *Cryptamphorella conara* (Foreman) gr.; 17- *Holocryptocanium* sp.; 18- *Cana* (?) sp.; 19- *Pantanellium* sp.; 20- *Pantanellium masirahense* Dumitrica; 21- *Archaeocenosphaera* sp.

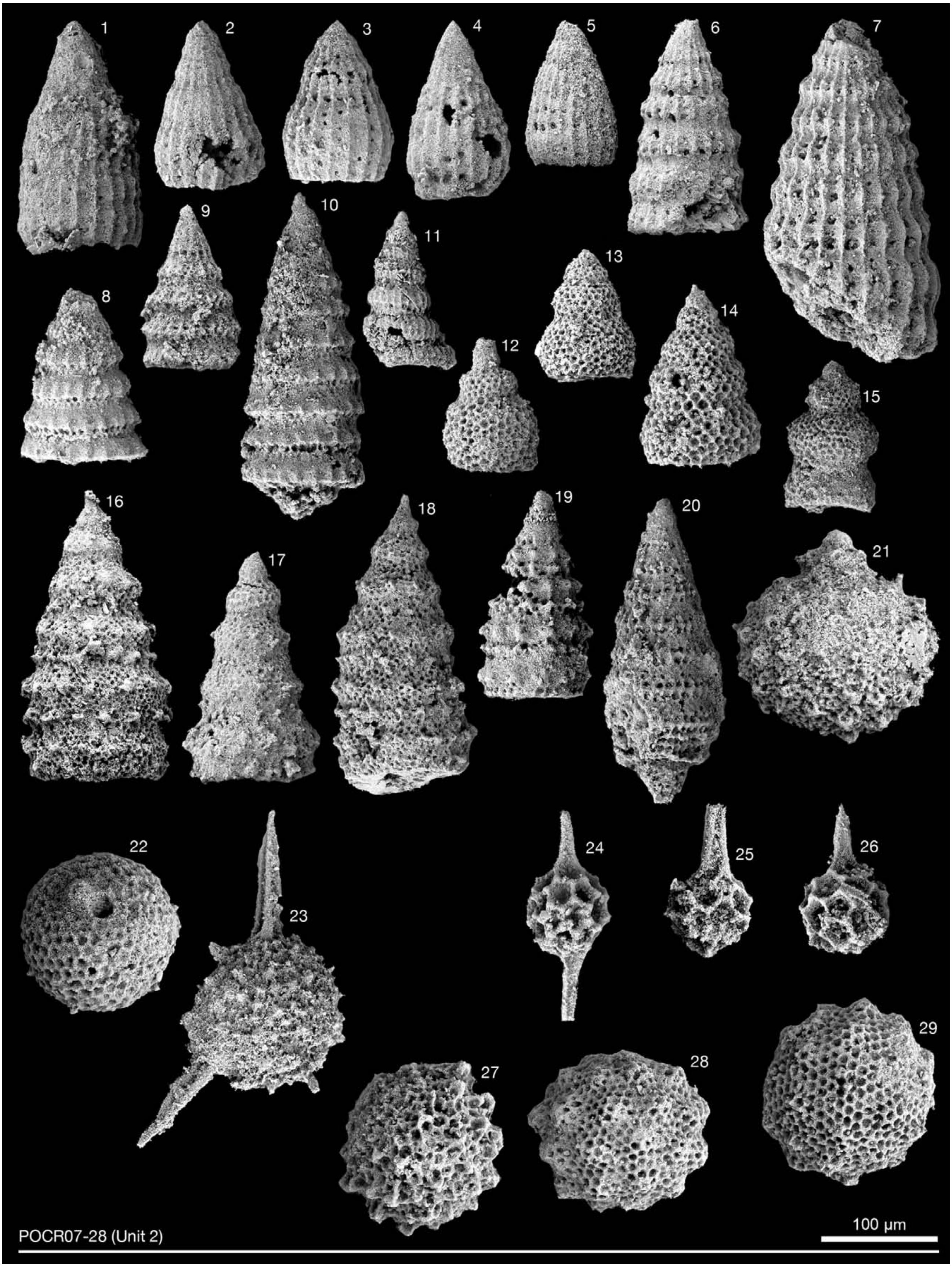

Plate 5 - Scanning Electron Microscope pictures of radiolarians from the Unit 2 of the Santa Rosa Accretionary Complex, Santa Elena Peninsula, northwestern Costa Rica. Sample POCR07-28 (late middle-late Aptian): 1- *Archaeodictyomitra* sp.; 2 and 4- *Thanarla brouweri* (Tan); 3- *Thanarla* cf. *brouweri* (Tan); 5- *Archaeodictyomitra mitra* Dumitrica; 6- *Dictyomitra* sp.; 7- *Archaeodictyomitra leptocostata* (Wu and Li); 8 and 10-.*Pseudodictyomitra* cf. *leptoconica* (Foreman); 9- *Svinitzium puga* (Schaaf); 11- *Pseudodictyomitra lodogaensis* Pessagno; 12 and 15- *Stichomitra* (?) sp.; 13- *Stichomitra* (?) *japonica* (Nakaseko and Nishimura); 14- *Stichomitra* (?) cf. *stocki* (Campbell and Clark); 16-18- *Xitus spicularius* (Aliev) *sensu* O'Dogherty (1994); 19- *Praexitus* cf. *verrucosus* Dumitrica; 20- *Svinitzium* aff. *mizutanii* Dumitrica; 21- *Hiscocapsa grutterinki* (Tan); 22- *Holocryptocanium* sp.; 23- *Becus horridus* (Squinabol); 24-26- *Pantanellium* cf. *masirahense* Dumitrica; 27- *Praeconocaryomma* sp.; 28 and 29- *Praeconosphaera* sp.

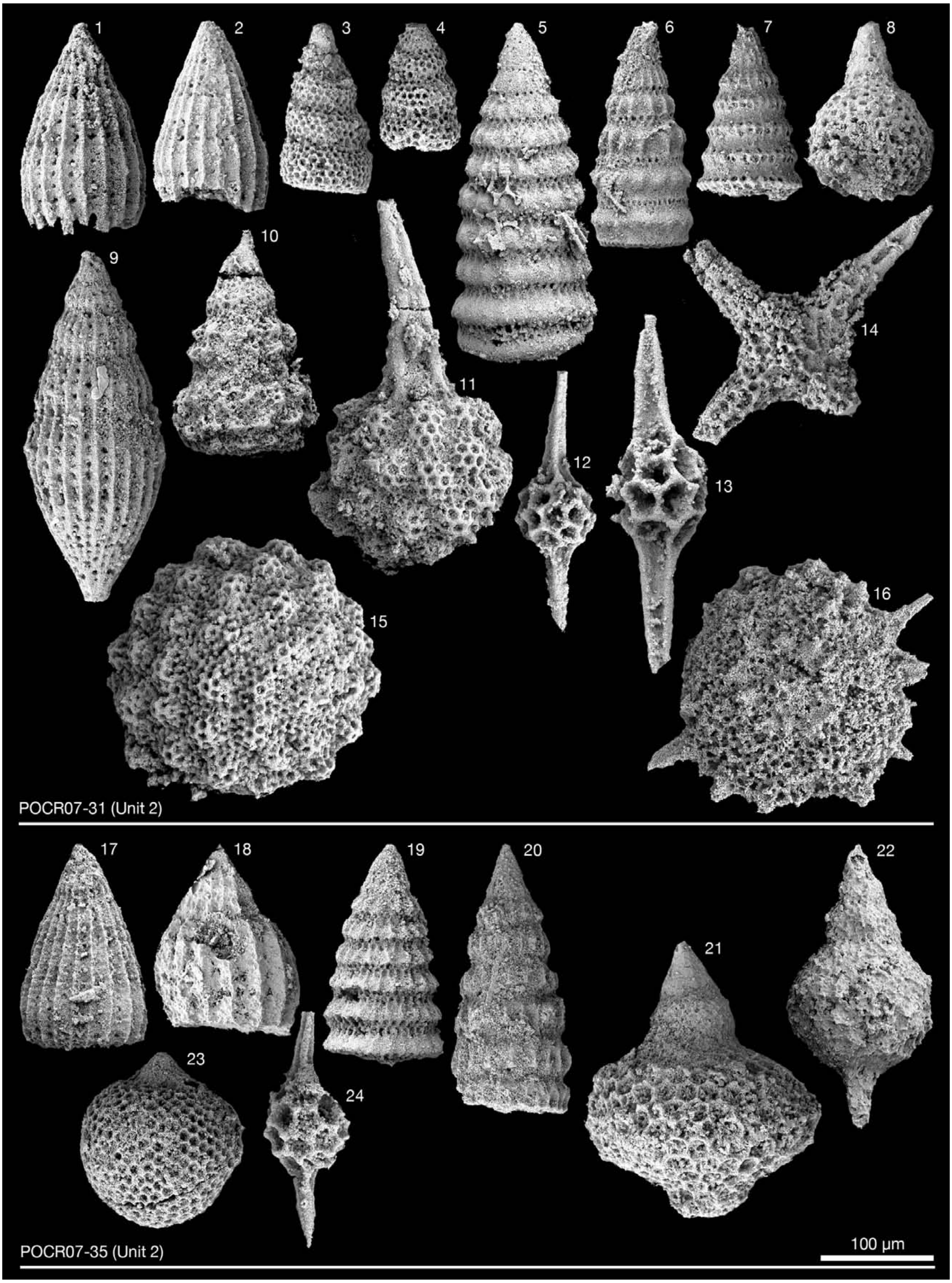

Plate 6 - Scanning Electron Microscope pictures of radiolarians from the Unit 2 of the Santa Rosa Accretionary Complex, Santa Elena Peninsula, northwestern Costa Rica. Sample POCR07-31 (late early to early middle Aptian): 1 and 2- *Thanarla brouweri* (Tan); 3 and 4- *Stichomitra* (?) *communis* Squinabol; 5- *Pseudodictyomitra* cf. *nodocostata* Dumitrica; 6- *Pseudodictyomitra lanceloti* Schaaf; 7- *Svinitzium puga* (Schaaf); 8- *Hiscocapsa* cf. *asseni* (Tan); 9- *Archaeodictyomitra lacrimula* (Foreman); 10- *Xitus* sp.; 11- *Acaeniotyle umbilicata* (RÜST); 12- *Pantanellium squinaboli* (Tan); 13- *Pantanellium* sp.; 14- *Crucella* sp.; 15- *Praeconosphaera sphaeroconus* (Rüst); 16- *Godia coronata* (Tumanda). Sample POCR07-35 (late Hauterivian-early middle Aptian): 17- *Thanarla brouweri* (Tan); 18- *Thanarla pacifica* Nakaseko and Nishimura; 19- *Pseudodictyomitra* aff. *carpatica* gr. (Lozyniak); 20- *Pseudodictyomitra lanceloti* Schaaf; 21- *Spinosicapsa typica* (Rüst); 22- *Spinosicapsa* sp.; 23- *Cryptamphorella conara* (Foreman) gr.; 24- *Pantanellium squinaboli* (Tan).

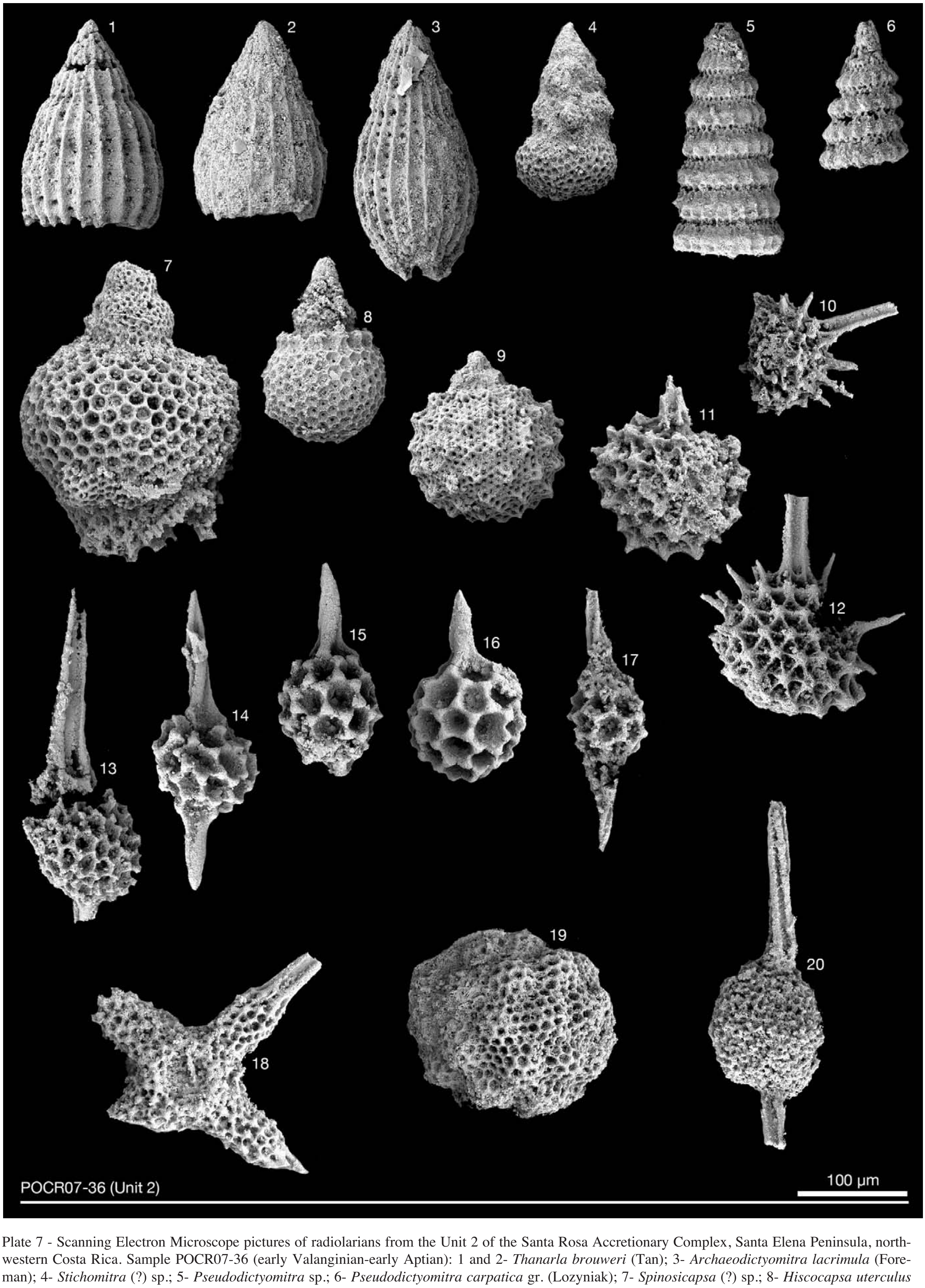

Plate 7 - Scanning Electron Microscope pictures of radiolarians from the Unit 2 of the Santa Rosa Accretionary Complex, Santa Elena Peninsula, northwestern Costa Rica. Sample POCR07-36 (early Valanginian-early Aptian): 1 and 2- *Thanarla brouweri* (Tan); 3- *Archaeodictyomitra lacrimula* (Foreman); 4- *Stichomitra* (?) sp.; 5- *Pseudodictyomitra* sp.; 6- *Pseudodictyomitra carpatica* gr. (Lozyniak); 7- *Spinosicapsa* (?) sp.; 8- *Hiscocapsa uterculus* (Parona); 9- *Hiscocapsa grutterinki* (Tan); 10-12- *Alievium regulare* (Wu and Li); 13- *Dicroa* sp.; 14-16- *Pantanellium squinaboli* (Tan); 17- *Pantanellium masirahense* Dumitrica; 18- *Crucella bossoensis* Jud; 19- *Praeconosphaera sphaeroconus* (Rüst); 20- *Archaeospongoprunum* sp.

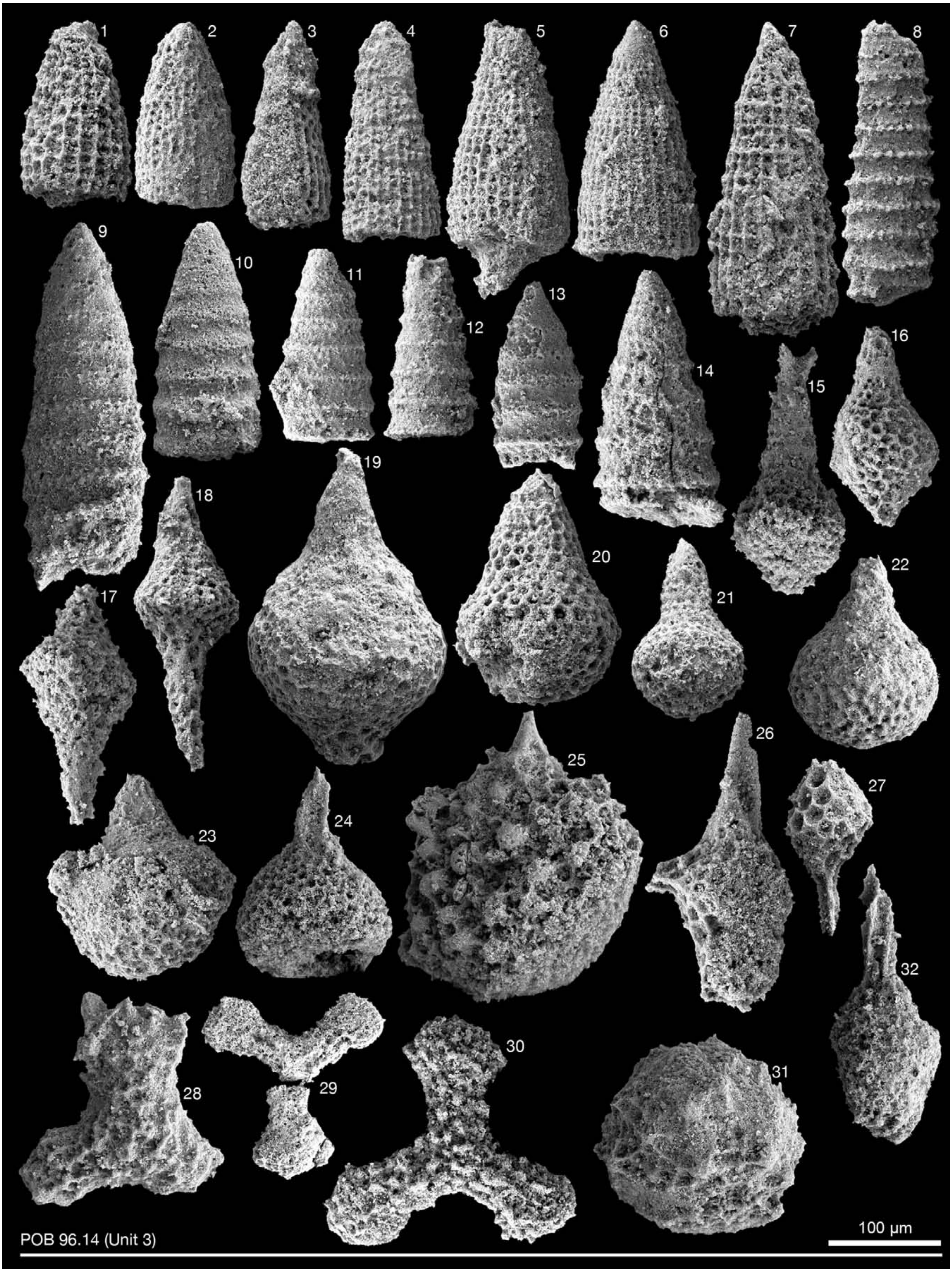

Plate 8 - Scanning Electron Microscope pictures of radiolarians from the Unit 3 of the Santa Rosa Accretionary Complex, Santa Elena Peninsula, northwestern Costa Rica. Sample POB96.14 (Pliensbachian): 1 and 5- *Parahsuum* spp.; 2- *Parahsuum ovale* Hori and Yao; 3 and 4- *Parahsuum* aff. *grande* Hori and Yao; 6- *Parahsuum snowshoense* (Pessagno); 7- *Parahsuum* aff. *stanleyense* (Pessagno); 8, 11 and 12- *Canoptum artum* Yeh; 9, 10 and 13- *Canoptum dixoni* Pessagno and Whalen; 14- *Canoptum* sp.; 15- *Katroma bicornus* De Wever; 16-18- *Katroma* sp.; 19- *Katroma* cf. *ninstintsi* Carter; 20- *Pseudoristola megaglobosa* Yeh; 21- *Pseudoristola* cf. *megaglobosa* Yeh; 22- Nassellaria gen et sp. indet.; 23- *Williriedellum* (?) sp.; 24- *Napora* (?) sp.; 25- Spumellaria gen. et sp. indet.; 26- *Anaticapitula anatiformis* (De Wever); 27- *Pantanellium cumshewaense* Pessagno; 28- *Paronella* sp.; 29 and 30- *Homeoparonaella* spp.; 31- *Praeconocaryomma* sp.; 32- *Archaeospongoprunum* sp.

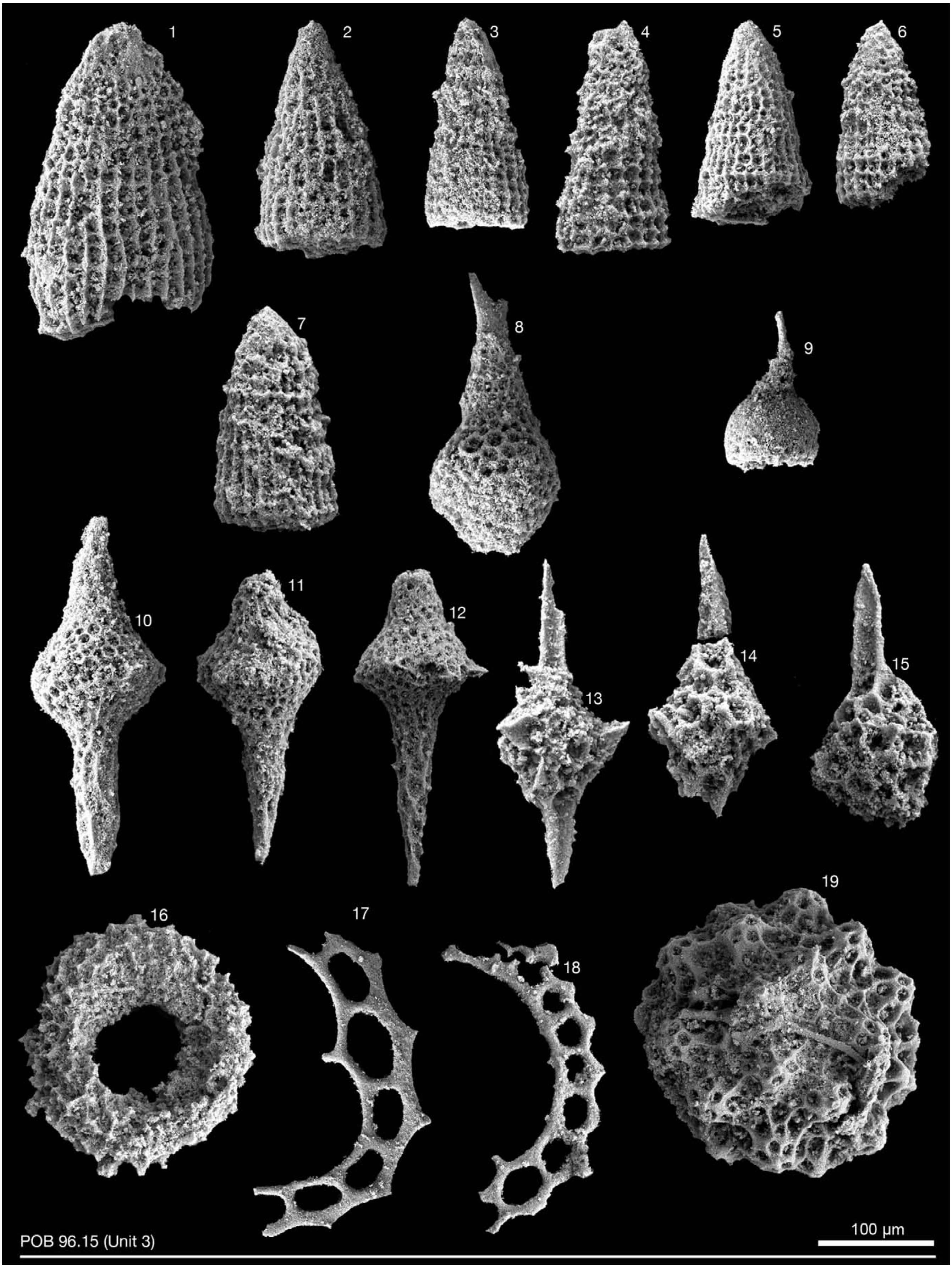

Plate 9 - Scanning Electron Microscope pictures of radiolarians from the Unit 3 of the Santa Rosa Accretionary Complex, Santa Elena Peninsula, northwestern Costa Rica. Sample POB96.15 (early Toarcian): 1- *Archaeodictyomitra* (?) sp.; 2, 3 and 5- *Parahsuum* aff. *grande* Hori and Yao; 4- *Parahsuum* aff. *stanleyense* (Pessagno); 6 and 7- *Parahsuum ovale* Hori and Yao; 8- *Katroma bicornus* De Wever; 9- *Eucyrtidiellum disparile* gr. Nagai and Mizutani; 10-12- *Katroma* cf. *clara* Yeh; 13 and 14- *Zartus mostleri* Pessagno and Blome; 15- *Trillus* cf. *elkhornensis* Pessagno and Blome; 16- *Orbiculiforma* (?) sp.; 17 and 18- *Parasaturnalis diplocyclis* (Yao); 19- *Praeconocaryomma bajaensis* Whalen.

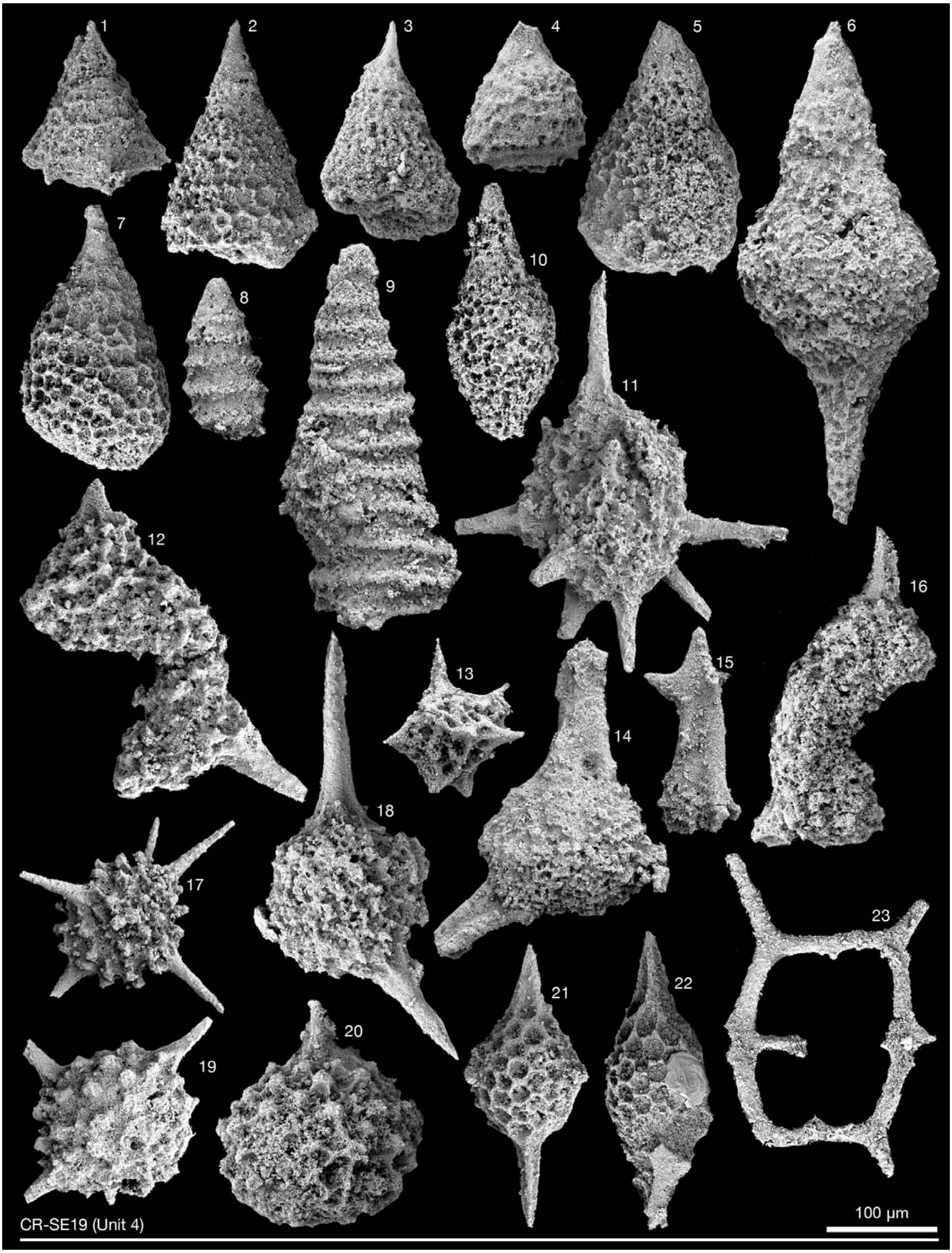

Plate 10 - Scanning Electron Microscope pictures of radiolarians from the Unit 4 of the Santa Rosa Accretionary Complex, Santa Elena Peninsula, north-western Costa Rica. Sample CR-SE19 (early-middle Pliensbachian): 1- *Napora* sp.; 2, 5, and 7- Nassellaria gen. et sp. indet.; 3- *Parahsuum* cf. *longiconicum* Sashida; 4- *Bipedis fannini* Carter; 6- *Katroma* cf. *ninstintsi* Carter; 8- *Canoptum* sp.; 9- *Canoptum columbiaense* Whalen and Carter; 10- *Pseudoeucyrtis* sp.; 11 and 13- Spumellaria gen. et sp. indet.; 12 and 16- *Cyclastrum asuncionense* Whalen and Carter; 14 and 18- *Triactoma* (?) sp.; 15- *Acaeniotylopsis* aff. *triacanthus* Kito and De Wever; 17 and 19- *Thurstonia* (?) *gibsoni* Whalen and Carter; 20- *Charlottea* (?) sp. C Gorican et al. (2006); 21- *Pantanellium* cf. *inornatum* Pessagno and Poisson; 22- *Pantanellium* sp.; 23- *Paleosaturnalis tetraradiatus* (Kozur and Mostler).

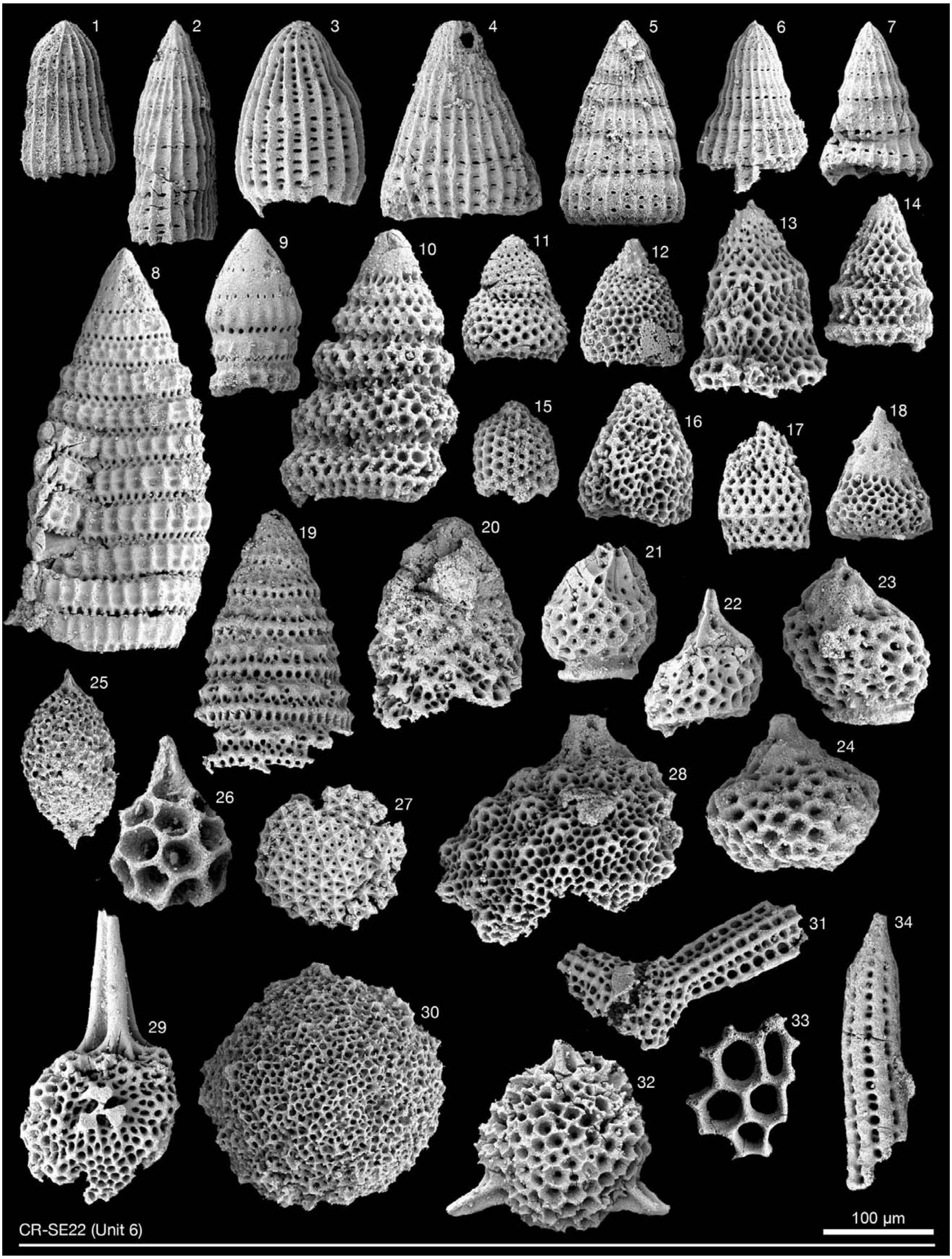

Plate 11 - Scanning Electron Microscope pictures of radiolarians from the Unit 6 of the Santa Rosa Accretionary Complex, Santa Elena Peninsula, northwestern Costa Rica. Sample CR-SE22 (late early Albian-early Turonian): 1- *Archaeodictyomitra undata* (Squinabol); 2- *Archaeodictyomitra montisserei* (Squinabol); 3- *Thanarla* aff. *brouweri* (Tan); 4- *Archaeodictyomitra* sp.; 5- *Dictyomitra* aff. *formosa* (Squinabol) *sensu* O'Dogherty (1994); 6 and 7- *Dictyomitra* spp.; 8- *Pseudodictyomitra* sp.; 9- *Pseudodictyomitra pseudomacrocephala* (Squinabol); 10- *Stichomitra* (?) sp.; 11- *Stichomitra* (?) cf. *japonica* (Nakaseko and Nishimura); 12, 13, and 16-18- Nassellaria gen. et sp. indet.; 14- *Stichomitra* (?) *tosaensis* (Nakaseko and Nishimura); 15- *Diacanthocapsa* (?) sp.; 19- *Xitus* aff. *vermiculatus* (Renz); 20- *Xitus* sp.; 21-23- *Rhopalosyringium mosquense* (Smirnova and Aliev); 24- *Rhopalosyringium* sp.; 25- *Archaeospongoprunum* sp.; 26- *Pantanellium* sp.; 27- *Cryptamhorella* sp.; 28- *Acaeniotyle* (?) cf. *glebulosa* (Foreman); 29- *Acaeniotyle* sp.; 30, 33, and 34- Spumellaria gen. et sp. indet.; 31- *Archaeotritrabs* sp.; 32- *Triactoma* sp.

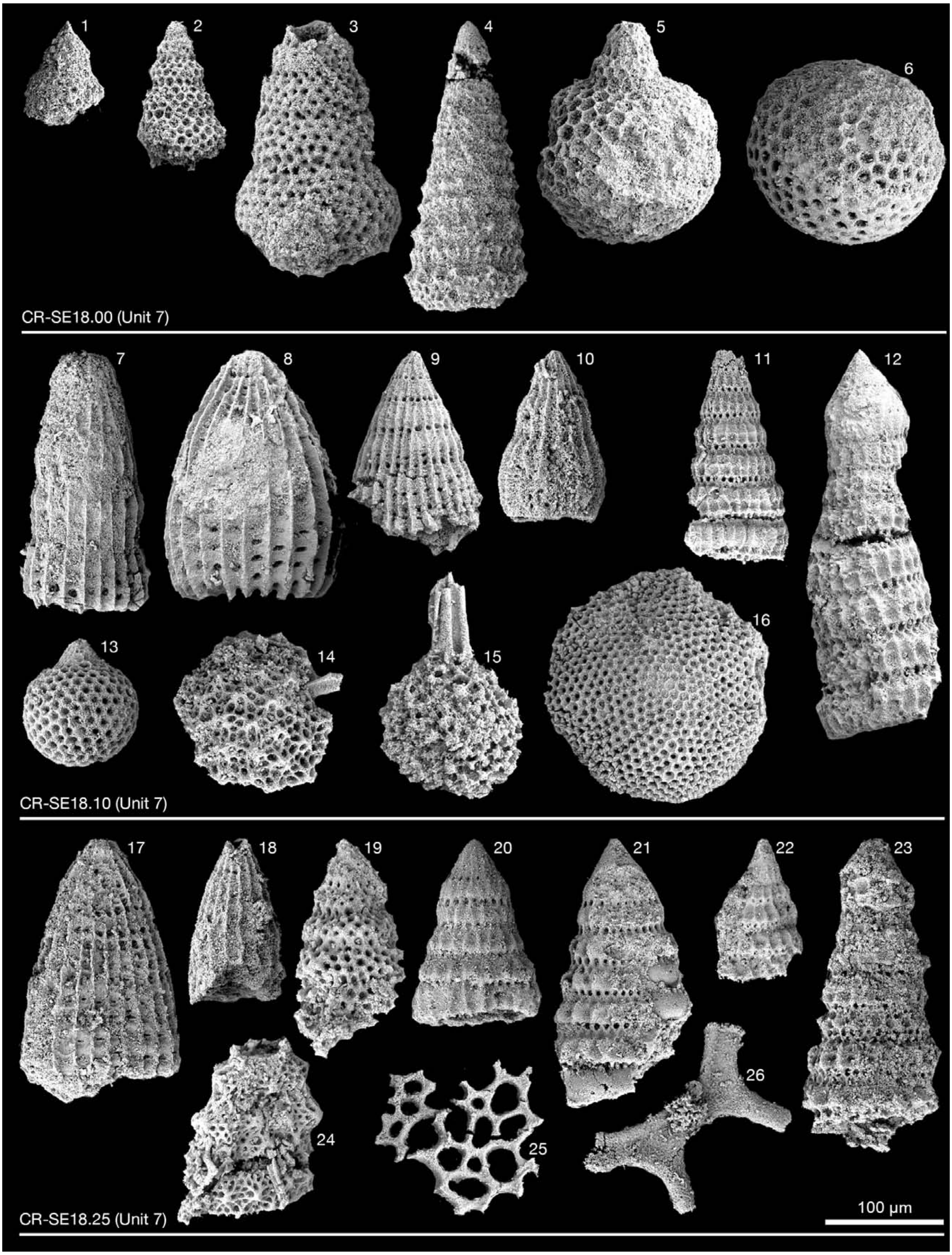

Plate 12 - Scanning Electron Microscope pictures of radiolarians from the Unit 7 of the Santa Rosa Accretionary Complex, Santa Elena Peninsula, northwestern Costa Rica. Sample CR-SE18.00 (late early Albian-early middle Albian): 1- Nassellaria gen. et sp. indet.; 2 and 3- *Stichomitra* (?) spp.; 4- *Crolanium spineum* (Pessagno); 5- *Hiscocapsa* sp.; 6- *Archaeocenosphaera* sp. Sample CR-SE18.10 (late early Albian-early middle Albian): 7- *Archaeodictyomitra* aff. *montisserei* (Squinabol); 8- *Thanarla* (?) sp.; 9- *Archaeodictyomitra* sp.; 10- *Thanarla* sp.; 11- *Pseudodictyomitra pentacolaensis* Pessagno; 12- *Pseudodictyomitra pseudomacrocephala* (Squinabol); 13- *Cryptamphorella conara* (Foreman) gr.; 14- *Praeconocaryomma universa* Pessagno; 15- *Alievium* (?) sp.; 16- Spumellaria gen. et sp. indet. Sample CR-SE18.25 (late early Albian-early middle Albian): 17 and 18- *Archaeodictyomitra* spp.; 19- *Stichomitra* (?) sp.; 20- *Loopus* aff. *nudus* (Schaaf); 21 and 22- *Pseudodictyomitra* spp.; 23- *Pseudodictyomitra pseudomacrocephala* (Squinabol); 24- *Xitus spicularius* (Aliev) *sensu* O'Dogherty (1994); 25- Spumellaria gen. et sp. indet.; 26- *Acanthocircus* aff. *hueyi* (Pessagno).

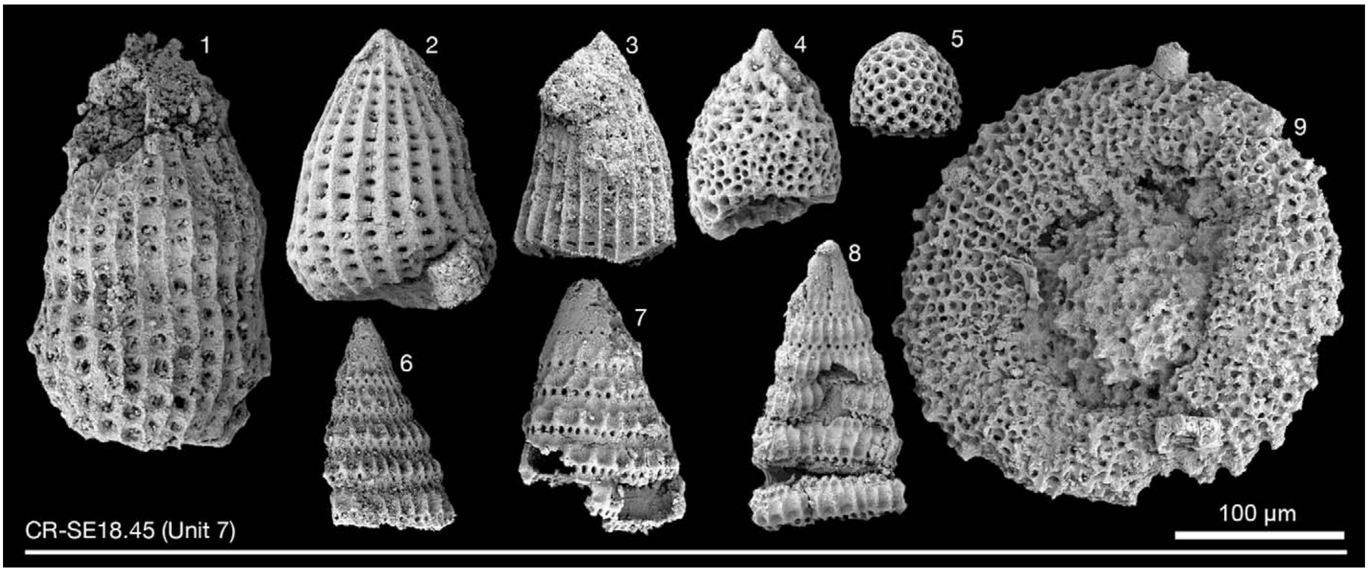

Plate 13 - Scanning Electron Microscope pictures of radiolarians from the Unit 7 of the Santa Rosa Accretionary Complex, Santa Elena Peninsula, northwestern Costa Rica. Sample CR-SE18.45 (late early Albian-early middle Albian): 1- *Archaeodictyomitra* sp.; 2- *Thanarla brouweri* (Tan); 3- *Archaeodictyomitra* aff. *montisserei* (Squinabol); 4- *Trimulus* (?) cf. *parmatus* O'Dogherty; 5- *Diacanthocapsa fossilis* (Squinabol); 6 and 7- *Pseudodictyomitra* spp.; 8- *Pseudodictyomitra paronai* (Aliev); 9- *Orbiculiforma railensis* Pessagno.